UNIVERSITY OF CALIFORNIA
Los Angeles

Interpreting the effect of environmental conditions on elemental partitioning in biogenic carbonates within the framework of Rayleigh fractionation

A thesis submitted in partial satisfaction of the requirements for the degree Master of Science in Geochemistry

by

Rosaleen Ella Gilmore

2013

ABSTRACT OF THE THESIS

Interpreting the effect of environmental conditions on elemental partitioning in biogenic carbonates within the framework of Rayleigh fractionation

by

Rosaleen Ella Gilmore

Master of Science in Geochemistry
University of California, Los Angeles, 2013
Professor Aradhna Tripati, Chair

The elemental composition of calcium carbonate ($CaCO_3$) precipitated by marine invertebrates varies with the physico-chemical properties of seawater, and is thus used for reconstructing past oceanic conditions, including temperature, pH, and seawater composition. Previous studies have used a Rayleigh fractionation model to interpret elemental partitioning within a range of calcitic and aragonitic organisms. This thesis contains analyses of elemental ratios for multiple marine invertebrates that were cultured from seawater under variable conditions using both new unpublished results and data from the literature. The partitioning of strontium, magnesium, barium, manganese, boron, lithium and uranium within these biogenic carbonates, and data from the literature for foraminifera and coccolithophores, are examined within a Rayleigh fractionation framework.

Application of a Rayleigh model to these systems requires constraints on elemental partitioning into inorganic $CaCO_3$. A survey of the literature shows that for some elements (e.g., Mn), there are very little data, while for others (e.g., Sr, Mg), there are a wide range of reported values. Given this uncertainty, I examine the impact that varying the nominal inorganic partition coefficient has on Rayleigh-derived estimates of calcium-utilization during calcification. The

elements examined in this thesis have different chemical and ionic properties (atomic mass, ionic radius, charge), and these properties impact how readily the element can be incorporated into the $CaCO_3$ lattice by replacing its constituents. A Rayleigh model allows one to examine how open the calcification system of an organism is, as well as how much calcium is remaining in the calcification reservoir after biomineralization is complete. I show that organisms that are evolutionarily similar to each other behave similarly in this model, and therefore are likely to use similar mechanisms for biomineralization; for example, organisms from the Crustacea phylum calcify from a relatively closed reservoir with a slow flushing rate, while organisms of the Mollusca phylum calcify from an open calcification pool and have a very fast flushing rate. There are still a few problems with the use of a Rayleigh model in the context of biological calcification; these issues are discussed in-depth throughout the study. An overview of the effects of changing pCO_2 and temperature on element partitioning in these invertebrates is examined. I used a combined understanding of organism physiology and Rayleigh fractionation geochemistry to elucidate how certain groups of marine calcifiers control their calcification, and how this control can influence elemental ratios in calcium carbonate that are sometimes used as paleo-proxies.

The thesis of Rosaleen Ella Gilmore is approved.

Robert Eagle

David Jacobs

Edwin Schauble

Aradhna Tripati, Committee Chair

University of California, Los Angeles

2013

Table of Contents

Acknowledgements

I would like to thank Justin Ries for providing samples of the organisms that he cultured at Woods Hole Oceanographic Institute, as well as Robert Eagle and Aradhna Tripati for performing the elemental analyses. I would also like to thank the members of my committee, Aradhna Tripati, Edwin Schauble, Robert Eagle, and David Jacobs, for their support and guidance with this research. This research was supported by a Hellman Fellowship as well as a grant from the American Chemical Society.

Introduction

This thesis presents data and calculations about the elemental composition of the calcium carbonate of twenty different marine invertebrate species for eight elements (Sr, Mg, Ba, Mn, B, Li, Cd, and U). A novel set of elemental data from a group of eighteen marine macroinvertebrates (Ries et al., 2009), along with previously published data on two microscopic calcifiers, are studied. Since element-to-calcium ratios are useful proxies for past ocean conditions, temperature and pH signals in both proven and potential proxy elements are examined. The impact of vital effects on paleoproxy signals is discussed, and a Rayleigh fractionation model is used to draw conclusions about the calcification processes in the organisms studied. Phylogenetic and evolutionary similarities in the process of calcification and the calcification reservoir in the organisms are demonstrated.

Background

Biomineralization is the process by which a biological organism produces a mineral. An example of biomineralization is the production of calcium carbonate ($CaCO_3$) by organisms such as corals, lobsters, scallops, and foraminifera. Calcium carbonate biomineralization is referred to as calcification, and is one of the predominant forms of biomineralization in the ocean, most commonly in the form of aragonite or calcite. In many marine organisms, calcification occurs in a fluid that originates from seawater. The calcifying environment may be manipulated to enable or enhance the rate of carbonate mineral precipitation. The chemistry of calcifying fluids may be biologically modified by enzymatic ion transport to increase concentrations of the ions needed for calcification (Constanz, 1986, McConnaughey, 1986, McConnaughey, 1989, Cohen and McConnaughey, 2003). It can also be controlled by organic macromolecules, which can dictate when calcification begins and ends, as well as the physical structure of the calcium carbonate produced (Dauphin, 2001).

As calcification proceeds, impurities are incorporated into the mineral lattice: ions of a similar size and charge may replace the calcium, carbon or oxygen atoms of $CaCO_3$. Although the specific controls are still debated, culturing and core-top studies show that these impurities and substitutions are typically dependent on the ambient conditions in which the calcium carbonate formed. This makes the elemental ratios of carbonates a proxy for past ocean conditions (Gaetani and Cohen, 2006, Barker et al., 2005, Lea, 2006).

Elements that have been utilized as paleoproxies include strontium, magnesium, barium, manganese, boron, lithium, cadmium and uranium. The measure of incorporation of these elements is expressed as an elemental ratio, X/Ca, where the concentration of the element X is

measured in respect to the concentration of calcium present in a sample of biogenic calcium carbonate.

One of the major concerns for using an elemental ratio as a paleoproxy is the lack of understanding as to how biological processes may influence the incorporation of elements into biominerals, which can create deviations from relationships constrained by experiments and theory on inorganic carbonate. Such deviations are known as 'vital effects'. One proposed source of vital effects is the effect of Rayleigh fractionation, which applies to organisms that use an enclosed calcifying reservoir. Rayleigh fractionation is relevant to vital effects because the concentration of elements in a closed reservoir are altered from the external environment as calcification progresses, which in turn alters the elemental ratios in the calcium carbonate precipitate. Here I present research that looks at the geochemistry of the calcium carbonate produced by twenty different marine calcifiers. Using a combined understanding of organism physiology, and a Rayleigh model to elucidate how certain groups of marine calcifiers control their calcification, I attempt to draw conclusions on how biological control can affect elemental ratios in calcium carbonate.

Changes in saturation state and ocean acidification

This thesis investigates modern marine invertebrates that sample environments from a range of $CaCO_3$ saturation states. The primary dataset I will consider comes from a suite of modern organisms cultured at variable carbonate saturation states. This range was achieved by manipulating pCO_2 across a range of values similar to what we might expect to achieve in the 21st century. In this case the cultured organisms were held at a constant temperature of 25°C, while CO_2 gas was bubbled through the seawater to produce four different pCO_2 treatments (Ries

et al., 2009). CO_2 levels in the atmosphere have been increasing since the beginning of the industrial revolution due to human activities. Anthropogenic CO_2 accumulating in the air results in increased global temperatures. Increased levels of atmospheric CO_2 also lead to an increase in the amount of dissolved inorganic carbon (DIC) in the ocean through dissolution. When excess CO_2 is removed from the atmosphere by the oceans, there is a shift in the dissolved inorganic carbon (DIC) system in seawater, resulting in increased hydrogen ion concentrations and reduced pH levels; this process is called ocean acidification. There is little doubt that ocean acidification is going to impact marine calcifiers (Doney et al., 2009a, Doney et al., 2009b, Riebesell et al., 2010, Cohen and Holcomb, 2009).

Overview of taxa studied

Twenty marine calcifiers from a very broad evolutionary and environmental range were studied for this thesis. Only a few of these organisms are studied in depth, while the rest are studied in comparison to the other organisms that are closely related to them. The broad taxonomic range of organisms, and physiological differences between these organisms, results in the organisms controlling the process of biomineralization quite differently (Mann, 2001). For example, some organisms calcify within a closed reservoir where the pH, calcium concentrations, and carbonate concentrations can be biologically altered to create an environment where calcification is favorable (McCulloch et al., 2012, Mackinder et al., 2010, Mackinder et al., 2011, Taylor et al., 2011). The physiologic control that organisms have on the transport pathways of calcium, carbon, and elements into the calcification reservoir, as well as the flushing time of the reservoir, are two important factors that are hypothesized to influence the X/Ca of the calcium carbonate produced and result in taxon-specific elemental partitioning into biominerals

(Elderfield et al., 1996). The present research reports the effects of changing saturation state on element-to-calcium ratios, and uses these data to draw conclusions about how these organisms control their calcification reservoir from a combination of observed elemental changes and the known physiology of the organisms. The work has implications for understanding how vital effects are created in element-to-calcium ratios that are used as paleoproxies, as well as placing new constrains on mechanisms of calcification in different organisms.

Table 1: ***A summary of the organisms studied in this project.***

Organism [a]	Scientific name [b]	Source [c]	Collection site [d]
Crustacea			
Lobster	*Homarus americanus*	J. Ries (Ries et al., 2009)	Gulf of Maine, ME
Blue Crab	*Callinectes sapidus*	J. Ries (Ries et al., 2009)	Chesapeake Bay, MD
Shrimp	*Penaeus plebejus*	J. Ries (Ries et al., 2009)	Atlantic Ocean, FL
Mollusca			
Bay Scallop	*Argopecten irradians*	J. Ries (Ries et al., 2009)	Nantucket Sound, MA
Oyster	*Crassostrea virginica*	J. Ries (Ries et al., 2009)	Buzzards Bay, MA
Blue Mussel	*Mytilus edulis*	J. Ries (Ries et al., 2009)	Buzzards Bay, MA
Hard Clam	*Mercenaria mercenaria*	J. Ries (Ries et al., 2009)	Nantucket Sound, MA
Soft Clam	*Mya arenaria*	J. Ries (Ries et al., 2009)	Nantucket Sound, MA
Conch	*Strombus alatus*	J. Ries (Ries et al., 2009)	Gulf of Mexico, FL
Whelk	*Urosalpinx cinerea*	J. Ries (Ries et al., 2009)	Buzzards Bay, MA
Periwinkle	*Littorina littorea*	J. Ries (Ries et al., 2009)	Buzzards Bay, MA
Limpet	*Crepidula fornicata*	J. Ries (Ries et al., 2009)	Buzzards Bay, MA
Annelida			
Serpulid Worm	*Hydroides crucigera*	J. Ries (Ries et al., 2009)	Nantucket Sound, MA
Echinodermata			
Purple Urchin	*Arbacia punctulata*	J. Ries (Ries et al., 2009)	Nantucket Sound, MA
Pencil Urchin	*Eucidaris tribuloides*	J. Ries (Ries et al., 2009)	Atlantic Ocean, FL
Cnidaria			
Temperate Coral	*Oculina arbuscula*	J. Ries (Ries et al., 2009)	Atlantic Ocean, NC
Rhodophyta			
Coralline Red Algae	*Neogoniolithon* sp.	J. Ries (Ries et al., 2009)	Atlantic Ocean, FL
Chlorophyte			
Halimeda	*Halimeda incrassata*	J. Ries (Ries et al., 2009)	Atlantic Ocean, FL
Foraminifera			
Foraminifera	*Orbulina universa*	Allen et al., 2011	Pacific Ocean, CA
Foraminifera	*Globigerina bulloides*	Yu et al., 2007	Various
Foraminifera	*Globorotalia inflata*	Yu et al., 2007	Various
Foraminifera	*Globigerina bulloides*	Lea et al., 1999	Pacific Ocean, CA
Foraminifera	*Orbulina universa*	Lea et al., 1999	Pacific Ocean, CA
Haptophyte			
Coccolithophore	*Coccolithus braarudii*	Stoll et al., 2012	Southern Atlantic Ocean
Coccolithophore	*Emiliania huxleyi*	Stoll et al., 2012	Various

[a] Common species names of the organisms with their phylum name in bold.
[b] Scientific name of each organism.
[c] Source of cultured organisms where we use newly collected data presented in this thesis for the first time, or the relevant citation where we use previously published data.
[d] Location where organisms were collected.

Table 2: ***Taxa studied in the newly collected dataset presented here on the cultured specimens provided by Justin Ries.***

Organism [a]	$CaCO_3$ morphology [b]	Elements analyzed [c]
Crustacean		
Lobster	HMC	Sr, Mg, Ba, Mn
Blue Crab	HMC	Sr, Mg, Ba, Mn
Shrimp	HMC	Sr, Mg, Ba, Mn
Mollusk		
Bay Scallop	LMC	Sr, Mg, Ba, Mn, B, Li, Cd, U
Oyster	LMC	Sr, Mg, Ba, Mn, B, Li, Cd, U
Blue Mussel	LMC > A	Sr, Mg, Ba, Mn, B, Li, Cd, U
Hard Clam	A >> HMC	Sr, Mg, Ba, B
Soft Clam	A >> LMC	Sr, Mg, Ba, B
Conch	A > LMC	Sr, Mg, Ba, B
Whelk	A > LMC	Sr, Mg, Ba, B
Periwinkle	LMC > A	Sr, Mg, Ba, Mn, B, Li, Cd, U
Limpet	A > LMC	Sr, Mg, Ba, B
Annelid		
Serpulid Worm	A + HMC	Sr, Mg, Ba, B
Echinoderm		
Purple Urchin	HMC	Sr, Mg, Ba, Mn, B, Li, Cd, U
Pencil Urchin	HMC	Sr, Mg, Ba, Mn
Cnidaria		
Temperate Coral	A	Sr, Mg, Ba, B, U
Rhodophyte		
Coralline Red Algae	HMC	Sr, Mg, Ba, Mn, B, Li, Cd, U
Chlorophyte		
Halimeda	A	Sr, Mg, Ba

[a] Common species names of the organisms with their phylum name in bold.
[b] Polymorph of calcium carbonate that is precipitated by the organism (Ries et al., 2009).
[c] Elements analyzed by Inductively-Coupled Plasma Mass Spectrometry (ICPMS), VISTA Inductively-Coupled Plasma Optical Emission Spectrometry (ICP-OES), or by a combination of both (calcium was analyzed in all cases to determine the X/Ca ratio). The second column lists the polymorph of calcium carbonate precipitated by each organism, 'LMC' stands for low-magnesium calcite, 'HMC' stands for high-magnesium calcite, and 'A' stands for aragonite. It should also be noted that some organisms precipitate a mixture of aragonite and either high- or low-magnesium calcite, and that mathematical notation is used to indicate the relative polymorph composition of the calcium carbonate precipitated by each organism. For example, 'A > LMC' means that the organism precipitates aragonite and some low-Mg calcite, and 'A >> LMC' means that the organism precipitates mostly aragonite and very little low-Mg calcite.

Phylum Crustacea

Three crustaceans are studied: the lobster *Homarus americanus*, the blue crab *Callinectes sapidus*, and the shrimp *Penaeus plebejus*. Crustaceans belong to the kingdom Animalia, the phylum Arthropoda, and the subphylum Crustacea (Pechenik, 1991). Crustaceans are covered by a hard exoskeleton that is segmented to allow movement (Hickman, 1973). This exoskeleton, also called the cuticle, is composed of a combination of the mineral calcium carbonate, the polysaccharide chitin, and several different proteins. The cuticle of crustaceans can be composed of anywhere between 0 and 90% calcium carbonate, with the stronger and harder parts of the skeleton containing more calcium carbonates, and the softer parts of the skeleton containing more chitin and proteins (Alexander, 1979).

Crustacean cuticle is composed of four distinct layers: the epicuticle, the exocuticle, the endocuticle, and the membranous layer, ordered from most external to most internal. The outer three layers contain calcium carbonate. The epicuticle is the thin waxy outer layer of the cuticle, which is composed of a mixture of calcite and a lipid-protein matrix. The exocuticle and the endocuticle are made up of lamellar chitin-protein fibers combined with calcite crystals (Alexander, 1979, Roer and Dillaman, 1984). The endocuticle is the most heavily calcified, as well as the thickest, part of the cuticle (Travis, 1955, Travis, 1965).

Evidence of the activity of carbonic anhydrase, Ca-ATPase, anion transporters, and internal storage pools of both calcium and carbonate has been extensively indicated in crustaceans (Roer and Dillaman, 1984, Luquet and Marin, 2004, Roer, 1980, Ahearn and Zhuang, 1996). The main source of calcium for crustaceans is exogenous, coming mainly from the surrounding water, although it has been shown that some of the calcium of the cuticle comes from the food consumed by the organism (Roer and Dillaman, 1984). The percentage of

percentage of exogenous and endogenous calcium incorporated varies by organism. The Rayleigh model cannot account for the use of endogenous calcium during calcification. Active calcium transport has been found in several species of crustaceans, including *Callinectes* (the blue crab studied here), although the affinity of the mechanism for calcium in *Callinectes* was quite low, indicating that it is not an incredibly efficient transportation mechanism (Roer and Dillaman, 1984). Isotopic labeling experiments performed by Roer and Dillaman, 1984 indicate the presence of carbonate storage compartments, whereas discrete calcium storage compartments seem less prevalent.

Phylum Mollusca

Nine different mollusk species are studied: the bay scallop *Argopecten irradians*, the oyster *Crassostrea virginica*, the blue mussel *Mytilus edulis*, the hard clam *Mercenaria mercenaria*, the soft clam *Mya arenaria*, the conch *Strombus alatus*, the whelk *Urosalpinx*, the periwinkle *Littorina littorea*, and the limpet *Crepidula fornicata*. Mollusks belong to the kingdom Animalia, the superphylum Lophotrochozoa, and the phylum Mollusca (Pechenik, 1991). The shells of mollusks consist of alternating layers of calcium carbonate and an organic matrix composed mostly of the protein chonchiolin, and are formed within a highly structured chitinous framework (Alexander, 1979, Hickman, 1973, Addadi et al., 2006). Mollusk shells are mostly calcium carbonate, with the organic matrix making up only about 5% of the whole shell (Alexander, 1979). The calcium- and carbon-concentrating mechanisms have not been as well identified or studied in the mollusks as in the crustaceans, although evidence for storage of calcium and carbonate ions, as well as of calcium carbonate mineral crystals, has been shown (Addadi et al., 2006, Watabe et al., 1976, Neff, 1972).

Phylum Annelida

The annelid studied here is the serpulid worm *Hydroides crucigera*. Annelids belong to the kingdom Animalia and the superphylum Lophotrochozoa, the same as mollusks, but they belong to the phylum Annelida (Pechenik, 1991). The annelid phylum consists of mostly worms, with the earthworm being a familiar member. Most of these organisms do not calcify; however the serpulid worm forms calcified tubes consisting of calcium carbonate with the assistance of the organic tube lining, which acts as a scaffold onto which the mineral is deposited by the organism (Tanur et al., 2010, Bernhardt et al., 1985). The biomineralization of the serpulid worm consists of fibrous and lamellar structures composed of calcium carbonate (Vinn, 2011). A thorough search of the literature has failed to produce any studies concerned with the transport of calcium or carbonate ions, or the process of calcification, in the serpulid worm.

Phylum Echinodermata

Two echinoderms are studied: the purple urchin *Arbacia punctulata* and the pencil urchin *Eucidaris tribuloides*. Echinoderms belong to the kingdom Animalia, the subkingdom Eumetazoa, and the phylum Echonidermata (Pechenik, 1991), and are a model organism that is used in many ocean acidification and marine biology studies. The endoskeleton and spines of sea urchins are composed of biomineralized calcium carbonate. The endoskeleton is embedded in the body wall, beneath the epidermal layer, and is made up of ossicles connected together to form one rigid test (Alexander, 1979). The spines are attached to the endoskeleton in a ball-and-socket type joint, with muscles connected to the bottoms of the spines to allow the urchin to keep the spines sticking out straight for protection from predators, or to move the spines around to

move or upright themselves (Hickman, 1973). The formation of the spines of sea urchins begins with the precipitation of precursor amorphous calcium carbonate, which later turns into high-magnesium calcite (Beniash et al., 1997). The spines are composed of an inner axial zone and an outer cortex; both are composed of calcite, and behave as a single crystal unit (Hickman, 1973). Evidence of carbonic anhydrase activity and active calcium and carbonate transport has been demonstrated in sea urchins (Benson and Wilt, 1992).

Phylum Cnidaria

The cnidarian studied here is the temperate coral *Oculina arbuscula*. Cnidarians come from the kingdom Animalia and the subkingdom Eumetazoa, just like echinoderms, but they belong to the phylum Cnidaria (also sometimes called the phylum Coelenterata) (Pechenik, 1991). Scleractinian corals, such as *Oculina arbuscula*, are marine animals that form coral reefs. The organism, or polyp, is not photosynthetic; however there are many phytoplankton and zooplankton that life as symbionts of the coral (Tambutté et al., 2011). Therefore, reef corals are dependent on photosynthesis. The calcification of scleractinian corals is in the form of aragonite and associated matric organics, and is precipitated in growth layers that form radially outward (Tambutté et al., 2011).

The source of calcium for scleractinian corals comes from the external seawater (Goreau, 1959, Muscatine, 1973, Gattuso et al., 1999) and is transported by passive diffusion except for at the site of calcification where active membrane transport has been discovered (Gattuso et al., 1999). Gagnon et al. (2012) indicate that all elements (calcium, strontium, boron, etc.) follow the same path of transport from the external seawater to the internal calcification space. The source of carbonate for biomineralization is a mixture of carbonate from the external seawater

and the metabolic products of the coral and its associated symbionts (Gattuso et al., 1999, Muscatine, 1973, Pearse, 1970, Pearse, 1971). In a radioisotopic study performed by Furla et al., 2000, it was shown that approximately 70-75% of the carbonate used for calcification came from metabolic products, while only 25-30% came from the external environment. Both light (photosynthesis) and symbiotic zooxanthellae are necessary for scleractinian corals to calcify to their highest potential (Goreau, 1959, Kawaguti and Sakumoto, 1948, Muscatine, 1973, Gattuso et al., 1999). Photosynthesis seems to be directly coupled to calcification, at least in some corals (Gattuso et al., 1999, Vandermeulen et al., 1972, Muscatine. 1973). It has been suggested that corals are able to raise the pH of their calcifying space to allow calcification to proceed more favorably (McCulloch et al., 2012). Evidence of carbonic anhydrase activity, active transporters, and calcium and carbonate reservoirs have been extensively researched (Furla et al., 2000, Muscatine, 1973, Kawaguti and Sakumoto, 1948, Gattuso et al., 1999), although there is still dissension about the precise mechanisms used, especially in carbonate storage and transport.

Phylum Rhodophyta

The coralline red algae *Neogoniolithon* sp. from the phylum Rhodophyta is studied. Unlike all of the organisms discussed above, the rhodophytes belong to the kingdom Plantae instead of the kingdom Animalia (Dawson, 1966). Coralline red algae calcify high-magnesium calcite in a two-stage process inside their cell walls (Bosence, 1991). This two-step calcification produces a layer of calcite just inside of, and parallel to, the cell wall, as well as a layer of radial calcite crystals that grow inwards towards the center of the cell (Bailey and Bisalputra, 1970, Alexandersson, 1974, Alexandersson, 1977, Garbary, 1978). There also appears to be some calcification that occurs extracellularly and cements cells together (Bosence, 1985) which is

problematic for the application of a Rayleigh model which presumes an enclosed calcification reservoir. The rate of calcification in coralline red algae is increased in the presence of light (Borowitzka, 1981, Gao et al., 1993), indicating that these algae may use the products of photosynthesis to maximize calcification while minimizing energetic costs. There is also radioisotopic evidence that the calcium and carbon that is taken up by coralline red algae is stored in separate compartments before they are transported to the sites of calcification (Borowitzka, 1979). An extensive literature review has failed to turn up any more information or experiments that could shed some light onto the molecular and cellular level of calcification in coralline red algae.

Phylum Chlorophyta

The chlorophyte studied here is *Halimeda incrassata*. Chlorophytes are from the kingdom Plantae, like the rhodophytes, and belong to the phylum Chlorophyta (Dawson, 1966). In halimeda, calcification begins inside the outermost layer of the cell wall. As calcification proceeds, the aragonite crystals that are precipitated grow rapidly in size, while moving inwards, away from the cell wall and into the cell. By the time calcification ceases, the biomineral aragonite takes up most of the space within the cell (Borowitzka and Larkum, 1977). Calcification in halimeda occurs within the extracellular space, completely separated from the exterior seawater (Borowitzka and Larkum, 1977). Evidence that halimeda change the pH at the site of calcification within their cells has been found based on radioisotopic experiments (Borowitzka and Larkum, 1976), and it is possible that this intercellular pH change is effected by the coupling of photosynthesis and calcification (Jensen et al., 1985). Although halimeda seems to alter the pH levels within its cells, there does not seem to be an active calcium or carbonate

concentrating mechanism present in these organisms (De Beer and Larkum, 2001). A carbonic anhydrase enzyme inhibitor study has shown that internal carbonic anhydrase is active, but external carbonic anhydrase is not (De Beer and Larkum, 2001).

Phylum Foraminifera

Foraminifera are the only organisms from the kingdom Protista that are studied in this research (Erez, 2003). Data from three different species of foraminifera from the literature are modeled: *Orbulina universa* (Allen et al., 2011, Lea et al., 1999), *Globigerina bulloides* (Lea et al., 1999, Yu et al., 2007), and *Globorotalia inflata* (Yu et al., 2007).

Foraminifera are single-celled organisms that surround themselves with a calcitic shell formed from tests. Foraminifera can have anywhere from one to more than ten tests, which are built sequentially outward from the protoplasm of the cell (Cusack and Freer, 2008). Every time a new test is constructed, each of the earlier tests is covered in a new layer of calcite (Erez, 2003). The process of biomineralization in foraminifera is regulated by various different proteins, which are essential to the proper formation of the tests (Cusack and Freer, 2008). The elemental composition of the calcite in foraminifera may vary throughout the structure of a single test (Hathorne et al., 2009). Evidence of a carbon concentrating mechanism and an enclosed calcification pool has been found in foraminifera (Rollion-Bard and Erez, 2010, de Nooijer et al., 2009, Erez et al., 2008, Erez, 2003, Bentov et al., 2009).

Phylum Haptophyta

Three strains of the species *Coccolithus braarudii*, and one strain of the species *Emiliania huxleyi*, from a study performed by Stoll et al., 2012, are modeled; coccolithophorids come from

the phylum Haptophyta. Coccolithophorids belong to the kingdom Chromalveolata and are the most evolutionarily distant from the higher animals of any organism studied here (Paasche, 2002).

Coccolithophorids are single-celled, microscopic organisms that range in size from about 5μm to 35μm in diameter. Coccolithophores produce plates, called coccoliths, made out of calcite that covers the entire surface of the cell. The coccoliths are composed entirely of calcite, but the baseplate onto which calcite is deposited is composed of various polysaccharides. Several polysaccharides and proteins have also been identified in the regulation of biomineralization in coccolithophores (Mann, 2001, Westbroek et al., 1989, Paasche, 2002). Calcification in coccolithophores occurs only within an enclosed pool, known as the coccolith vesicle, and is under a high level of biological control (Young and Henriksen, 2003, Paasche, 2002). Carbon- and calcium-concentrating mechanisms, carbonic anhydrase activity, and active carbon and calcium transport have been well established (Mackinder et al., 2010, Mackinder et al., 2011, Taylor et al., 2011, Gussone et al., 2006, Bach et al., 2011, Buitenhuis et al., 1999, Iglesias-Rodriguez et al., 2002, Rickaby et al., 2010, Leonardos et al., 2009).

Table 3: ***Summary of the calcification systems of the macroinvertebrates studied***

Phylum [a]	Enclosed reservoir [b]	pH control [c]	Active transport [d]	Enzyme activity [e]	Coupling with photosynthesis [f]
Crustacea			yes	yes	
Mollusca			yes	yes	
Annelida					
Echinodermata			yes	yes	
Cnidaria	potentially	potentially	yes	yes	yes
Rhodophyta			yes		yes
Chlorophyte	yes	yes	no	yes	yes
Foraminifera	yes	yes	yes		
Haptophyta	yes	yes	yes	yes	potentially

[a] Phylum studied.
[b] Evidence of an enclosed reservoir within which calcium carbonate is precipitated.
[c] Evidence that the organisms of that phylum can control the pH level at the cite of calcification.
[d] Evidence of active transport of calcium and/or carbon within the organisms of that phylum.
[e] Evidence that enzymatic activity (generally internal and/or external carbonic anhydrase) is active and either increasing the rate, or reducing the energetic cost, of calcification.
[f] Evidence of a coupling of photosynthesis and calcification to reduce the energetic costs of calcification in the organisms of that phylum.

In this table, 'yes' means that evidence has been found that indicates that the process is occurring in the organisms of that phylum, 'no' means that evidence has been found that proves that the process is not occurring in the organisms of that phylum, 'potentially' means that there is still debate about whether or not the process occurs in that phylum, and a blank space indicates that no evidence has been found for the process in that phylum, either because that phylum is not well studied or because the process does not occur. This table summarizes the text of the section above to provide a visual representation about what is known to be occurring in the organisms studied in this thesis, as well as what is not known about the organisms. All references and details on the information presented in this table can be found in the 'overview of taxa studied' section above.

Carbonate system parameters and calcification

Organisms were cultured at a range of pCO_2 levels; levels of 400, 600, 900, and 2850 ppm were chosen to mimic potential ocean acidification conditions. The 400 ppm pCO_2 level is equivalent to average conditions in the oceans today, the 600 ppm and 900 ppm levels are expected over the next century or two, and the 2850 ppm level was chosen to show how organisms react under very elevated pCO_2 conditions that will hopefully never be witnessed on Earth.

The carbonate system consists of the total concentration of dissolved inorganic carbon (DIC) which speciates into carbon dioxide (CO_2), carbonic acid (H_2CO_3), bicarbonate (HCO_3^-) and carbonate ion (CO_3^{2-}):

$$CO_{2(g)} \rightleftharpoons CO_{2(aq)} + H_2O \rightleftharpoons H_2CO_3^* \rightleftharpoons HCO_3^- + H^+ \rightleftharpoons CO_3^{2-} + H^+$$

At lower pH levels (more acidic) this reaction will shift to the left and more carbon dioxide will be present than any other carbon species. At higher pH levels (more basic) the reaction will shift to the right and more bicarbonate and carbonate ions will be present in the ocean. Marine calcifiers are affected by both the carbonate system and the pH of the ocean. Calcification is affected by the carbonate system since it requires high concentrations of either bicarbonate or carbonate ion to proceed:

$$Ca^{2+} + HCO_3^- \rightleftharpoons CaCO_3 + H^+$$

$$Ca^{2+} + CO_3^- \rightleftharpoons CaCO_3$$

In addition, calcification cannot proceed at too acidic of a pH, since the calcium carbonate saturation state is pH-dependent. The calcium carbonate saturation state is a measure of whether or not there is enough calcium and carbonate available in the surrounding water to allow the formation of calcium carbonate to proceed favorably (Dickson, 2009).

Elemental ratios studied

The element-to-calcium ratios that are considered in this research are Sr/Ca, Mg/Ca, Ba/Ca, Mn/Ca, B/Ca, Li/Ca, Cd/Ca and U/Ca. These ratios have all been previously studied as paleoproxies, to varying degrees, with Mg/Ca and Sr/Ca having been extensively studied (Cohen et al., 2001, Dueñas-Bohórquez et al., 2011, Gagnon et al., 2013, Lea, 2006, Lea et al., 1999, Gabitov and Watson, 2006, Saulnier et al., 2012), and Mn/Ca having been barely studied at all. The partitioning of these elements into calcium carbonate is differentially influenced by environmental parameters (such as temperature and saturation state).

Table 4: ***A summary of the atomic and ionic properties of the elements being studied.***

Element [a]	Atomic number [b]	Atomic Mass (amu) [c]	Effective ionic Radius (pm) [d]	Ionic charge [e]
Calcium	20	40.08	1.14	+2
Strontium	38	87.62	1.32	+2
Magnesium	12	24.30	0.86	+2
Barium	56	137.33	1.49	+2
Manganese	25	54.94	0.97 (hs)	+2
			0.79 (hs)	+3
			0.67	+4
Boron	5	10.81	0.15 *	+3
			0.25 **	+3
Lithium	3	6.94	0.90	+1
Cadmium	48	112.41	1.09	+2
Uranium	92	238.03	0.87	+6

[a] The element being studied.
[b] The atomic number of the element.
[c] The atomic mass.
[d] The effective ionic radius of the ion for the associated charges in the right hand column for an assumed coordination number of six (Nesse, 2004).
[e] The ionic charges that are of interest in this study.

Since boron is incorporated differently from the other elements, 3-coordinate * and 4-coordinate** are more relevant.

It should be noted for this table, that the more similar an element is to calcium in size and charge, the more likely it is to replace calcium carbonate during calcification.

Strontium

Strontium-to-calcium ratios have been extensively studied in coral, foraminifera and coccolithophores. Sr/Ca has been shown to vary linearly with sea surface temperature (SST) decreasing with increasing temperature in corals (Cardinal et al., 2001, Sun et al., 2004, Marshal and McCulloch, 2002). Sr/Ca is also affected by calcification rate (Cohen et al., 2001, Saenger et al., 2008, Kisakürek et al., 2008), pressure due to depth in the water column (Rosenthal et al., 1997, McCorkle et al., 1995), the Sr/Ca conditions of the ocean (Lea, 2006) and pH (Lea et al., 1999, Russell et al., 2004). A study by Raitzsch et al. (2010) looked at the correlation between calcite saturation state and Sr/Ca in two species of foraminifera; they found that the Sr/Ca composition of one species was completely unaffected, while the other species showed a significant trend with calcite saturation state (Raitzsch et al., 2010). The fact that Sr/Ca has been found to correlate with more than one environmental condition seriously complicates the use of Sr/Ca as a paleoproxy because calcification rate, depth, ambient Sr/Ca, and pH conditions must all be constrained before a variation in Sr/Ca observed in a sample of carbonate can be absolutely attributed to a variation in the temperature in which it was precipitated.

Strontium incorporation into inorganic calcium carbonate has also been studied extensively. The inorganic partition coefficients for strontium partitioning in calcite that can be found in the literature range from 0.020 (Nehrke et al., 2007) to 0.350 (Gabitov and Watson, 2006) with a median of 0.07 (Curti, 1999) and a mean value of 0.1154 (Tang et al., 2008, Drake et al., 2012, Elderfield et al., 1996, Dawber and Tripati, 2012, Tesoriero and Pankow, 1996, Lorens, 1981, Lea et al., 1995, Kitano et al., 1971, Katz, 1973, Pingitore and Eastman, 1986). For this study, the inorganic partition coefficient for strontium in calcite used is 0.120 (Gabitov and Watson, 2006), which is the value that comes closest to the mean.

The inorganic partition coefficients for strontium partitioning in aragonite are not as extensive studied as for calcite. The coefficients that can be found in the literature range from 1.133 (Gaetani and Cohen, 2006) to 1.24 (Gagnon et al., 2007) with a median of 1.183 and a mean value of 1.185 (Dietzel et al., 2004). For this study, the inorganic partition coefficient for strontium in aragonite used is 1.193 (Dietzel et al., 2004), which is one of the two median values that comes closest to the mean.

Magnesium

Magnesium-to-calcium ratios have also been well studied, particularly in foraminifera, and are generally considered a good proxy for sea surface temperature since Mg/Ca tends to increase with increasing temperatures (Barker et al., 2005, Lear et al., 2000, Lear et al., 2010, Rosenthal et al., 1997, Wei et al., 2000, Hathorne et al., 2009, Kisakürek et al., 2008, Russell et al., 2004). Although Mg/Ca has a strong correlation with temperature, salinity (Hastings et al., 1998, Lea et al., 1999, Lea 2006, Kisakürek et al., 2008), pH (Lea et al., 1999, Lea 2006), and ambient ocean Mg/Ca (Lear et al., 2000) also exert some control over the amount of magnesium that is incorporated into biogenic calcium carbonate. A few studies have found that pH has a negligible effect on the Mg/Ca ratios found in foraminiferal calcite at ambient ocean pH (8.1-8.3), but at a pH of less than 8, that pH was a major factor for the incorporation of magnesium into calcite (Kisakürek et al., 2008, Russell et al., 2004). A study by Raitzsch et al. (2010) looked at the correlation between calcite saturation state and Mg/Ca in two species of foraminifera; they found that the Mg/Ca composition of one species was completely unaffected, while the other species showed a significant trend with calcite saturation state (Raitzsch et al., 2010).

Magnesium incorporation into inorganic calcium carbonate has been relatively well studied. The inorganic partition coefficients for magnesium partitioning in calcite that can be found in the literature range from 0.0123 (Freitas et al., 2006) to 0.097 (Drake et al., 2012) with a median of 0.0181 (Freitas et al., 2006) and a mean value of 0.04042 (Saulnier et al., 2012, Dawber and Tripati, 2012, Mucci an Morse, 1983, Mucci, 1987, Oomori et al., 1987, Katz, 1973). For this study, the inorganic partition coefficient for magnesium in calcite used is 0.0190 (Freitas et al., 2006), which is one of the two median values that comes closer to the mean.

The inorganic partition coefficients for magnesium partitioning in aragonite are relatively well studied. The coefficients that can be found in the literature range from 0.000275 (Gagnon et al., 2007) to 0.001333 (Gaetani and Cohen, 2006) with a median of 0.001027 (Gaetani and Cohen, 2006) and a mean value of 0.0008774. For this study, the inorganic partition coefficient for magnesium in aragonite used is 0.001027 (Gaetani and Cohen, 2006), which is the median value.

Barium

The paleoproxy potential of barium-to-calcium ratios has not been interrogated as robustly as Sr/Ca and Mg/Ca, and there is no consensus about what Ba/Ca correlates well with. The Ba/Ca ratio of calcium carbonate is affected by the ambient Ba/Ca of the ocean (Lea and Spero, 1992), which can be interpreted as a signal for increased rainfall (Horta-Puga and Carriquiry, 2012) since rainfall removes barium from soil and deposits this excess barium in the ocean through runoff (Hönisch et al., 2011). Ba/Ca has also been indicated as a proxy for productivity (Prakash Babu et al., 2002, McManus et al., 1999), alkalinity (McManus et al., 1999) and depth (McCorkle et al., 1995). A study performed by Hönisch et al. (2011) showed

that the Ba/Ca ratios of foraminiferal calcite are not affected by pH, salinity, temperature, or symbiont photosynthesis.

Barium incorporation into inorganic calcium carbonate has been relatively well studied. The inorganic partition coefficients for barium partitioning in calcite that can be found in the literature range from 0.015 (Curti, 1999) to 0.10 (Gillikin et al., 2006) with a median of 0.070 and a mean value of 0.06375 (Elderfield et al., 1996, Tesoriero and Pankow, 1996, Pingitore and Eastman, 1986, Boyle et al., 1995). For this study, the inorganic partition coefficient for barium in calcite used is 0.08 (Elderfield et al., 1996), which is one of the two median values.

The inorganic partition coefficients for barium partitioning in aragonite have not been studied as extensively. The coefficients that can be found in the literature range from 1.521 (Dietzel et al., 2004) to 2.817 (Gaetani and Cohen, 2006) with a median of 2.11 (Gaetani and Cohen, 2006) and a mean value of 2.149. For this study, the inorganic partition coefficient for barium in aragonite used is 2.11 (Gaetani and Cohen, 2006), which is the median value.

Manganese

Manganese-to-calcium ratios have not been well studied. Mn/Ca has been shown to have a seasonal effect in scallops that is not directly correlated with temperature (Freitas et al., 2006), as well as being an indicator of ambient Mn/Ca ratios and redox conditions in foraminfera (Glock et al., 2012). The three manganese ions of interest for this study are Mn^{2+}, Mn^{3+}, and Mn^{4+}, with the Mn^{3+} and Mn^{4+} ions being highly insoluble and Mn^{2+} being soluble in the absence of hydrogen sulfide, but only stable in environments with very low oxygen levels. This redox chemistry among the manganese ions may be the reason for use of manganese incorporation into calcium carbonate as a proxy for the redox properties of ambient seawater.

Manganese incorporation into inorganic calcium carbonate has not been studied extensively. The inorganic partition coefficients for Mn^{2+} partitioning in calcite that can be found in the literature range from 8.5 (Drake et al., 2012) to 30 (Elderfield et al., 1996) with a median of 14.8 (Drake et al., 2012) and a mean value of 17.7 (Dromgoole and Walter, 1990, Lorens, 1981, Lea et al., 1995). For this study, the inorganic partition coefficient for manganese into calcite used is 14.8 (Drake et al., 2012), which is the median value. An extensive search of the literature has failed to produce any inorganic partition coefficients for manganese in aragonite. The sensitivity of manganese to redox conditions, combined with a short oceanic residence time (~50 years, Sarmiento and Gruber, 2006), makes it very difficult to constrain the concentration of Mn^{2+} in seawater, and may lead to errors in these analyses.

Boron

The B/Ca paleo-pH proxy is a relatively new paleoproxy, and thus is very promising even though all of the complications of the proxy have not been constrained as of yet. There are two species of boron in the ocean that are incorporated into calcium carbonate; boric acid $B(OH)_3$ and borate ion $B(OH)_4^-$, with borate ion being taken up preferentially into calcium carbonate. The boron pH proxy is based on the speciation of boron in seawater, and therefore in calcium carbonate, being pH dependent (Hemming and Hanson, 1992, Klochko et al., 2009). B/Ca is shown to correlate well with the carbonate system in foraminifera (Rae et al., 2011, Yu and Elderfield, 1997, Foster 2008, Tripati et al., 2011, Yu et al., 2007) and coccolithophores (Stoll et al., 2012). B/Ca also seems to correlate with temperature in coral (Sinclair et al., 1998, Fallon et al., 1999) and growth rate in foraminifera (Ni et al., 2007).

Boron incorporation into inorganic calcium carbonate has been well studied. The inorganic partition coefficients for boron partitioning in calcite that can be found in the literature range from 0.00127 (the lowest value in the range found by He et al., 2013) to 2.0 (the highest value in the range found by Allen and Hönisch, 2012) with a median of 0.00213 and a mean value of 0.641 (Allen et al., 2011). For this study, the inorganic partition coefficient for boron in calcite used is 0.0017, which is the average of the values found in the He et al. (2013) study. These inorganic partition coefficients were calculated for an approximate pH range of 7.4 to 8.8 on the free hydrogen ion scale.

The inorganic partition coefficients for boron partitioning in aragonite are not well studied. There are two coefficients that can be found in the literature, 0.0016 (Allison et al., 2010) and 0.981 (Hemming et al., 1995). For this study, the inorganic partition coefficient for boron in aragonite used is 0.0016 (Allison et al., 2010).

Lithium

Lithium-to-calcium has been proposed as another temperature paleoproxy in foraminifera (Marriott et al., 2004a), coral (Marriott et al., 2004a), and brachiopods (Delaney et al., 1989), as well as in inorganic experiments (Marriott et al., 2004b). However. Li/Ca also correlates with salinity (Marriott et al., 2004b), silicate weathering (Hathorne and James, 2006), carbonate saturation state (Hall and Chan, 2004, Lear et al., 2010), and depth (Hall and Chan, 2004).

Lithium incorporation into inorganic calcite has been relatively well studied. The inorganic partition coefficients for lithium partitioning in calcite that can be found in the literature range from 0.00025 (Elderfield et al., 1996) to 3.82 (Marriott et al., 2004a) with a median of 0.0031 (Marriott et al., 2004a) and a mean value of 0.7656 (Dawber and Tripati, 2012,

Murray, 1991, Okumura and Kitano, 1986). For this study, the inorganic partition coefficient for lithium in calcite used is 0.00195, which is the average of the values found in the Marriott et al. (2004a) study. It should be noted that the 3.82 value is an outlier, and that the next highest inorganic partition coefficient for lithium incorporation in calcite is 0.0040 (Dawber and Tripati, 2012, Okumura and Kitano, 1986). An extensive search of the literature has failed to produce any inorganic partition coefficients for lithium in aragonite.

Cadmium

Cadmium-to-calcium ratios correlate well with phosphate and nutrient concentrations in foraminifera (Rosenthal et al., 1997, Patton et al., 2011, Rickaby and Elderfield, 1999, Marchitto and Broecker 2006, Mashiotta et al., 1997) and upwelling in coral (Matthews 2007). Since upwelling and nutrient concentrations in surface waters are contributory, this is good for the use of Cd/Ca as a nutrient paleoproxy. However, temperature (Rickaby and Elderfield, 1999) and depth (McCorkle et al., 1995, Matthews 2007) have also been shown to have an affect on the Cd/Ca composition of foraminiferal calcite. Cadmium behaves as a nutrient in the ocean (Cossa et al., 1992, Bruland et al., 1985), resulting in it having a short residence time in the ocean. Since cadmium has a short residence time, its concentration at the time of calcification is very hard to constrain and may result in an error when a Rayleigh model is applied to cadmium incorporation in calcification.

Cadmium incorporation into inorganic calcium carbonate has not been well studied. The inorganic partition coefficients for cadmium partitioning in calcite that can be found in the literature range from 7.0 (Elderfield et al., 1996) to 110.0 (Curti, 1999) with a median of 27.85 (Curti, 1999) and a mean value of 43.18 (Ólafsson, 1983, Lorens, 1981, Tesoriero and Pankow,

1996, Davis et al., 1987). For this study, the inorganic partition coefficient for cadmium in calcite used is 41.0 (Curti, 1999), which is one of the two median values. An extensive search of the literature has failed to produce any inorganic partition coefficients for cadmium in aragonite.

Uranium

Uranium-to-calcium ratios have been studied as a temperature paleoproxy in coral (Cardinal et al., 2001, Min et al., 1995, Shen and Dunbar, 1995) and foraminifera (Yu et al., 2008, Russell et al., 2004). Uranium is generally incorporated into calcium carbonate by interactions with uranyl (UO_2^{2+}) in the seawater. U/Ca ratios show a seasonal effect that is not well correlated with temperature in corals (Sinclair et al., 1998), are impacted by the redox chemistry of the local environment in which calcification occurs in foraminifera (Boiteau et al., 2012), and correlate with the growth rate of foraminifera (Ni et al., 2007).

Uranium incorporation into inorganic calcium carbonate has been studied. The inorganic partition coefficients for uranium partitioning in calcite that can be found in the literature range from 0.046 (Elderfield et al., 1996) to 0.20 (Meece and Benninger, 1993) with a median of 0.046 (Meece and Benninger, 1993) and a mean value of 0.09733 (Russell et al., 1994). For this study, the inorganic partition coefficient for uranium in calcite used is 0.123, which is the average of the values found in the Meece and Benninger (1993) study.

The inorganic partition coefficients for uranium partitioning in aragonite are not well studied. Meece and Benninger (1993) reported finding a range of coefficients between 1.8 and 9.8. For this study, the inorganic partition coefficient for uranium in aragonite used is 5.8, which is the average of the values found in the Meece and Benninger (1993) study.

The fact that many of these element-to-calcium ratios seem to correlate with several hydrographic parameters can pose challenges to proxy development. A potential approach to circumvent some of these issues includes using a combination of culture- and field-based calibrations. Careful culturing techniques can provide constraints on the physical, chemical, and biological processes that impact the incorporation of these elements into biogenic calcium carbonate. The patterns of elemental incorporation produced in a controlled laboratory setting can then be applied to the patterns found from field-based research.

Variations between calcium carbonate polymorphs

Calcium carbonate has at least eight polymorphs; here we are concerned with calcite and aragonite, which are the two most common biominerals. Calcite has a trigonal or hexagonal (rhombohedral) crystal structure, while aragonite forms an orthorhombic crystal structure (Nesse, 2004). Calcite is much more stable than aragonite, having a higher saturation state in seawater.

Inorganic calcite and aragonite also differ in how elements are incorporated into their lattices. Calcite tends to take up manganese and cadmium preferentially, while discriminating against strontium, magnesium, barium, boron, lithium and uranium. Aragonite tends to take up strontium, barium and uranium preferentially, while discriminating against magnesium and boron. Since aragonite and calcite behave differently in respect to these elements due to their crystal structure, it is logical that organisms that produce calcite may have different element incorporation behavior than organisms that produce aragonite.

Vital effects and biology

As discussed above, the use of element-to-calcium ratios as proxies can be complicated by assumptions about the systematics governing calcification. When there is a variation in a dataset that is not known or understood it is often called a 'vital effect'. Vital effects may be caused by biological alteration of the calcification environment, such as an organism using an enclosed reservoir in which calcification is precipitated, or by having active biological processes like proton pumping that changes the chemical composition of calcifying fluids. As a result, the chemistry of this reservoir may be biologically altered, there may be elemental fractionation in the pathway to come from the exterior seawater to the interior calcification reservoir, thus the reservoir may not be at equilibrium with the outside seawater. Any of these biologically mediated alterations of the calcification environment will produce disequilibrium X/Ca ratios in calcium carbonate produced by an organism and potentially compromise the use of a particular measurement as a paleoceanographic proxy.

An example to illustrate this effect involves coccolithophores. These organisms alter the pH of the vesicle where they produce their calcite coccoliths (Buitenhuis et al., 1999, Iglesias-Rodriguez et al., 2002, Rickaby et al., 2010, Leonardos et al., 2009). Since calcification occurs in the coccolith vesicle, any elemental or isotopic pH proxy will record the pH of the coccolith vesicle and not the pH of the ambient environment. This creates a problem for proxy-based reconstructions. A solution is to use a species-specific calibration that takes into account how a certain species alters the chemistry at the site of calcification, however these calibrations are less accurate than if the organism did not alter the pH at the site of calcification. The use of an enclosed calcification reservoir that may not be at equilibrium with the external environment is another factor that needs to be considered when developing a process-based understanding of

elemental partitioning into biogenic carbonates; it has been hypothesized that in some cases, elemental ratios may be explained by Rayleigh fractionation (Elderfield et al., 1996, Gagnon et al., 2007).

Previous work using Rayleigh-type models to study calcification and paleo-proxies

Rayleigh fractionation was first developed to understand the chemistry of a liquid/gas mixture over time within an enclosed space. Later, Rayleigh fractionation was used to understand the trace element composition of minerals produced in melts that occurred in closed systems (Rayleigh, 1902, Shaw, 2006, Albarède, 2003). A closed system, in this context, is created when a body of fluid is separated from its parent fluid, and kept isolated from that fluid while a solid is precipitated from the fluid. The concept of Rayleigh fractionation, as understood in petrology, is based on the premise that as a mineral crystallizes out of a melt, while remaining out of chemical contact with the parent fluid, that preferentially incorporates (or discriminates against) an element, the composition of the melt will evolve over time. The elemental composition of the mineral produced will vary as a function of the percentage of melt remaining due to a distillation effect.

The same concept can be used to understand the precipitation of calcium carbonate within an enclosed calcification reservoir that is not in communication with the external seawater (Elderfield et al., 1996, Dawber and Tripati, 2012, Gaetani and Cohen, 2006, Gaetani et al., 2011, Gagnon et al., 2007). In the case of calcification, it is the concentration of calcium remaining in the reservoir, instead of the amount of liquid melt remaining, when the solid is precipitated or removed from the reservoir.

Elderfield et al. (1996) uses a Rayleigh fractionation model to look at calcification in benthic foraminifera. This study looks at the Sr/Ca, Ba/Ca, and Cd/Ca compositions of core top and live-captured foraminifera of the species *Amphisorus hemprichii*, *Amphistegina lobifera*, *Uvigerina spp.*, *Cibicidoides wuellerstorf*, and *Hoeglundina elegans*. The inorganic partition coefficients (α) used in that study are $\alpha_{Sr} = 0.044$ (compared to the $\alpha_{Sr} = 0.120$ from Gabitov and

Watson, 2006 that is used in this thesis), $\alpha_{Ba} = 0.08$ (which is the value used in this thesis), and $\alpha_{Cd} = 7.0$ (compared to the $\alpha_{Cd} = 41.0$ from Curti, 1999 that is used in this thesis). Elderfield et al. (1996) conclude that a Rayleigh model can be used to calculate the fraction of calcium remaining in the calcification reservoir (F values), and that these F values can be used to draw conclusions about the size of the calcification reservoir and the speed of calcification in foraminifera.

Dawber and Tripati (2012) also use a Rayleigh model to look at the elemental compositions of the calcium carbonate produced by benthic foraminifera. The study analyzes Sr/Ca, Mg/Ca, B/Ca, and Li/Ca in core top samples of *Oridorsalis umbonatus*. The inorganic partition coefficients (α) used in the study are $\alpha_{Sr} = 0.04$ (the same value used by Elderfield et al., 1996, but different from the value used in this thesis: $\alpha_{Sr} = 0.120$ from Gabitov and Watson, 2006), $\alpha_{Mg} = 0.0573$ (from Katz, 1973, but different from the value used in this thesis: $\alpha_{Mg} = 0.019$ from Freitas et al., 2006), $\alpha_{B} = 0.38$ (from Hemming et al., 1995, compared to the $\alpha_{B} = 0.0017$ from He et al., 2013 that is used in this thesis), and $\alpha_{Li} = 0.004$ (compared to the $\alpha_{Li} = 0.00195$ from Marriott et al., 2004a that is used in this thesis). Dawber and Tripati (2012) concluded that the fraction of calcium remaining in the calcification reservoir is a function of the carbonate saturation state in which the organisms are grown.

Two other studies performed by Gagnon et al. (2007) and Gaetani and Cohen (2006) look at the validity of applying a Rayleigh fractionation model to corals. Gagnon et al. (2007) looks at Sr/Ca and Mg/Ca in the scleractinian deep-sea coral *Desmophyllum dianthus* and concludes that there is an internal calcification reservoir in *D. dianthus* that produces a Rayleigh fractionation-effect in the elemental composition of most of the skeleton (although not in the central band of the coral skeleton). Gaetani and Cohen (2006) examines Sr/Ca, Mg/Ca, and

Ba/Ca in a brain coral, *Diploria labyrinthiformis,* from Bermuda, and concludes that a Rayleigh fractionation is occurring during calcification in *D. labyrinthiformis*.

Approach taken in this work

This study examines whether the use of a Rayleigh fractionation model can provide insights into the calcification process in a range of marine organisms. This work is novel because it examines an extensive array of macroinvertebrates that have never been studied in this context before. A geochemical model is used to draw conclusions about the biochemical transport and storage processes occurring within organisms during calcification, as well as examining how these biochemical processes can change the elemental composition of calcium carbonate precipitated by the organism from the surrounding environment. As mentioned in the section concerned with the organisms studied in this research, many calcifying organisms are known to use an enclosed space (often called the calcification reservoir or the site of calcification) from which the elements that form the calcium carbonate are taken. Just as with melts that incorporate elements, the elemental composition of the calcium carbonate produced from an enclosed reservoir will be different than if it were precipitated inorganically in well-mixed ambient seawater. Vital effects in elemental-based proxies are not well understood, but may in part be explained by such a process.

Methods

Experimental conditions

Eighteen marine invertebrates were cultured by Justin Ries at Woods Hole Oceanographic Institute in a sixty day experiment in 25°C, 32ppt seawater with varying pCO_2 levels (Ries et al., 2009, Ries, 2011). There were four pCO_2 treatments representing modern (400 ppm) and future elevated (600 ppm, 900 ppm, 2850 ppm) carbon dioxide ocean conditions. The calcitic organisms cultured include bay scallop, blue crab, lobster, purple urchin, pencil urchin, coralline red algae, oyster, shrimp, blue mussel and periwinkle. The aragonitic organisms cultured include limpet, halimeda, hard clam, soft clam, conch and temperate coral. Serpulid worm and whelk produce a mixture of calcite and aragonite, and were also cultured. It should be noted that, although these organisms can be found in 25°C, 32ppt conditions, some of the organisms may have experienced temperature and salinity stress which would impact their biogeochemical processes. Another caveat to note is that, although every effort was made to collect only newly formed calcification, some of the old calcification material may have been included in these analyses due to the difficulty of separating the new from the old. A detailed synopsis of these organisms and their properties can be found in Tables 1 and 2.

Analytical methods

After the sixty-day experiment was completed, Aradhna Tripati and Robert Eagle analyzed the elemental compositions of the calcium carbonate skeletons of the organisms. Samples comprising 200 to 1000 micrograms of calcium carbonate were cleaned in a dilute alkali-buffered solution of hydrogen peroxide to remove organic matter in accordance with the oxidative cleaning protocol of Barker et al. (2003). Cleaned samples were dissolved in quartz-

distilled 0.075 M nitric acid; samples were centrifuged after complete digestion, and the supernatant was removed. This solution was then analyzed on a Varian Vista inductively-coupled plasma optical emission spectrophotometer (ICP-OES) to determine calcium concentrations, Mg/Ca, and Sr/Ca ratios using matrix-matched intensity ratios (de Villiers et al., 2003). We routinely achieved analytical accuracy and precision on the X/Ca ratioscomparable to those reported by de Villiers et al. (2003). Typical reproducibility of our method based on replicate samples and standards is better than 3% for Mg/Ca and Sr/Ca (% relative standard deviation). Samples were then diluted to 100 ppm calcium concentrations, and more precise X/Ca ratios were determined from matrix-matched intensity ratios (Yu et al., 2005) on a Perkin-Elmer Elan DRC II quadrupole inductively coupled plasma mass spectrometer (ICP-MS). We routinely achieved analytical accuracy and precision on the X/Ca ratios comparable to those reported by Yu et al., (2005). Typical reproducibility of our method based on replicate samples and standards is better than 3% for Ba/Ca, Mn/Ca, Cd/Ca, and U/Ca, 1.6% for Mg/Ca, B/Ca and Li/Ca, and better than 0.7% for Sr/Ca (% relative standard deviation).

A brief overview of the data taken from the literature

The data taken from the literature for this research include three studies on foraminifera (Allen et al., 2011, Lea et al., 1999, Yu et al., 2007) and one study on coccolithophores (Stoll et al., 2012). Allen et al., 2011 cultured live foraminifera (species *Orbulina universa*) that were collected in the North Pacific Ocean near the Wrigley Institute for Environmental Studies on Santa Catalina Island in California; these cultured foraminifera were exposed to varying levels of pH and their boron-to-calcium ratios were analyzed. Yu et al., 2007 collected two different species of foraminifera (*Globigerina bulloides* and *Globorotalia inflata*)

from sediment cores of various depths, ages, conditions and locations (ranging in location from the North Atlantic to the South Atlantic to the South Pacific); boron-to-calcium ratios were analyzed in these foraminifera. Lea et al., 1999 cultured live foraminifera (species *Globigerina bulloides* and *Orbulina universa*) that were collected in the North Pacific Ocean near the Wrigley Institute for Environmental Studies on Santa Catalina Island in California; these cultured foraminifera were exposed to varying temperature, pH, and salinity conditions and the magnesium- and strontium-to-calcium ratios were analyzed. Stoll et al., 2012 cultured four different strains of two different species of coccolithophores (species *Coccolithus braarudii* strain AC 400 and *Emiliania huxleyi* strains RCC 1256, RCC 1212, and RCC 1238) that were bought from an algal culturing facility; pH levels were varied, two of the strains were cultured at 17°C and two were cultured at 20°C, and boron-to-calcium ratios were measured.

Rayleigh model

Below is a mathematical description of the Rayleigh fractionation model along with an explanation of the equations that are used in this study. The original Rayleigh distillation equation for trace element incorporation in melts is expressed:

$$C_{RES} = C_O F^{\alpha-1}$$

where C_{RES} is the concentration of the element in the reservoir at the time of crystallization, C_O is the initial concentration of the trace element in the melt, F is the fraction of melt remaining in the liquid state, and α is the partition coefficient for the element into the mineral phase (Albarède, 2003).

This Rayleigh distillation equation was converted by Elderfield et al., (1996) to be relevant to element incorporation during biomineralization within the calcification reservoir. Elderfield et al., (1996) defined the ratio of the X/Ca ratio of the calcium carbonate to the X/Ca ratio of the ambient seawater as the empirical partition coefficient (D):

$$D = \frac{\frac{X}{Ca_{CaCO3}}}{\frac{X}{Ca_{SW}}}$$

where $(X/Ca)_{CaCO3}$ is the element-to-calcium ratio of the calcium carbonate produced by the organism, $(X/Ca)_{SW}$ is the element-to-calcium ratio of ambient seawater, and D is the empirical partition coefficient. For this study, the mean ocean concentrations reported by Millero et al., 2008 were used to calculate D-values of Sr/Ca and Mg/Ca. Mean ocean concentrations from Broecker and Peng, 1982 were used to calculate D-values of Ba/Ca, Mn/Ca, B/Ca, Li/Ca, Cd/Ca, and U/Ca. D can also be defined in terms of the fraction of calcium remaining in the calcification reservoir at the time of biomineralization using an inorganic partition coefficient (α):

$$D = \frac{1 - F^{\propto}}{1 - F}$$

where D is the empirical partition coefficient defined above, α is the inorganic partition coefficient for element X into the polymorph of calcium carbonate being produced, and F is the fraction of calcium remaining in the calcification reservoir. The inorganic partition coefficient (α) is the measure of how easily a particular element is incorporated into the polymorph of calcium carbonate being observed in inorganic experiments. This coefficient is dependent on temperature, and varies across inorganic precipitation experiments. The X/Ca ratio of ambient seawater at present is known for most of the elements discussed here; the Mn/Ca and Cd/Ca ratios of the ocean are very difficult to constrain and are discussed below. The X/Ca ratio of the

calcium carbonate is experimentally determined by mass spectrometry, as discussed in the analytical methods section. F can be calculated using this equation as long as D and α are known.

Table 5: ***A compilation of mean ocean element concentrations with associated references used to calculate the empirical partition coefficient (D) values presented in this research.***

Element [a]	Mean Ocean Concentration (µmol/kg) [b]	Reference [c]
Calcium	1.03*10^4	Broecker and Peng, 1982
Calcium	1.02821*10^4	Millero et al., 2008
Strontium	90.7	Millero et al., 2008
Magnesium	5.28171*10^4	Millero et al., 2008
Barium	0.10	Broecker and Peng, 1982
Manganese	5*10^-3	Broecker and Peng, 1982
Boron	4.2*10^2	Broecker and Peng, 1982
Lithium	25	Broecker and Peng, 1982
Cadmium	7*10^-4	Broecker and Peng, 1982
Uranium	1.3*10^-2	Broecker and Peng, 1982

[a] Element of interest.
[b] Value of mean oceanic concentration for that element.
[c] Literature source from which this value was obtained.

Table 6*: The X/Ca ratios calculated from the mean ocean element concentrations presented in Table 5.*

Element-to-Calcium [a]	X/Ca ratio [b]	Reference [c]
Sr/Ca	0.00882	Millero et al., 2008
Mg/Ca	5.14	Millero et al., 2008
Ba/Ca	9.7E-06	Broecker and Peng, 1982
Mn/Ca	4.85E-07	Broecker and Peng, 1982
B/Ca	0.041	Broecker and Peng, 1982
Li/Ca	0.0024	Broecker and Peng, 1982
Cd/Ca	7E-08	Broecker and Peng, 1982
U/Ca	1.3E-06	Broecker and Peng, 1982

[a] Element-to-calcium ratio of interest.
[b] Calculated mean oceanic X/Ca ratio.
[c] Literature source from which the values for this calculation were obtained.

Table 7: ***A compilation of the inorganic partition coefficients for X/Ca ratios in both aragonite and calcite.***

X/Ca [a]	Inorganic Partition Coefficient (α) [b]	Reference [c]	Notes [d]
Calcite			
Sr/Ca	0.12	Gabitov and Watson, 2006	
Mg/Ca	0.019	Freitas et al., 2006	from Oomori et al., 1987
Ba/Ca	0.08	Elderfield et al., 1996	from Boyle et al., 1995
Mn/Ca	14.8	Drake et al., 2012	from Lorens, 1981
B/Ca	0.0017	He et al., 2013	average value
Li/Ca	0.00195	Marriott et al., 2004a	average value
Cd/Ca	41	Curti, 1999	from Tesoriero and Pankow, 1996
U/Ca	0.123	Meece and Benninger, 1993	average value
Aragonite			
Sr/Ca	1.193	Dietzel et al., 2004	
Mg/Ca	0.001027	Gaetani and Cohen, 2006	
Ba/Ca	2.11	Gaetani and Cohen, 2006	
B/Ca	0.0016	Allison et al., 2010	
U/Ca	5.8	Meece and Benninger, 1993	average value

[a] Element-to-calcium ratio.
[b] Value of the inorganic partition coefficient used in this study.
[c] Literature source from which this value was obtained.
[d] Notes about the value.

A thorough search of the literature produced many different inorganic partition coefficients; generally the median value closest to the mean of all the coefficients found in the literature was chosen. These values were determined experimentally by observing the partitioning behavior of calcite and aragonite that was precipitated inorganically. It should be noted that when an inorganic partition coefficient is greater than 1, that the element is taken up preferentially into the mineral, whereas an inorganic partition coefficient of less than 1 indicates that the mineral discriminates against that element relative to calcium.

Table 8: ***A list of the highest and lowest values recorded for the partitioning of each element into calcite and aragonite with their associated sources.***

X/Ca	Inorganic Partitioning Coefficient (α)	Reference	Notes
Calcite			
Sr/Ca	0.02	Nehrke et al., 2007	
	0.35	Gabitov and Watson, 2006	
Mg/Ca	0.0123	Freitas et al., 2006	from Mucci and Morse, 1983
	0.097	Drake et al., 2012	from Katz et al., 1973
Ba/Ca	0.015	Curti, 1999	from Tesoriero and Pankow, 1996
	0.1	Gillikin et al., 2006	
Mn/Ca	8.5	Drake et al., 2012	from Dromgoole and Walter, 1990
	30	Elderfield et al., 1996	from Lea et al., 1995
B/Ca	0.00127	He et al., 2013	lowest value found
	2.0	Allen and Hönisch, 2012	highest value found
Li/Ca	0.00025	Elderfield et al., 1996	from Murray, 1991
	3.82	Marriott et al., 2004a	
Cd/Ca	7	Elderfield et al., 1996	from Ólafsson, 1983
	110	Curti, 1999	from Davis et al., 1987
U/Ca	0.046	Elderfield et al., 1996	from Russell et al., 1994
	0.2	Meece and Benninger, 1993	
Aragonite			
Sr/Ca	1.133	Gaetani and Cohen, 2006	
	1.24	Gagnon et al., 2007	
Mg/Ca	0.000275	Gagnon et al., 2007	
	0.00133	Gaetani and Cohen, 2006	
Ba/Ca	1.521	Dietzel et al., 2004	
	2.817	Gaetani and Cohen, 2006	
B/Ca	0.0016	Allison et al., 2010	
	0.981	Hemming et al., 1995	
U/Ca	1.8	Meece and Benninger, 1993	
	9.8	Meece and Benninger, 1993	

[a] Element-to-calcium ratio.
[b] Value of the inorganic partition coefficient used in this study.
[c] Literature source from which this value was obtained.
[d] Notes about the value.

This table shows the highest and lowest values found in a search of the literature; the inorganic partition coefficients are better defined for some elements than for others, and there can be a large amount of variation between studies. For instance, for strontium incorporation into

aragonite, the outlying values are 1.133 and 1.24, which are quite similar. In contrast, lithium incorporation into calcite has outlying coefficients of 0.00025 and 3.82 reported in the literature. This variation can create errors in the calculations presented in this thesis. See Table 41 in the Appendix for a complete list of the inorganic partition coefficients found in the literature.

Caveats of the Rayleigh model

There are several potential problems with the Rayleigh model presented in this study. For a Rayleigh model to be applied to the calcification system of an organism, calcification must occur in an enclosed space that is separated from ambient seawater. Many of the organisms studied here are known to calcify within an enclosed reservoir. It is very probable that most marine calcification occurs within an enclosed reservoir, however further experimentation is needed for several of these organisms. If an organism calcifies within a space that is not completely closed, a Rayleigh model is not applicable.

There could be a major error in the cadmium and manganese empirical partition coefficient calculations because the concentrations of Cd and Mn in the ambient seawater in which these organisms were grown are not known. The mean concentrations of elements in the ocean are used to calculate the empirical partition coefficient (D) values in the Rayleigh model presented in this research. Cadmium is a nutrient with a short residence time in the ocean. Manganese also has a short residence time in the ocean; in addition the concentration of Mn^{2+} is highly dependent on the ambient redox conditions and can vary greatly over space and time. Therefore, the concentrations of both cadmium and manganese are very hard to constrain for the seawater in which the organisms were grown, and may result in an error in the empirical partition coefficient calculations within the framework of a Rayleigh model.

As shown in the Results section below, there are a few problems with the F-values calculated by the Rayleigh model. Both impossibly high and impossibly low F-values are reported. An F-value greater than 1 is impossible since there can never be more than 100% calcium remaining in the calcification reservoir. An F-value that is less than ~10^-2 is impossibly low since it is unlikely that calcification would continue to proceed when so little

calcium is present in the calcification reservoir. There is also no correlation between F-values calculated from different elements for the same organism. When the F-values calculated from each element do not agree within the same organism, there is either a major problem with the inorganic partition coefficient being used, or a problem with the use of a Rayleigh model for that organism. The implications of these problems are presented in the discussion section below.

Results

Elemental patterns of incorporation into calcite and aragonite:

Macroinvertebrates from Ries et al. (2009) study

In Figure 1, blue markers represent organisms that precipitate calcite, and purple markers represent organisms that precipitate aragonite. Presenting plots of empirical partition coefficient (D) versus the fraction of calcium remaining after calcification (F) for each element and every organism would have taken too much space and would have been highly repetitive; therefore, following are a selection of one calcitic and one aragonitic (when possible) organism for the partitioning of each element, and tables of the calculations from all of the organisms studied can be found in Figures 11-18 in the Appendix. A representative set of figures is shown to span the range of taxa and show the types of elemental partitioning observed. There are no plots of aragonitic organisms for manganese, lithium, or cadmium because I was unable to find inorganic partition coefficients for these elements into aragonite in the literature, and without that coefficient, F cannot be calculated. There are no plots of calcitic organisms for boron because the empirical partition coefficients produced in all of the calcitic samples resulted in unreal numbers when calculating the value of F. Although the trends shown in the plots that are presented below are uniform through all calcitic and aragonitic organisms respectively, the values of both the empirical partition coefficient (D) and the fraction of calcium remaining in the calcification reservoir (F) vary between elements within the same organism, as well as between organisms with respect to the same element. The following calculations are representative of the trends seen in all of the organisms, although not the numerical ranges.

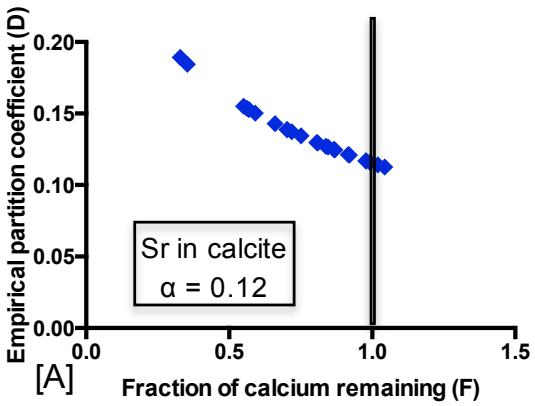
Empirical partition coefficient (D)
0.20
0.15
0.10
0.05
0.00
0.0
0.5
1.0
1.5
Sr in calcite
α = 0.12
[A]
Fraction of calcium remaining (F)

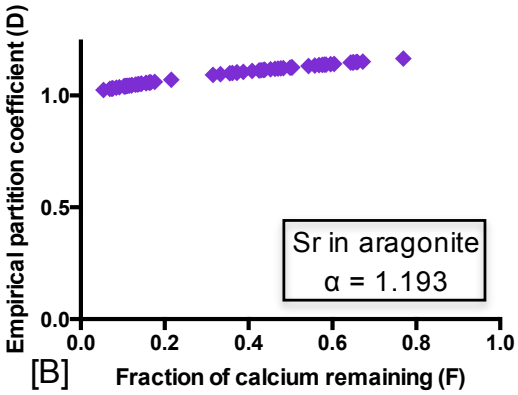
Empirical partition coefficient (D)
1.0
0.5
0.0
0.0
0.2
0.4
0.6
0.8
1.0
Sr in aragonite
α = 1.193
[B]
Fraction of calcium remaining (F)

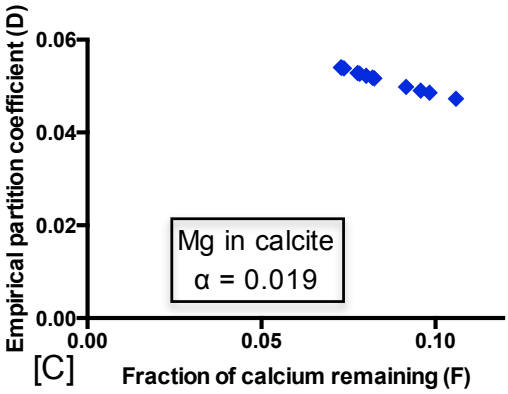
Empirical partition coefficient (D)
0.06
0.04
0.02
0.00
0.00
0.05
0.10
Mg in calcite
α = 0.019
[C]
Fraction of calcium remaining (F)

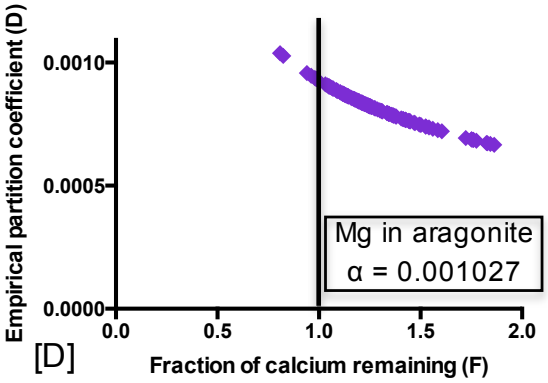
Empirical partition coefficient (D)
0.0010
0.0005
0.0000
0.0
0.5
1.0
1.5
2.0
Mg in aragonite
α = 0.001027
[D]
Fraction of calcium remaining (F)

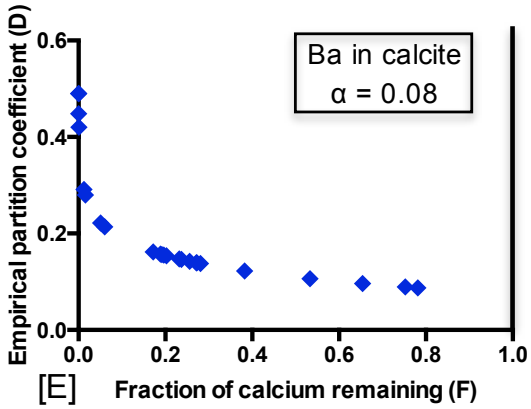
Empirical partition coefficient (D)
0.6
0.4
0.2
0.0
0.0
0.2
0.4
0.6
0.8
1.0
Ba in calcite
α = 0.08
[E]
Fraction of calcium remaining (F)

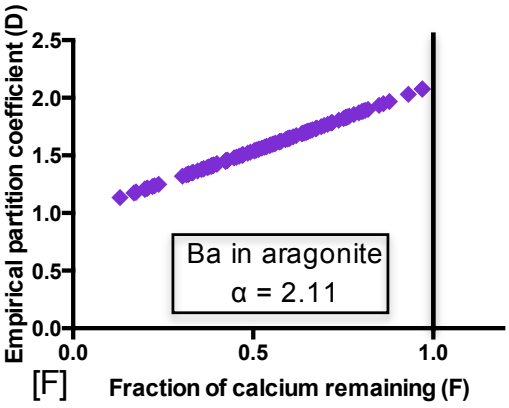
Empirical partition coefficient (D)
2.5
2.0
1.5
1.0
0.5
0.0
0.0
0.5
1.0
Ba in aragonite
α = 2.11
[F]
Fraction of calcium remaining (F)

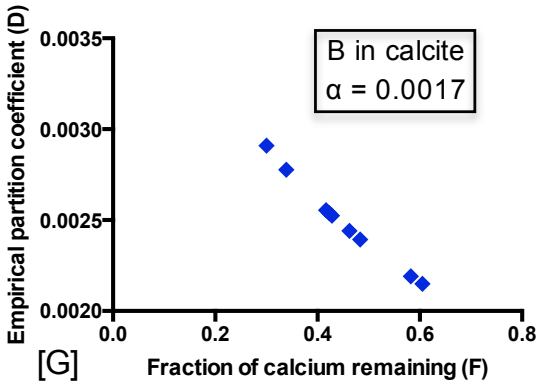
Empirical partition coefficient (D)
0.0035
0.0030
0.0025
0.0020
0.0
0.2
0.4
0.6
0.8
B in calcite
α = 0.0017
[G]
Fraction of calcium remaining (F)

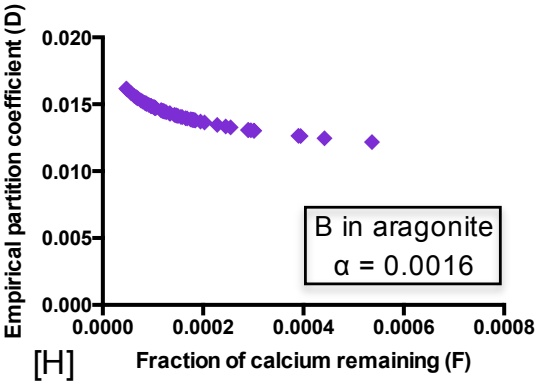
Empirical partition coefficient (D)
0.020
0.015
0.010
0.005
0.000
0.0000
0.0002
0.0004
0.0006
0.0008
B in aragonite
α = 0.0016
[H]
Fraction of calcium remaining (F)

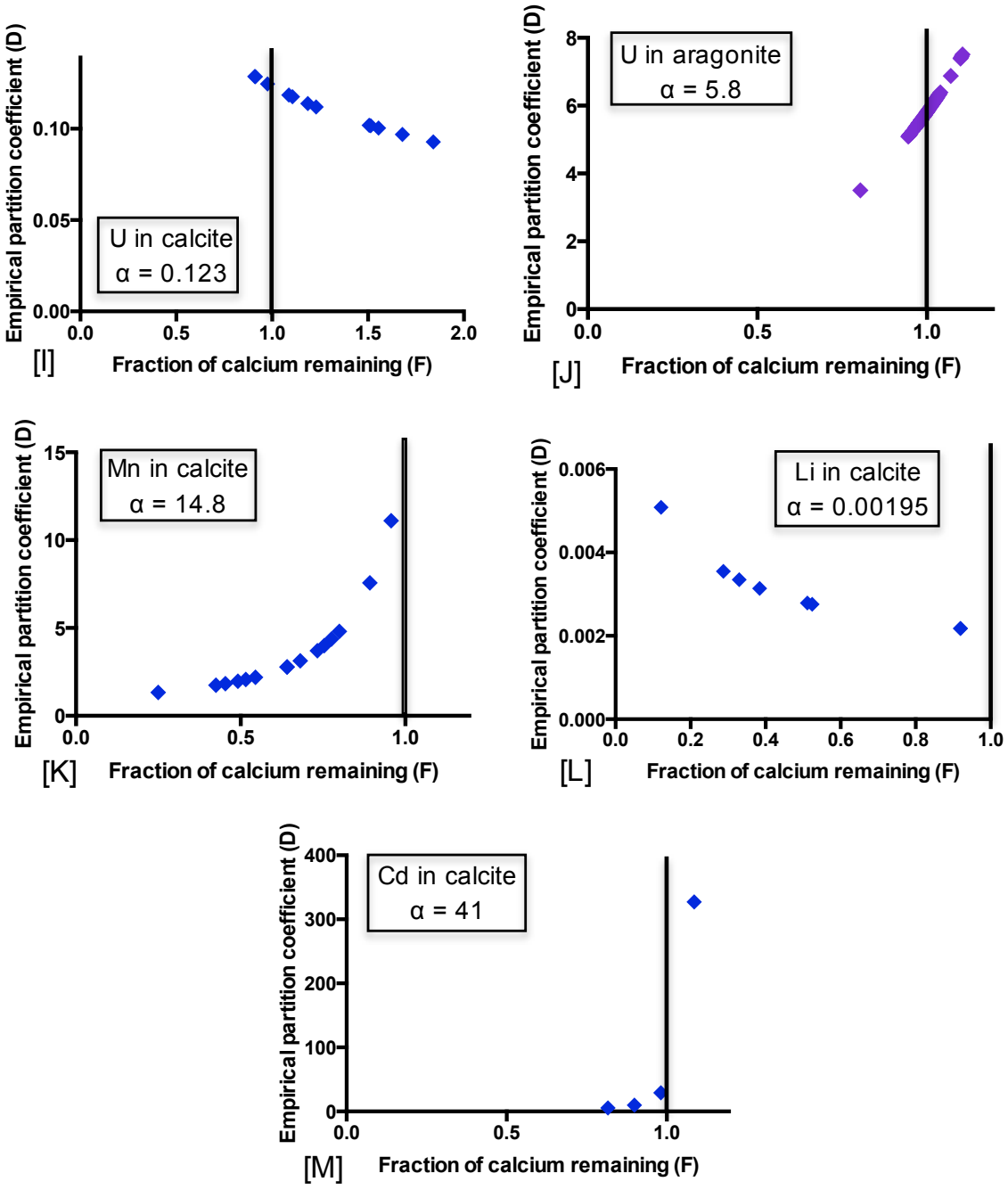

Figure 1: ***Calculations based on strontium, magnesium, barium, manganese, boron, lithium, cadmium and uranium incorporation in calcitic and aragonitic marine invertebrates.*** Presented here are calculations of the empirical partition coefficient (D) (y-axis) versus the fraction of calcium remaining in the calcification reservoir after calcification (F) (x-axis). These calculations represent data for [A] strontium incorporation in the calcitic periwinkle *Littorina littorea*, [B] strontium incorporation in the aragonitic coral *Oculina arbuscula*, [C] magnesium incorporation in the calcitic coralline red algae *Neogoniolithon* sp., [D] magnesium incorporation in the aragonitic coral *Oculina arbuscula*, [E] barium incorporation in the calcitic periwinkle *Littorina littorea*, [F] barium incorporation in the aragonitic coral *Oculina arbuscula*, [G] boron

incorporation in the calcitic oyster *Crassostrea virginica,* [H] boron incorporation in the aragonitic coral *Oculina arbuscula*, [I] uranium incorporation in the calcitic coralline red algae *Neogoniolithon* sp., and [J] uranium incorporation in the aragonitic coral *Oculina arbuscula,* [K] manganese incorporation in the calcitic purple urchin *Arbacia punctulata*, [L] lithium incorporation in the calcitic blue mussel *Mytilus edulis*, and [M] cadmium incorporation in the calcitic bay scallop *Argopecten irradians*. There are vertical black lines where F=1; any data to the right of the line is impossible since F cannot exceed a value of 1; this phenomenon will be discussed in detail both later in the results section as well as in the discussion section.

Strontium incorporation in macroinvertebrates

The plotting of empirical partition coefficient (D) versus the fraction of calcium remaining in the calcification reservoir (F) for the incorporation of strontium into calcite [Figure 1a] produces a gradual negative slope that is slightly curved. The plotting of D versus F for the incorporation of strontium into aragonite [Figure 1b] produces a gradual positive and exponential curve. These two organisms were chosen to represent the general trend created by the Rayleigh model for strontium incorporation during calcification; see Figure 11 in the appendix for the calculations for all of the organisms studied.

Magnesium incorporation in macroinvertebrates

The plotting of D versus F for both the incorporation of magnesium into calcite [Figure 1c] and aragonite [Figure 1d] produce a gradual negative exponential trend. These two organisms were chosen to represent the general trend created by the Rayleigh model for magnesium incorporation during calcification; see Figure 12 in the appendix for the calculations for all of the organisms studied.

Barium incorporation in macroinvertebrates

The plotting of D versus F for the incorporation of barium into calcite [Figure 1e] produces a negative curve. The plotting of D versus F for the incorporation of barium into aragonite [Figure 1f] produces a positive linear trend. These two organisms were chosen to represent the general trend created by the Rayleigh model for barium incorporation during calcification; see Figure 13 in the appendix for the calculations for all of the organisms studied.

Manganese incorporation in macroinvertebrates

The plotting of D versus F for the incorporation of manganese into calcite [Figure 1k] produces a steep positive trend that is slightly curved. The purple urchin was chosen to represent the general trend created by the Rayleigh model for manganese incorporation in calcite during calcification; see Figure 14 in the appendix for the calculations for all of the calcitic organisms studied.

Boron incorporation in macroinvertebrates

The plotting of D versus F for the incorporation of boron into calcite [Figure 1g] produces a negative linear trend. The plotting of D versus F for the incorporation of boron into aragonite [Figure 1h] produces a slightly curved negative trend. These two organisms were chosen to represent the general trend created by the Rayleigh model for boron incorporation during calcification; see Figure 15 in the appendix for the calculations for all of the organisms studied.

Lithium incorporation in macroinvertebrates

The plotting of empirical partition coefficient (D) versus the fraction of calcium remaining in the calcification reservoir after biomineralization has ended (F) for the incorporation of lithium into calcite [Figure 1l] produces a curved trend with a negative slope. The blue mussel was chosen to represent the general trend created by the Rayleigh model for lithium incorporation in calcite during calcification; see Figure 16 in the appendix for the calculations for all of the calcitic organisms studied.

Cadmium incorporation in macroinvertebrates

The plotting of D versus F for the incorporation of cadmium into calcite [Figure 1m] produces a steep, positive exponential curve. The bay scallop was chosen to represent the general trend created by the Rayleigh model for cadmium incorporation in calcite during calcification; see Figure 17 in the appendix for the calculations for all of the calcitic organisms studied.

Uranium incorporation in macroinvertebrates

The plotting of D versus F for the incorporation of uranium into calcite [Figure 1i] produces a gradual negative exponential curve. The plotting of D versus F for the incorporation of uranium into aragonite [Figure 1j] produces a positive linear trend. These two organisms were chosen to represent the general trend created by the Rayleigh model for uranium incorporation during calcification; see Figure 18 in the appendix for the calculations for all of the organisms studied.

In a few of the figures presented above (Figure 1k: Mn in calcite, Figure 1h: B in aragonite, and Figure 1j: U in aragonite), some of the values that are calculated for F are larger than 1, which is physically impossible since there can never be more than 100% calcium remaining (F=1). It may be worth examining if these high F-values are being caused by more calcium being brought into the calcification reservoir as calcification proceeds, thereby bringing more calcium into the reservoir than was there as the biomineralization process began. This would indicate that the organism has a relatively open calcification reservoir with a relatively short flushing time. Since the Rayleigh model presumes a closed calcification reservoir, this would be detrimental to the use of the model in this context. It has been pretty well demonstrated that most organisms have a closed calcification reservoir (Borowitzka and Larkum, 1977, Rollion-Bard and Erez, 2010, de Nooijer et al., 2009, Erez et al., 2008, Erez, 2003, Bentov et al., 2009, Young and Henriksen, 2003, Paasche, 2002). Therefore, this result should not be taken as an indication that the calcification reservoir of an organism is open if a large F value is calculated; rather compare the F values in between organisms to compare the openness of the organisms' calcification systems (as can be seen in the section 'Groupings of organisms in the same phylum with respect to Rayleigh model' below).

In the calculation for cadmium incorporation in calcite (Figure 1m) the value calculated for F is incredibly small, indicative of the organisms using nearly all of the calcium in their reservoir during calcification. If an organism actually consumed so much calcium within their calcification reservoir it raises the issue of how they were able to maintain the saturation state of calcium carbonate at a high enough level to allow calcification to continue. This, therefore, presents an issue for the model results that produce a very small F value, and may indicate a problem with the inorganic partition coefficient used in the calculation. Another possibility is

that the cadmium concentrations of the water in which the organisms were grown was dissimilar from the estimated mean ocean cadmium concentrations, and this error occurred in the calculation of the empirical partition coefficient (D).

See Table 16 in the Discussion section for a synopsis of these results. See Tables 18 through 31 in the Appendix for the tabulated data on which these calculations are based, along with the statistical analysis of this data.

Foraminifera and Coccolithophores from various studies

The calculations and plots presented in this thesis on the calcification of foraminifera and coccolithophores are based on data from the Allen et al. (2011), Yu et al. (2007), Lea et al. (1999) and Stoll et al. (2012) studies. In the figures concerning foraminifera and coccolithophores, there is a color assigned to each species that is studied, as listed in Table 9:

Table 9: ***A list of the marker color that represents each species in the following plots.***

[a]	Species [b]	Marker color [c]	Literature [d]
Foraminifera	*Orbulina universa*	Red	Allen et al., 2011, Lea et al., 1999
Foraminifera	*Globorotalia inflata*	Pink	Yu et al., 2007
Foraminifera	*Globigerina bulloides*	Purple	Yu et al., 2007, Lea et al., 1999
Coccolithophore	*Coccolithus braarudii*	Orange	Stoll et al., 2012
Coccolithophore	*Emiliania huxleyi*	Blue	Stoll et al., 2012

[a] List of whether the organism is a foraminifera or a coccolithophore.
[b] Scientific genus and species name of each of the organisms studied.
[c] Color of marker used in the figures below.
[d] List of the studies that looked at each species. It should be noted that in Stoll et al., 2012, there were three strains of the species *E. huxleyi* studied, so they are represented in shades of blue ranging from the dark navy (strain RCC 1256), to the medium royal blue (strain RCC 1212), to the light sky blue (strain RCC 1238) in each of the plots.

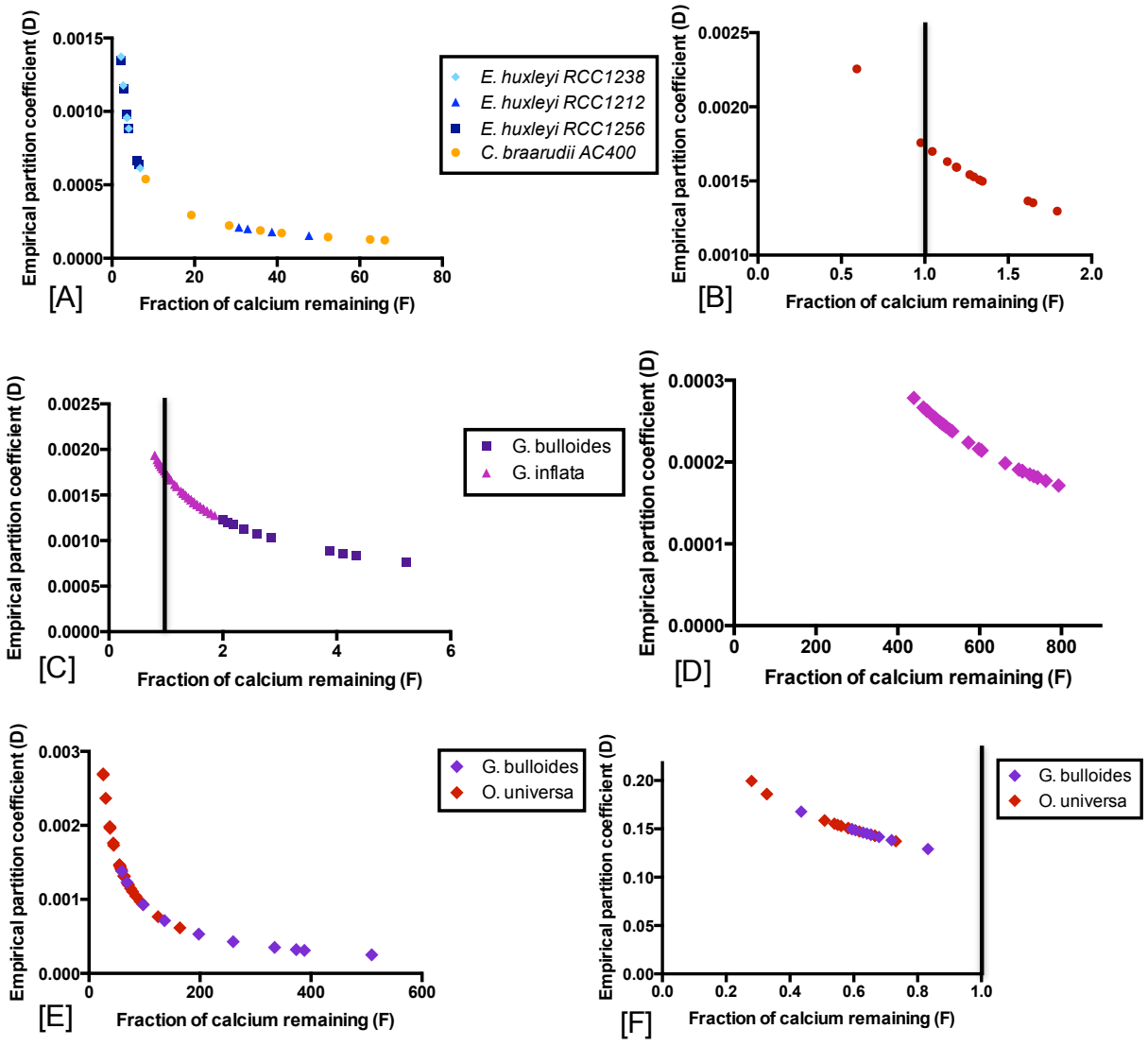

Figure 2: ***Calculations based on boron, magnesium, and strontium incorporation in calcitic foraminifera from Stoll et al., 2012, Allen et al., 2011, Yu et al., 2007, and Lea et al., 1999.*** Presented here are calculations of the empirical partition coefficient (D) (y-axis) versus the fraction of calcium remaining in the calcification reservoir after calcification (F) (x-axis). These calculations represent data for [A] boron incorporation in the coccolithophore species *C. braarudii* (orange) and three different strains of the species *E. huxleyi* (shades of blue) from Stoll et al., 2012, [B] boron incorporation in the foraminiferal species *O. universa* (red) from Allen et al., 2011, [C] boron incorporation in the foraminiferal species *G. bulloides* (purple) and *G. inflata* (pink) from Yu et al., 2007, [D] magnesium incorporation in the foraminifera species *G. inflata* from Yu et al., 2007, [E] magnesium incorporation in the foraminifera species *G. bulloides* (purple) and *O. universa* (red) from Lea et al., 1999, and [F] strontium incorporation in the two species of foraminifera studied by Lea et al., 1999. There are vertical black lines where F=1; any data to the right of the line is impossible since F cannot exceed a value of 1; this phenomenon will be discussed in detail both later in the results section as well as in the discussion section. It should be noted that Figures 2 a, d, and e do not have visible black lines since F=1 is too close to the axis to be distinguished, but all of the F values are greater than 1.

Boron incorporation in Coccolithophores and Foraminifera

A comparison of the empirical partition coefficient (D) and the fraction of calcium remaining in the calcification reservoir after biomineralization has ended (F) for the incorporation of boron in two species of coccolithophores and three species of foraminifera from Stoll et al., 2012, Allen et al., 2011, and Yu et al., 2007 are presented in Figures 2 a, b, and c. It is interesting that organisms of the same coccolithophore species, but of different strains, differentiate when comparing their D and F values. The three strains of *E. huxleyi* show different patterns of boron incorporation; *E. huxleyi* RCC1238 and RCC1256 produce higher empirical partition coefficients and smaller F values, while *E. huxleyi* RCC1212 *C. braarudii* AC400 have smaller empirical partition coefficients and larger F values. Although no foraminifera of the same species were studied, differences are seen between the foraminiferal species are seen. *O. universa* have the highest empirical partition coefficient and the smallest fraction of calcium remaining in their calcification reservoir after calcification compared to the organisms of the other phylums. *G. inflata* have the lowest empirical partition coefficient and the largest fraction of calcium remaining in their calcification reservoir after calcification compared to the organisms of the other phylums. *G. bulloides* fall in between the other two species in respect to both D and F values. The partitioning of boron into calcite in coccolithophores and foraminifera follow the same trend as in the cultured calcitic organisms.

Magnesium incorporation in Foraminifera

A comparison of the empirical partition coefficient (D) and the fraction of calcium remaining in the calcification reservoir after biomineralization has ended (F) for the incorporation of magnesium in three different species of foraminifera from Yu et al., 2007 and

Lea et al., 1999 are presented in Figures 2 d and e. These three foraminifera also show difference between species; the species show the same trends in their incorporation of magnesium as were seen in their incorporation of boron in Figures 2 a, b, and c. The partitioning of magnesium into calcite in foraminifera follow the same trend as in the cultured calcitic organisms, and produce extremely high F values.

Strontium incorporation in Foraminifera

A comparison of the empirical partition coefficient (D) and the fraction of calcium remaining in the calcification reservoir after biomineralization has ended (F) for the incorporation of strontium in two species of foraminifera are presented in Figure 2f. Both species show similar values in calculated D and F values, but *O. universa* have slightly higher empirical partition coefficient and slightly smaller fraction of calcium remaining in their calcification reservoir compared to *G. bulloides*. The partitioning of magnesium into foraminiferal calcite follows the same trend as in the cultured calcitic organisms.

Rayleigh fractionation and temperature, pH, or pCO_2 levels

Presented below are several plots looking at the empirical partition coefficient (D) versus the fraction of calcium remaining in the calcification reservoir (F) as calculated by the Rayleigh model with the additional variable of the temperature, pH, or pCO_2 conditions in which the organisms were grown. The pH or pCO_2 levels are denoted by shades of blue (calcite) or purple (aragonite). The more acidic conditions (lower pH and higher pCO_2 levels) are denoted by light shades of blue or purple, while more basic conditions (higher pH and lower pCO_2 levels) are denoted by dark shades of blue and purple. The temperature levels are denoted by shades of red orange and yellow, with red denoting colder temperatures and yellow denoting warmer temperatures. The seven organism and element combinations shown below are the only combinations that show any apparent trend when comparing the Rayleigh model calculations to the carbonate system and temperature conditions in which they were grown. The organisms shown include both cultured organisms and the data found in the literature.

Macroinvertebrates from Ries et al. (2009) study

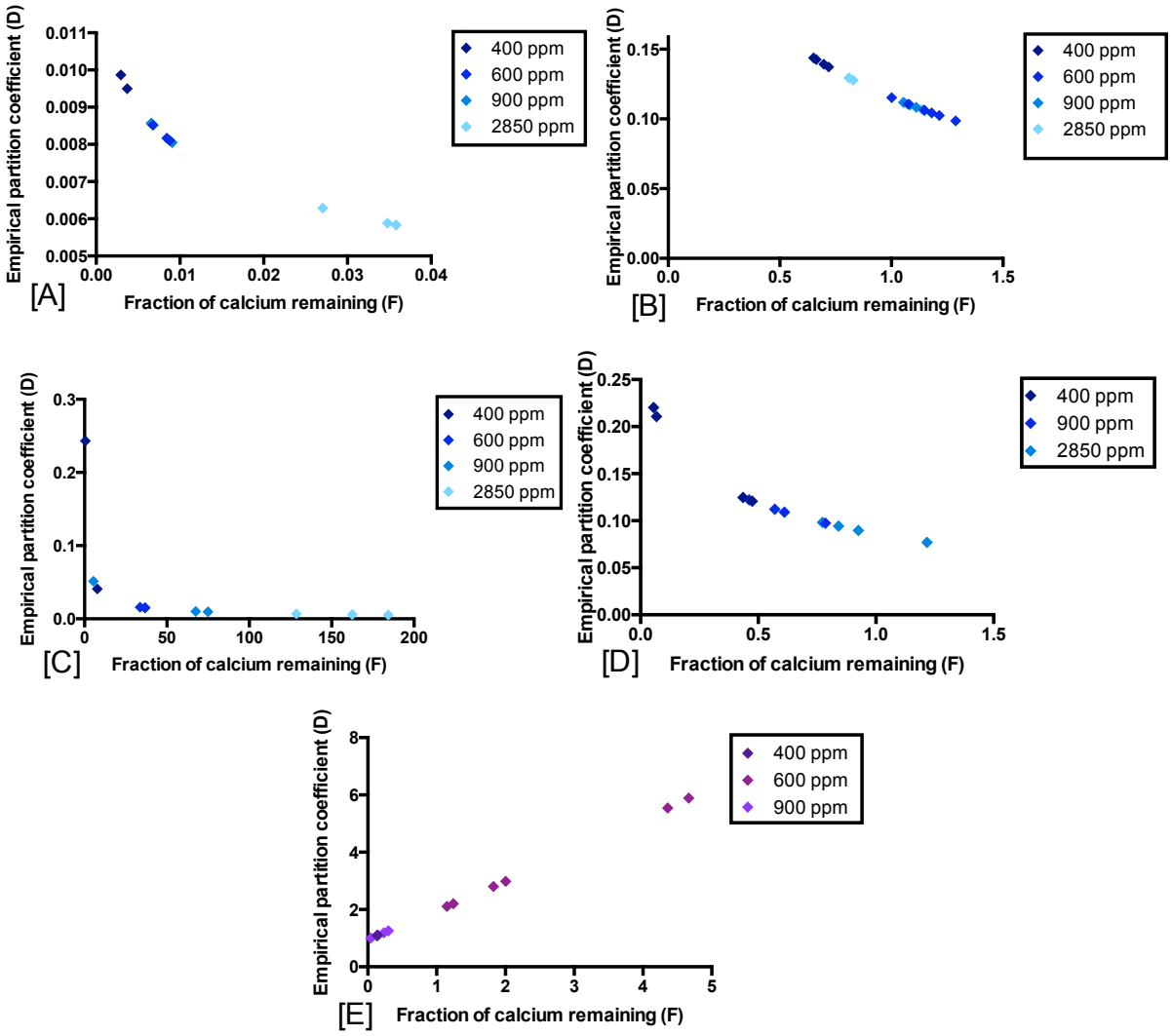

Figure 3: ***Calculations based on element incorporation in cultured marine calcifiers.*** These plots of the empirical partition coefficient (D) (y-axis) versus the fraction of calcium remaining in the calcification reservoir after calcification (F) (x-axis) are for [A] boron incorporation in the calcitic purple urchin *Arbacia punctulata*, [B] strontium incorporation in the calcitic oyster *Crassostrea virginica*, [C] uranium incorporation in the calcitic purple urchin *Arbacia punctulata*, [D] barium incorporation in the calcitic oyster *Crassostrea virginica*, and [E] barium incorporation in the aragonitic hard clam *Mercenaria mercenaria*. The pCO_2 levels the organisms were cultured in are shown by the shades of blue for the calcitic organisms and purple for the aragonitic organisms, with the highest (more acidic) pCO_2 level in light shades and the lowest (more basic) pCO_2 level in dark shades. These organisms were grown in culture; therefore, these pCO_2 values are the precise pCO_2 levels that these organisms were exposed to throughout the sixty-day culture experiment (Ries et al., 2009).

Table 10: ***Statistical data for Figure 3.***

Figure [a]	Organism [b]	Element [c]	R^2 [d]	P-value [e]	Significance [f]
3a	Purple urchin	Boron	0.8863	< 0.0001	Significant
3b	Oyster	Strontium	0.0008591	0.9081	Not Significant
3c	Purple urchin	Uranium	0.1413	0.2546	Not Significant
3d	Oyster	Barium	0.1435	0.1211	Not Significant
3e	Hard clam	Barium	0.1619	0.0978	Not Significant

[a] Figure for which the statistical data is being reported.
[b] the common name of the organism being studied.
[c] the element being studied
[d] The Pearson R^2 value for the data.
[e] The Pearson P-value for the data.
[f] Whether or not there is a significant trend. Statistical significance is reported whenever the P-value is less than 0.05.

It should be noted that the statistics presented in this table were calculated for the empirical partition coefficient versus the pCO_2 treatment to represent the trend between element incorporation and the pCO_2 level in which the organism was raised.

Boron incorporation in the calcitic purple urchin with pCO_2

Figure 3a examines the spread of pCO_2 treatments within the Rayleigh model of the purple urchin for boron incorporation. There is a trend that shows that the urchins grown in the lower pCO_2 levels have higher empirical partition coefficients and smaller fractions of calcium remaining in the reservoir after calcification than the urchins grown in the higher pCO_2 levels.

Strontium incorporation in the calcitic oyster with pCO_2

Figure 3b examines the spread of pCO_2 treatments within the Rayleigh model of the oyster for strontium incorporation. There is not a definite trend shown for strontium incorporation in oysters; the highest and the lowest pCO_2 treatments group together with high empirical partition coefficients and small fractions of calcium remaining in their calcification reservoir compared to the two middle pCO_2 treatments, which also group together. This trend is

shown again in barium incorporation in the aragonitic hard clam in Figure 3e, as discussed below.

Uranium incorporation in the calcitic purple urchin with pCO_2

Figure 3c examines the spread of pCO_2 treatments within the Rayleigh model of the purple urchin for uranium incorporation. There is a trend that indicates that the urchins grown in the lower pCO_2 levels have higher empirical partition coefficients and smaller fractions of calcium remaining in the reservoir after calcification than the urchins grown in the higher pCO_2 levels.

Barium incorporation in the calcitic oyster with pCO_2

Figure 3d examines the spread of pCO_2 treatments within the Rayleigh model for the oyster for barium incorporation. Similar to Figures 3 a and c, the trend indicates that the oysters grown in the lower pCO_2 levels have higher empirical partition coefficients and smaller fractions of calcium remaining in the reservoir after calcification than the oysters grown in the higher pCO_2 levels.

Barium incorporation in the aragonitic hard clam with pCO_2

Figure 3e examines the spread of pCO_2 treatments within the Rayleigh model for the hard clam for barium incorporation. Similar to Figure 3b, there is no definite trend shown for barium incorporation in the hard clam; the highest and the lowest pCO_2 treatments group together with low empirical partition coefficients and small fractions of calcium remaining in their calcification reservoir compared to the middle pCO_2 treatment which has large empirical partition coefficients and fractions of calcium remaining.

Foraminifera from various studies with pH

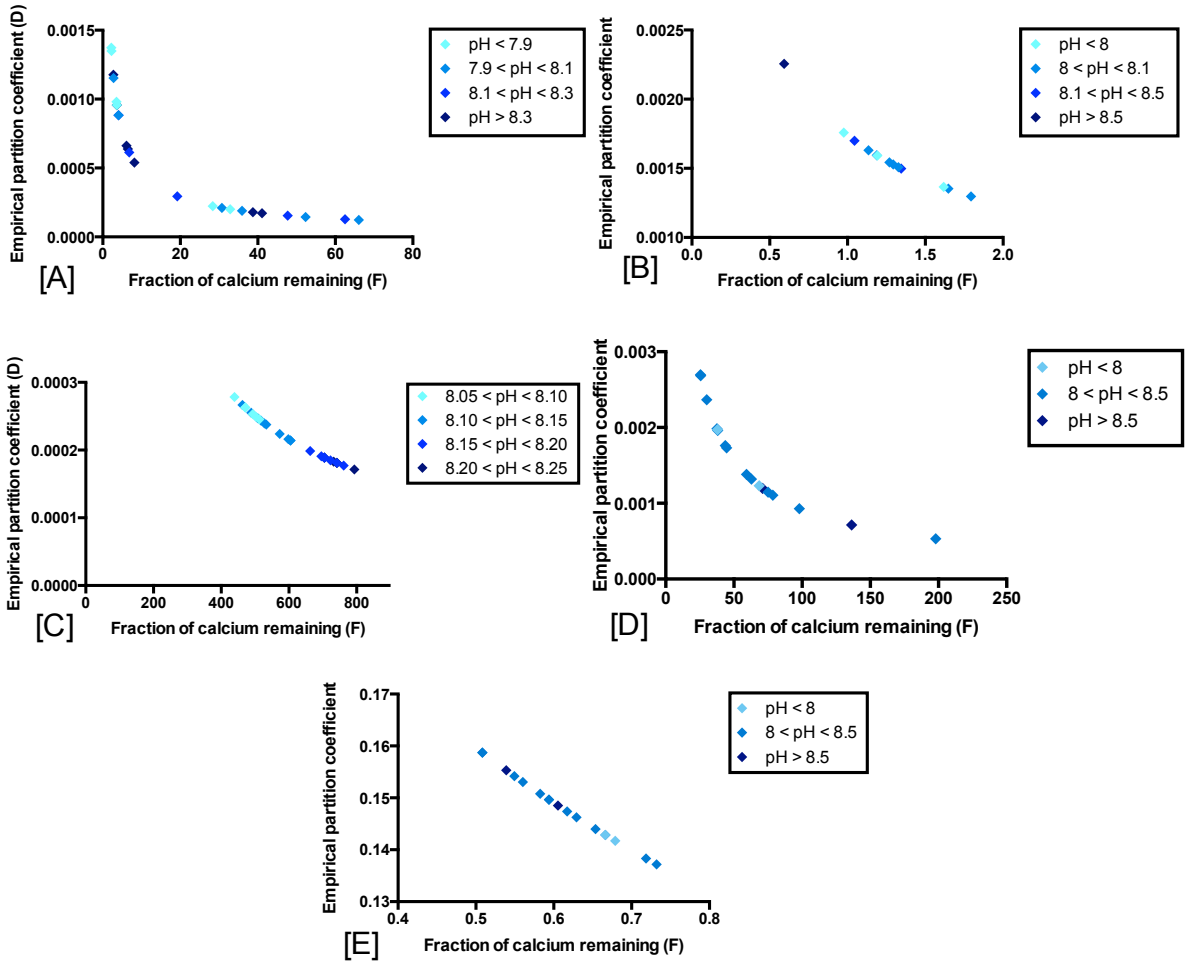

Figure 4: ***Calculations based on boron, magnesium, and strontium incorporation in calcitic coccolithophores and foraminifera from Stoll et al., 2012, Allen et al., 2011, Yu et al., 2007 and Lea et al., 1999 with respect to pH.*** These plots of the empirical partition coefficient (D) (y-axis) versus the fraction of calcium remaining in the calcification reservoir after calcification (F) (x-axis) are for [A] boron incorporation in the coccolithophore species *C. braarudii* (orange) and three different strains of the species *E. huxleyi* (shades of blue) from Stoll et al., 2012, [B] boron incorporation in the foraminiferal species *O. universa* (red) from Allen et al., 2011, [C] magnesium incorporation in the foraminifera *G. inflata* from Yu et al., 2007, [D] magnesium incorporation in the foraminiferal species *O. universa* and *G. bulloides* from Lea et al., 1999, and [E] strontium incorporation in the two foraminifera species from Lea et al., 1999, all with respect to pH level. The pH level the organism was found in is shown by the shades of blue, with the lowest (most acidic) pH in light blue and the highest (most basic) pH in dark blue. The pH levels from Stoll et al., 2012, Allen et al., 2011, and Yu et al., 2007 are in the total pH scale; the pH levels in Lea et al., 1999 are in the NBS free hydrogen ion scale. Note that Figure 4e is zoomed in to better show the spread of data points.

Table 11: ***Statistical data for Figure 4.***

Figure [a]	Organism [b]	Element [c]	R^2 [d]	P-value [e]	Significance [f]
4a	Coccolithophores	Boron	0.02214	0.4878	Not Significant
4b	Foraminifera	Boron	0.5772	0.0026	Significant
4c	Foraminifera	Magnesium	0.7602	< 0.0001	Significant
4d	Foraminifera	Magnesium	0.03558	0.4684	Not Significant
4e	Foraminifera	Strontium	0.1496	0.1251	Not Significant

[a] Figure for which the statistical data is being reported.
[b] the common name of the organism being studied.
[c] the element being studied
[d] The Pearson R^2 value for the data.
[e] The Pearson P-value for the data.
[f] Whether or not there is a significant trend. Statistical significance is reported whenever the P-value is less than 0.05.

It should be noted that the statistics presented in this table were calculated for the empirical partition coefficient versus the pCO_2 treatment to represent the trend between element incorporation and the pCO_2 level in which the organism was raised.

Boron incorporation in two calcitic coccolithophore species with pH

Figure 4a examines the spread of pH values within the Rayleigh model for boron incorporation of the coccolithophore species *C. braarudii* and *E. huxleyi* from the Stoll et al., 2012 study. There is no definite trend with pH in the two coccolithophores from this study.

Boron incorporation in a calcitic foraminifera species with pH

Figure 4b examines the spread of pH values within the Rayleigh model for boron incorporation of the foraminifera species *O. universa* from the Allen et al., 2011 study. There is no definite trend with pH in the two coccolithophores from this study.

Magnesium incorporation in calcitic foraminifera *G. inflata* with pH

Figure 4c examines the spread of pH values within the Rayleigh model for magnesium incorporation of the foraminiferal species *G. inflata* from the Yu et al., 2007 study. There is a trend that indicates that the foraminifera grown in lower pH levels have higher empirical partition coefficients and smaller fractions of calcium remaining in the reservoir after calcification than the foraminifera that were grown in higher pH levels.

Magnesium incorporation in two calcitic foraminifera species with pH

Figure 4d examines the spread of pH values within the Rayleigh model for magnesium incorporation of the foraminiferal species *O. universa* and *G. bulloides* from the Lea et al., 1999 study. There is no definite trend with pH in the two foraminifera from this study.

Strontium incorporation in two calcitic foraminifera species with pH

Figure 4e examines the spread of pH values within the Rayleigh model for strontium incorporation of the foraminiferal species *O. universa* and *G. bulloides* from the Lea et al., 1999 study. There is no definite trend with pH in the two foraminifera from this study.

Foraminifera from Yu et al. (2007) and Lea et al., 1999 studies with temperature

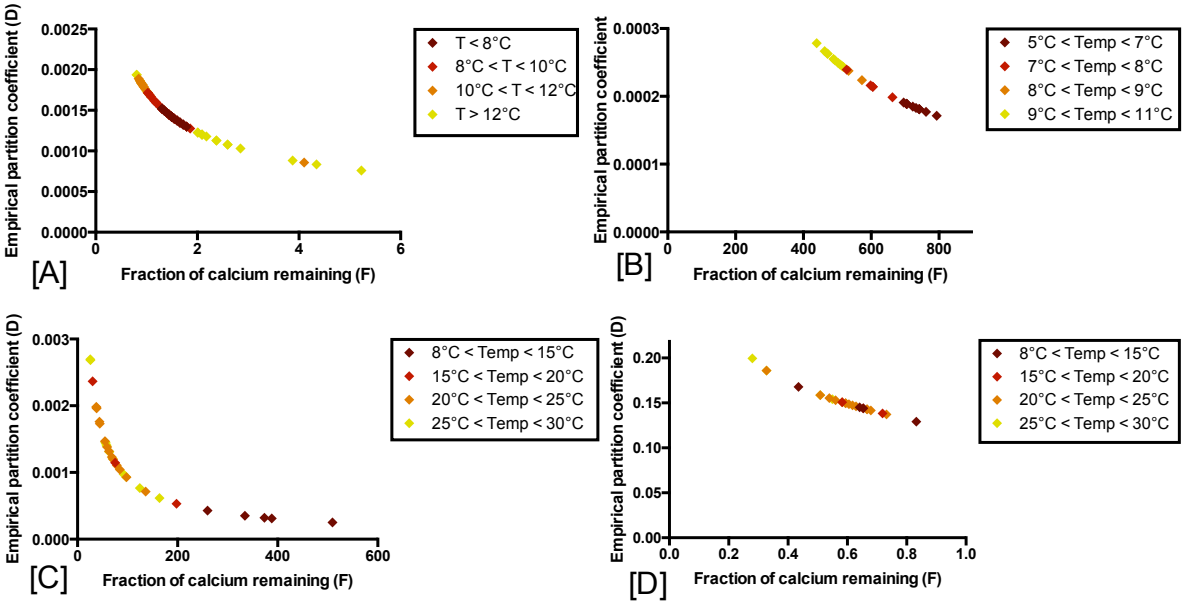

Figure 5: ***Calculations based on boron, magnesium, and strontium incorporation in calcitic coccolithophores and foraminifera from Stoll et al., 2012, Allen et al., 2011, Yu et al., 2007 and Lea et al., 1999 with respect to temperature.*** These plots of the empirical partition coefficient (D) (y-axis) versus the fraction of calcium remaining in the calcification reservoir after calcification (F) (x-axis) are for [A] boron incorporation in the foraminifera *G. inflata* and *G. bulloides* from Yu et al., 2007, [B] magnesium incorporation in the foraminifera *G. inflata* from Yu et al., 2007, [C] magnesium incorporation in the foraminiferal species *O. universa* and *G. bulloides* from Lea et al., 1999, and [D] strontium incorporation in the two foraminifera species from Lea et al., 1999, all with respect to temperature. The temperature is denoted by shades of red to yellow, with red representing colder temperatures and yellow representing warmer temperatures.

Table 12: ***Statistical data for Figure 5.***

Figure [a]	Organism [b]	Element [c]	R^2 [d]	P-value [e]	Significance [f]
5a	Foraminifera	Boron	0.006213	0.4707	Not Significant
5b	Foraminifera	Magnesium	0.9900	< 0.0001	Significant
5c	Foraminifera	Magnesium	0.2487	0.0020	Significant
5d	Foraminifera	Strontium	0.2248	0.0166	Significant

[a] Figure for which the statistical data is being reported.
[b] the common name of the organism being studied.
[c] the element being studied
[d] The Pearson R^2 value for the data.
[e] The Pearson P-value for the data.
[f] Whether or not there is a significant trend. Statistical significance is reported whenever the P-value is less than 0.05.

It should be noted that the statistics presented in this table were calculated for the empirical partition coefficient versus the temperature to represent the trend between element incorporation and the temperature conditions in which the organism was raised.

Boron incorporation in two calcitic foraminifera species with temperature

Figure 5a examines the spread of temperature values within the Rayleigh model for boron incorporation of the foraminifera species *G. inflata* and *G. bulloides* from the Yu et al., 2012 study. There is a visible trend that indicates that the foraminifera grown in colder temperatures have higher empirical partition coefficients and smaller fractions of calcium remaining in the reservoir after calcification than the foraminifera that were grown in warmer temperatures. The statistical analysis does not agree with the visual analysis of this trend with a p-value of 0.4707.

Magnesium incorporation in the calcitic foraminifera *G. inflata* with temperature

Figure 5b examines the spread of temperature conditions within the Rayleigh model for magnesium incorporation of the foraminiferal species *Globorotalia inflata* from the Yu et al., 2007 study. There is a trend that indicates that the foraminifera grown in warmer temperatures have higher empirical partition coefficients and smaller fractions of calcium remaining in the reservoir after calcification than the foraminifera that were grown in colder temperatures. There is some overlap in the temperature conditions, but there is a definite trend.

Magnesium incorporation in two calcitic foraminifera species with temperature

Figure 5c examines the spread of temperature conditions within the Rayleigh model for magnesium incorporation of the foraminiferal species *O. universa* and *G. bulloides* from the Lea et al., 1999 study. There is a trend that indicates that the foraminifera grown in warmer temperatures have higher empirical partition coefficients and smaller fractions of calcium

remaining in the reservoir after calcification than the foraminifera that were grown in colder temperatures. There is some overlap in the temperature conditions, but there is an apparent trend.

Strontium incorporation in two calcitic foraminifera species with temperature

Figure 5d examines the spread of temperature conditions within the Rayleigh model for strontium incorporation of the foraminiferal species *O. universa* and *G. bulloides* from the Lea et al., 1999 study. There is a trend that indicates that the foraminifera grown in warmer temperatures have higher empirical partition coefficients and smaller fractions of calcium remaining in the reservoir after calcification than the foraminifera that were grown in colder temperatures. There is some overlap in the temperature conditions, but there is an apparent trend.

Element-to-calcium ratios as proxies for pCO_2, pH, and temperature

Element-to-calcium ratios and pCO_2 in macroinvertebrates from Ries et al. (2009) study

Below are four plots of X/Ca vs. aragonite saturation state for boron-to-calcium and lithium-to-calcium ratios in several cultured macroinvertebrates. Aragonite saturation state (Ω) is used as a measure of pCO_2 where a pCO_2 level of 400 ppm is equivalent to Ω = 2.5, 600 ppm is equivalent to Ω = 2.0, 900 ppm is equivalent to Ω = 1.5, and 2850 ppm is equivalent to Ω = 0.7. Aragonite saturation state is used instead of pCO_2 level to reduce the spread of data and present a clearer representation of the data. These four plots are the only organism-element combinations that show a trend with pCO_2 levels from the cultured macroinvertebrates in this study. In the following plots the organisms that precipitate calcite are represented by blue markers; since the serpulid worm precipitates a mixture of calcite and aragonite, it is represented with black markers.

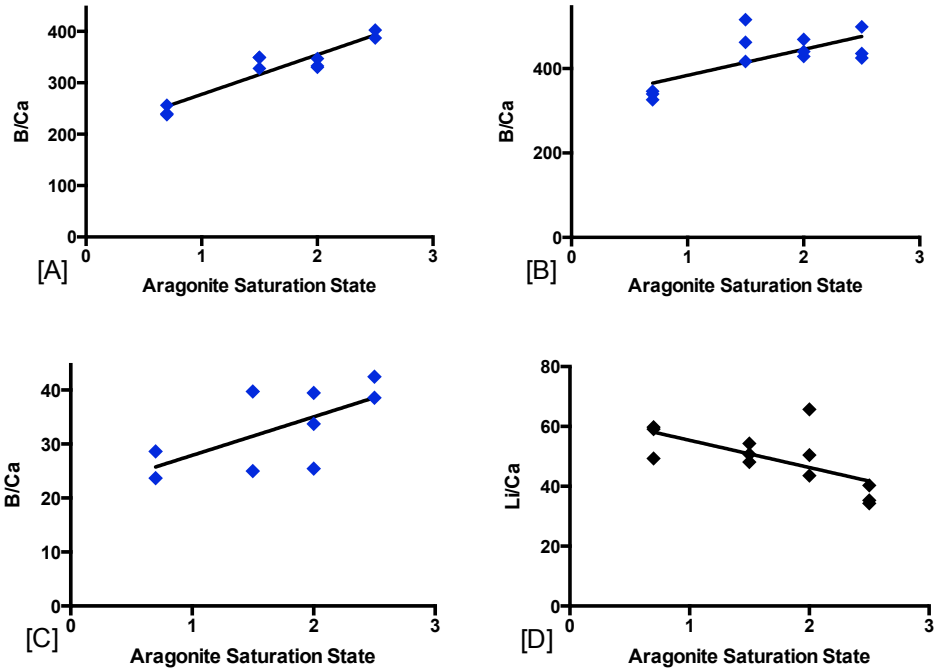

Figure 6: ***Plots of boron and incorporation various macroinvertebrates as a function of aragonite saturation state.*** These plots of element-to-calcium ratios (y-axis) versus aragonite saturation state (x-axis) are for [A] B/Ca ratios in the purple urchin *Arbacia punctulata*, [B] B/Ca

ratios in the coralline red algae *Neogoniolithon* sp., [C] B/Ca ratios in the bay scallop *Argopecten irradians*, and [D] Li/Ca ratios in the serpulid worm *Hydroides crucigera*. The statistical analyses for these plots can be found in Table 13.

Table 13: ***Statistical data for Figure 6.***

Figure [a]	R^2 [b]	P-value [c]	Slope [d]	y-intercept [e]	Significance [f]
6a	0.8694	< 0.0001	77.10 ± 9.962	200.4 ± 17.18	Significant
6b	0.4918	0.0110	61.49 ± 19.77	322.4 ± 35.62	Significant
6c	0.4243	0.0574	7.129 ± 3.139	20.77 ± 5.729	Not Significant
6d	0.4219	0.0223	-9.093 ± 3.366	64.47 ± 6.066	Significant

[a] Figure for which the statistical data is being reported.
[b] The Pearson R^2 value for the data.
[c] The Pearson P-value for the data.
[d] The slope of the line through all of the data points, along with error.
[e] The y-intercept of the line through all of the data points where x=0, along with error.
[f] Whether or not there is a significant trend. Statistical significance is reported whenever the P-value is less than 0.05.

Boron incorporation in purple urchin as a function of the carbonate system

Figure 6a examines the correlation between element incorporation and the carbonate system for B/Ca ratios in the purple urchin. There is a definitive trend that indicates that more boron is incorporated in the calcite of the purple urchin at higher aragonite saturations states, lower pCO_2 concentrations and higher pH levels. The p-value for this trend is <0.0001, signifying that there is a very strong correlation between B/Ca ratios and the carbonate system in purple urchins.

Boron incorporation in coralline red algae as a function of the carbonate system

Figure 6b examines the correlation between element incorporation and the carbonate system for boron incorporation in the coralline red algae. Similar to Figure 6a, there is a trend

that indicates that more boron is incorporated into the calcite of the coralline red algae at higher aragonite saturations states, lower pCO_2 concentrations and higher pH levels. The p-value for this trend is 0.0110, suggesting that there is a correlation between B/Ca ratios and the carbonate system in coralline red algae, although the correlation is not as strong as the one seen in the purple urchin in Figure 6a. The curve in the data points shown in this plot indicate that there may be a threshold effect in boron incorporation, where boron incorporation is uniform until the ambient conditions drop below a certain aragonite saturation state and then much less boron is incorporated. This threshold effect is not seen in the purple urchin, which shows a uniform decrease in boron incorporation with decreasing aragonite saturation state.

Boron incorporation in bay scallop as a function of the carbonate system

Figure 6c examines the correlation between element incorporation and the carbonate system for boron incorporation in the bay scallop. Similar to Figures 6 a and b, there is a trend that indicates that more boron is incorporated into the calcite of the coralline red algae at higher aragonite saturations states, lower pCO_2 concentrations and higher pH levels. The p-value for this trend is 0.0570; indicating that the trend is not a statistically since this study is using the typical p-value cut-off of 0.05 to represent significance.

Lithium incorporation in serpulid worm as a function of the carbonate system

Figure 6d examines the correlation between element incorporation and the carbonate system for lithium incorporation in the serpulid worm. There is a trend that indicates that less lithium is incorporated in the calcification of the serpulid worm at higher aragonite saturations states, lower pCO_2 concentrations and higher pH levels. The p-value for this trend is 0.0223,

signifying that there is a correlation between Li/Ca ratios and the carbonate system in serpulid worms. Similar to boron incorporation in coralline red algae (Figure 6b), there may be a threshold effect in lithium incorporation in the serpulid worm.

Element-to-calcium ratios and pH in foraminifera and coccolithophores:

Below are comparisons of B/Ca, Mg/Ca and Sr/Ca with pH in foraminifera and coccolithophores from the studies performed by Allen et al., 2011, Yu et al., 2007, Lea et al., 1999, and Stoll et al., 2012. Some of the following data shows a significant correlation between the X/Ca ratio being studied and pH and some do not. This data is the elemental proxy comparison with pH that corresponds to the Rayleigh model calculations in Figures 2 and 4 above.

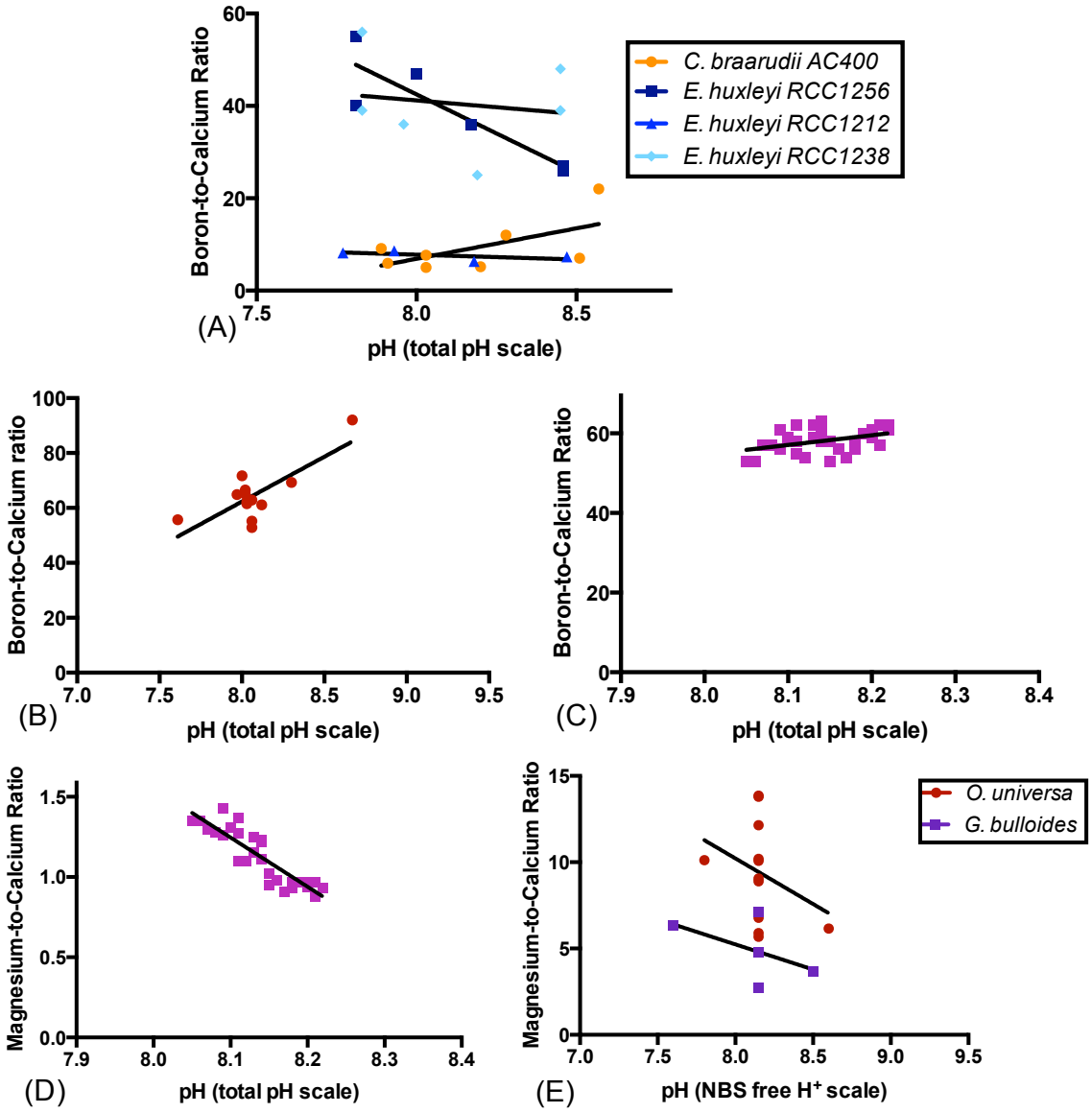

Figure 7: ***Plots of boron and magnesium incorporation and ambient pH levels in several species of foraminifera and coccolithophores.*** The plots shown here compare the element-to-calcium ratios of calcite (y-axis) versus the ambient pH in which the organisms were grown (x-axis) for several different species of foraminifera and coccolithophores from studies performed by Stoll et al. (2012), Allen et al. (2011), Yu et al. (2007), and Lea et al. (1999). Figure 7a presents data from Stoll et al. (2012) which is for boron incorporation in calcite and includes two different species of coccolithophores, and three strains of one of the species: *Coccolithus braarudii* (orange), and *Emiliania huxleyi* (blue). There are three different strains of *E. huxleyi* presented here: strain RCC1256 (dark navy blue), strain RCC 1212 (medium royal blue), and strain RCC 1238 (light turquoise blue). Figure 7b presents data from Allen et al. (2011) looking at boron incorporation in the calcitic foraminifera *Orbulina universa* (red). Figures 7c and 7d present data from Yu et al. (2007) for the foraminifera species *Globorotalia inflata* (pink). Figure 7c is for boron incorporation in calcite and Figure 7d is for magnesium incorporation in calcite. Figure 7e presents data from Lea et al. (1999) for the foraminifera *Orbulina universa* (red) and *Globigerina bulloides* (purple) and magnesium incorporation in calcite.

Table 14: ***Statistical data for Figure 7.***

Figure [a]	Species [b]	R^2 [c]	P-value [d]	Slope [e]	y-intercept [f]	Significance [g]
7a	AC400	0.3686	0.1104	13.19 ± 7.046	-98.59 ± 57.64	Not Significant
7a	RCC1256	0.7845	0.0189	-33.81 ± 8.861	313.0 ± 71.97	Significant
7a	RCC1212	0.3859	0.3788	-2.079 ± 1.854	24.41 ± 15.00	Not Significant
7a	RCC1238	0.02556	0.7622	-5.871 ± 18.12	88.16 ± 147.2	Not Significant
7b	*O. universa*	0.5972	0.0020	32.66 ± 8.087	-199.0 ± 65.32	Significant
7c	*G. inflata*	0.1585	0.0325	24.42 ± 10.83	-140.7 ± 88.17	Significant
7d	*G. inflata*	0.7905	< 0.0001	-3.070 ± 0.304	26.11 ± 2.476	Significant
7e	*O. universa*	0.09817	0.3214	-5.284 ± 5.065	52.50 ± 41.33	Not Significant
7e	*G. bulloides*	0.2689	0.3707	-2.909 ± 2.769	28.51 ± 22.47	Not Significant

[a] Figure for which the statistical data is being reported.
[b] The species or strain of the line being analized.
[c] The Pearson R^2 value for the data.
[d] The Pearson P-value for the data.
[e] The slope of the line through all of the data points, along with error.
[f] The y-intercept of the line through all of the data points where x=0, along with error.
[g] Whether or not there is a significant trend. Statistical significance is reported whenever the P-value is less than 0.05.

Boron incorporation in calcitic coccolithophores with pH from Stoll et al. (2012)

Figure 7a is a plot of B/Ca ratios in coccolithophore calcite with respect to pH based on data from Stoll et al., 2012 is presented above. This data does not support the correlation between pH and B/Ca ratios; in addition to the trends for all but the RCC1256 strain of *E. huxleyi* being statistically insignificant, the trends are also in different directions (both positive and negative slopes). *E. huxleyi* strains RCC1212 and RCC1238 both show straight lines with minimal variation over 0.7 units of pH change (slopes of -2.079 ± 1.854 and -5.871 ± 18.12, respectively). *E. huxleyi* strain RCC1256 has a negative slope (-33.81 ± 8.861), with B/Ca ratios decreasing with increasing pH, while *C. braarudii* strain AC400 has a positive slope (+13.19 ± 7.046) meaning that B/Ca ratios are increasing with increasing pH. It should be noted that the R^2 values for the trendlines through these points range from 0.02556 to 0.78446, and P-values range

from 0.0189 to 0.7622, indicating that there may be an underlying trend, but that there are also some complicating factors. In addition to not showing a correlation between B/Ca and pH, this data also presents variability on both the species and strain levels, which complicates the proxy potential of boron.

Boron incorporation in calcitic foraminifera with pH from Allen et al. (2011)

Figure 7b is a plot of B/Ca ratios in foraminiferal calcite with respect to pH based on data from Allen et al., 2011 is presented above. It has been reported in both foraminifera and coccolithophores that there is a correlation between B/Ca and pH (Rae et al., 2011, Yu and Elderfield, 1997, Foster 2008, Tripati et al., 2011, Yu et al., 2007, Stoll et al., 2012); this data supports that hypothesis, showing a significant trend with a P-value of 0.0020.

Boron incorporation in calcitic foraminifera with pH from Yu et al. (2007)

Figure 7c is a plot of B/Ca ratios in foraminiferal calcite with respect to pH based on data from Yu et al., 2007 is presented here. There is a trend between B/Ca and pH based on this plot since the trends are statistically significant, although the accuracy of the trend is questionable. The R^2 value of this correlation is low (0.1585) and the P-value is high (0.0325), but the trend is significant. The use of the B/Ca paleoproxy to recreate past pH conditions will need a better correlation between B/Ca and pH before it can be completely trusted.

Magnesium incorporation in calcitic foraminifera with pH from Yu et al. (2007)

Figure 7d is a plot of Mg/Ca ratios in foraminiferal calcite with respect to pH based on data from Yu et al., 2007 is presented here. It has been reported in foraminifera that there is a

correlation between Mg/Ca and pH (Lea et al., 1999, Lea 2006), and this data supports that hypothesis, showing a statistically significant trend between Mg/Ca and pH.

Magnesium incorporation in calcitic foraminifera with pH from Lea et al. (1999)

Figure 7e is a plot of Mg/Ca ratios in foraminiferal calcite with respect to pH based on data from Lea et al., 1999 is presented here. This data shows a trend that is opposite to what was reported by Yu et al., 2007 and is shown in Figure 7d, and is also statistically insignificant with P-values of 0.3214 for *O. universa* and 0.3707 for *G. bulloides*. Although the Yu et al., 2007 study was performed several years after the Lea et al., 1999 study, there was no comment made on the contradiction they found with the findings of the Lea et al., 1999 study.

Element-to-calcium ratios and temperature in foraminifera and coccolithophores:

Below are comparisons of B/Ca, Mg/Ca and Sr/Ca with temperature in foraminifera from the studies performed by Allen et al., 2011, Yu et al., 2007 and Lea et al., 1999. The study performed by Stoll et al., 2012 looking at B/Ca and temperature in coccolithophores is excluded because it was already discussed in the section on species- and strain-specificity. Some of the following data shows a correlation between the X/Ca ratio being studied and temperature and some do not. Most of the data conflicts with the data from the other experiments; for example, Yu et al., 2007 shows a very strong correlation between Mg/Ca and temperature, and then the data from Lea et al., 1999 show no correlation between Mg/Ca and temperature. This data is the elemental proxy comparison with pH that corresponds to the Rayleigh model calculations in Figures 2 and 5 above.

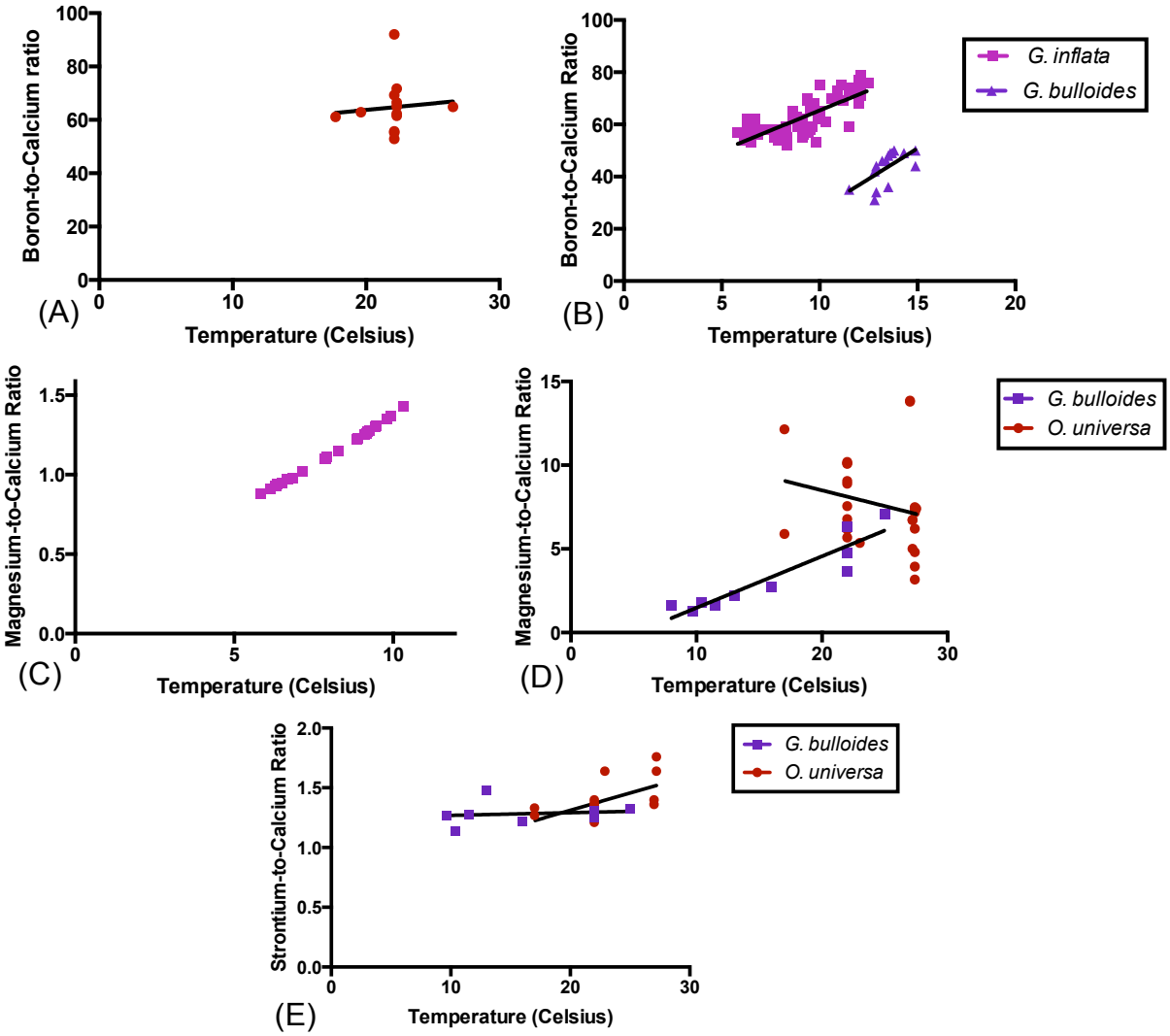

Figure 8: ***Plots of boron, magnesium, and strontium incorporation and ambient temperatures in several species of foraminifera.*** The plots shown here compare the element-to-calcium ratios of calcite (y-axis) versus the ambient ocean temperature in which the organisms were grown (x-axis) for several different species of foraminifera from studies performed by Allen et al. (2011), Yu et al. (2007), and Lea et al. (1999). Figure 8a presents data from Allen et al. (2011) looking at boron incorporation in the calcitic foraminifera *Orbulina universa* (red). Figure 8b presents data from Yu et al. (2007) on the incorporation of boron in the foraminifera species *Globorotalia inflata* (pink) and *Globigerina bulloides* (purple). Figure 8c presents data from Yu et al. (2007) on the incorporation of magnesium in the foraminifera species *Globorotalia inflata* (pink). Figures 8d and 8e present data from Lea et al. (1999) for the foraminifera species *Orbulina universa* (red) and *Globigerina bulloides* (purple). Figure 8d is for magnesium incorporation in calcite and Figure 8e is for strontium incorporation in calcite.

Table 15: ***Statistical data for Figure 8.***

Figure [a]	Species [b]	R^2 [c]	P-value [d]	Slope [e]	y-intercept [f]	Significance [g]
8a	*O. universa*	0.00918	0.7555	0.4869 ± 1.525	53.99 ± 33.64	Not Significant
8b	*G. inflata*	0.5794	< 0.0001	3.061 ± 0.3139	34.75 ± 2.965	Significant
8b	*G. bulloides*	0.3924	0.0125	4.688 ± 1.618	-19.51 ± 21.80	Significant
8c	*G. inflata*	0.9974	< 0.0001	0.119 ± 0.0011	0.169 ± 0.009	Significant
8d	*G. bulloides*	0.8516	0.0001	0.3080 ± 0.045	-1.602 ± 0.774	Significant
8d	*O. universa*	0.0534	0.2559	-0.1883 ± 0.16	12.26 ± 4.000	Not Significant
8e	*G. bulloides*	0.0212	0.7081	0.0022 ± 0.006	1.247 ± 0.102	Not Significant
8e	*O. universa*	0.3381	0.0230	0.0289 ± 0.011	0.7332 ± 0.25	Significant

[a] Figure for which the statistical data is being reported.
[b] The species of the line being analized.
[c] The Pearson R^2 value for the data.
[d] The Pearson P-value for the data.
[e] The slope of the line through all of the data points, along with error.
[f] The y-intercept of the line through all of the data points where x=0, along with error.
[g] Whether or not there is a significant trend. Statistical significance is reported whenever the P-value is less than 0.05.

Boron incorporation in calcitic foraminifera with temperature from Allen et al. (2011)

Figure 8a is a plot of B/Ca ratios in foraminiferal calcite with respect to temperature based on data from Allen et al., 2011 is presented above. It has been reported in coral that there is a correlation between B/Ca and temperature (Sinclair et al., 1998, Fallon et al., 1999), however, this data does not show a significant correlation between temperature and the boron-to-calcium ratio of calcite with a P-value of 0.7555.

Boron incorporation in calcitic foraminifera with temperature from Yu et al. (2007)

Figure 8b is a plot of B/Ca ratios in foraminiferal calcite with respect to temperature based on data from Yu et al., 2007 is presented here. There is a statistically significant trend between B/Ca and temperature based on this plot, which is unfortunate for the development of a B/Ca pH proxy since temperature will produce interference in the pH signal of the proxy. It

should be noted that the data set for *G. inflata* is a collection of two sample sets; one of the sample sets for *G. inflata* comes from a multiple samples out of a single sediment core (CHAT 16K in the Southern Ocean), and the other sample set comes from many box core tops taken on a transect that covers approximately 30° of latitude and 10° of longitude in the Northern Atlantic Ocean from a combination of the NEAPACC and APNAP cruises.

Magnesium incorporation in calcitic foraminifera with temperature from Yu et al. (2007)

Figure 8c is a plot of Mg/Ca ratios in foraminiferal calcite with respect to temperature based on data from Yu et al., 2007 is presented here. It has been reported in many marine calcifiers that Mg/Ca ratios increase with increasing ocean temperatures (Barker et al., 2005, Lear et al., 2000, Lear et al., 2010, Rosenthal et al., 1997, Wei et al., 2000), and this data supports that hypothesis very well with a P-value of < 0.0001 for the *G. inflata* data set.

Magnesium incorporation in calcitic foraminifera with temperature from Lea et al. (2007)

Figure 8d is a plot of Mg/Ca ratios in foraminiferal calcite with respect to temperature based on data from Lea et al., 1999 is presented here. These trends are distinct from those reported by Yu et al., 2007 in Figure 8c for other species. Although Mg/Ca ratios are considered a relatively robust proxy for temperature, there are still major variations being found with the trendlines on this plot having P-values of 0.2559 for *O. universa* and 0.0001 for *G. bulloides* (the *O. universa* data is not statistically significant, while the *G. bulloides* data is statistically significant. There must be some signal overlying the temperature signal in the Mg/Ca composition, however what that signal is, is impossible to say without further data.

Strontium incorporation in calcitic foraminifera with temperature from Lea et al. (2007)

Figure 8e is a plot of Sr/Ca ratios in foraminiferal calcite with respect to temperature based on data from Lea et al., 1999 is presented here. It has been reported in many marine calcifiers that Sr/Ca ratios decrease with increasing ocean temperatures (Cardinal et al., 2001, Sun et al., 2004, Marshal and McCulloch, 2002); not only is the trend for *G. bulloides* insignificant while the trend for *O. universa* is barely statistically significant (P-values of 0.7081 and 0.0230, respectively), but it also has slopes in the opposite direction than has been reported, increasing with increasing ocean temperatures instead of decreasing (positive slopes instead of negative).

Groupings of organisms in the same phylum with respect to Rayleigh model

Presented below are comparisons of the empirical partition coefficient (D) and the fraction of calcium remaining in the calcification reservoir after biomineralization is complete (F) found in the cultured organisms that produce calcite. Shades of blue are used to represent the organisms of the phylum Crustacea, red represents the coralline red algae of the phylum Rhodophyta, shades of green represent the phylum Echinodermata, and shades of purple represent the phylum Mollusca. The organisms have similar D and F values to other organisms within their phyla, indicating that there is some genetic or physiological similarity in calcification systems between organisms that have comparable evolutionary histories. In all of the elements studied here, except for cadmium, the organisms tend to group together with other organisms of the same phylum; however, strontium, magnesium, and manganese produce the most obvious separations and are discussed below. The effect of the inorganic partition coefficient chosen on the Rayleigh model calculations is discussed in this thesis. It should be noted that the inorganic partition coefficient will change the absolute values of F calculated, but does not impact the spread of organisms in relation to each other. Therefore, the trends shown below will not change if different inorganic partition coefficients are used for the calculations. Plots of D versus F with phylogenetic groupings can be found in Figure 19 in the Appendix.

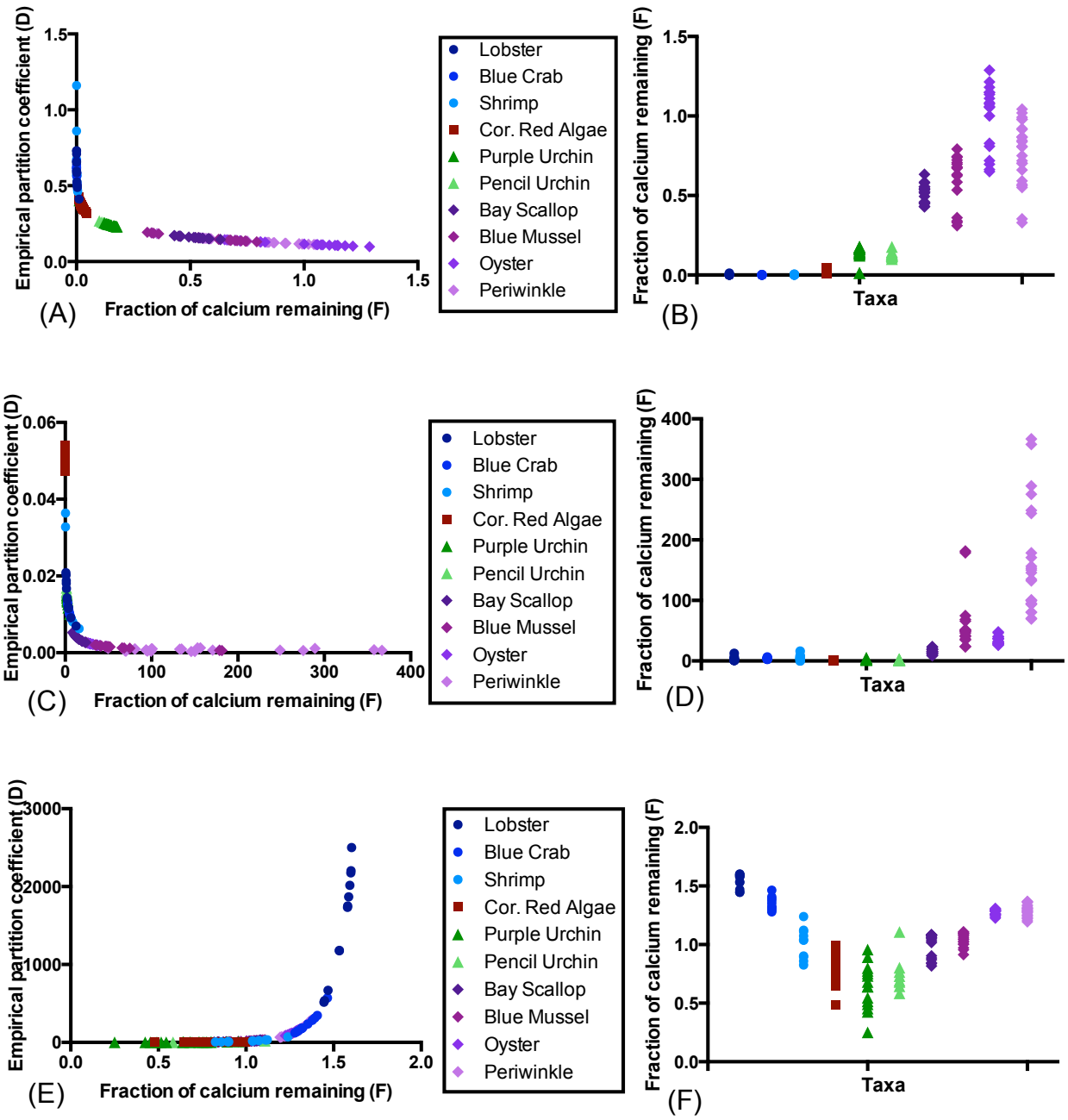

Figure 9: ***Calculations based on element partitioning into by marine invertebrates with reference to phylogenetic similarities in calcification.*** Figure 9a presents a calculation of the empirical partition coefficient (D) (y-axis) versus the fraction of calcium remaining in the calcification reservoir after calcification (F) (x-axis) for strontium incorporation in all of the organisms that precipitate calcite studied by Ries et al. (2009). Figure 9b presents the F values calculated for strontium incorporation in Figure 9a (y-axis) as a function of the organism being studied (x-axis). Figure 9c presents a D versus F calculation for magnesium incorporation in all of the calcitic organisms and Figure 9d presents the F values calculated for magnesium incorporation in Figure 9c (y-axis) as a function of the organism being studied (x-axis). Figure 9e presents a D versus F calculation for manganese incorporation in all of the calcitic organisms

and Figure 9f presents the F values calculated for magnesium incorporation in Figure 9e (y-axis) as a function of the organism being studied (x-axis).

Phylogenetic similarities in strontium incorporation in the calcitic macroinvertebrates

Figure 9a presents a comparison of the empirical partition coefficient (D) and the fraction of calcium remaining in the calcification reservoir after biomineralization has ended (F) for the incorporation of strontium across all of the calcitic organisms studied here results in the organisms grouping around the other organisms in the same phylum. Figure 9b presents the F value of each calcitic organism to show the trends between these organisms. The organisms of the phylum Crustacea have the highest empirical partition coefficient and the smallest fraction of calcium remaining in their calcification reservoir after calcification compared to the organisms of the other phylums. The crustaceans also have a large range in the empirical partition coefficients, but a small range in the F values produced. The organisms of the phylum Mollusca have the lowest empirical partition coefficient and the largest fraction of calcium remaining in their calcification reservoir after calcification compared to the organisms of the other phylums. The mollusks also have a small range in the empirical partition coefficients, but a large range in the F values produced. The sea urchins of the phylum Echinodermata and the coralline red algae of the phylum Rhodophyta range in between the crustaceans and the mollusks, with the echinoderms being more similar to the mollusks while the rhodophytes are more similar to the crustaceans in this plot.

The trend in F values across the suite of organisms studied here may indicate the mechanism of calcification, and calcium or carbon transport and storage during calcification in each of these organisms. In particular, the flushing rate, or the 'openness', of the site of calcification can be determined by the fraction of calcium remaining in the reservoir (Elderfield

et al., 1996, Dawber and Tripati, 2012). An organism with a small F value can be assumed to have a closed reservoir from which it calcifies with a very long flushing time, since the organism is using up all of the calcium and the organism is not replenishing the calcium supply as would be beneficial for calcification to be favorable. On the other hand, an organism with a large F value can be assumed to have a more open reservoir from which it calcifies with a shorter flushing time, since the organism does not seem to be depleting its calcification reservoir.

Phylogenetic similarities in magnesium incorporation in the calcitic macroinvertebrates

Figure 9c shows a similar trend as Figure 9a of the organisms of the same phylum grouping together, although there is an overlap between the coralline red algae, crustaceans, and sea urchins. The coralline red algae have the highest empirical partition coefficient and the smallest fraction of calcium remaining in their calcification reservoir after calcification compared to the organisms of the other phylums, followed by crustaceans and sea urchins. The mollusks have the lowest empirical partition coefficient and the largest fraction of calcium remaining in their calcification reservoir after calcification compared to the organisms of the other phylums.

Figure 9d presents the trend in F values across the suite of calcitic organisms analyzed for magnesium in order to determine how each organism handles its calcification reservoir and transport, and shows a very similar pattern as Figure 9b. According to this data, the coralline red algae tend to have a more closed calcification reservoir and a longer flushing time, while the mollusks seem to have a more open reservoir with a short flushing time and the urchins fall in between. However, almost all of the organisms presented here have F values above 1; since this problem is only extensively seen in magnesium incorporation into calcite in this study, the

accuracy of the inorganic partition coefficients for Mg in calcite found in the literature should be further researched.

Phylogenetic similarities in manganese incorporation in the calcitic macroinvertebrates

Figure 9e shows a different trend from Figures 9a and 9c, with many of the phyla overlapping each other, although still grouping together with other organisms of their phyla. The coralline red algae and the urchins have the lowest empirical partition coefficient and the smallest fraction of calcium remaining in their calcification reservoir after calcification compared to the organisms of the other phylums. The crustaceans and the mollusks have the highest empirical partition coefficient and the largest fraction of calcium remaining in their calcification reservoir after calcification compared to the organisms of the other phylums. Figure 9f presents the trend in F values across the suite of calcitic organisms analyzed for manganese in order to determine how each organism handles its calcification reservoir and transport.

Although there is some overlap among the phyla, the general trends between phyla seen in strontium incorporation in calcite (Figures 1 a and b) are seen in all elements except for manganese. The calculations for barium, lithium, and uranium incorporation into calcite can be found in the appendix in Figure 19. Boron and cadmium incorporation into calcite produced too many unreal numbers in the F calculation to be plotted.

A thought experiment on the importance of the inorganic partition coefficient used

Presented in Table 16 below are calculations of the fraction of calcium remaining in the calcification reservoir (F) using the highest and lowest inorganic partition coefficients reported in the literature over the range of empirical partition coefficients produced. These calculations were performed to elucidate how the chosen inorganic partition coefficient will change the results of the Rayleigh model. In addition to the calculations of the outlying values, Figure 10 shows D versus F calculations using the lowest and highest reported inorganic partition coefficients for strontium incorporation in calcite. Such calculations could be used to eliminate the appearance of F-values greater than 1 and indicate which inorganic partition coefficients are more accurate. However, several of the element-polymorph combinations will produce F-values greater than 1 or unreal numbers with all of the reported inorganic partition coefficients. It should be noted that the use of a different inorganic partition coefficient will change the absolute values of F calculated, but does not affect how the organisms compare to each other.

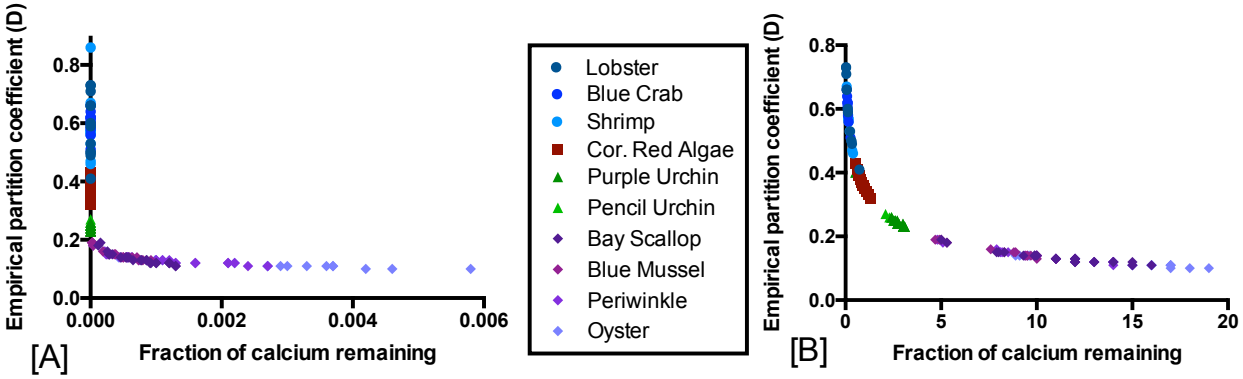

Figure 10: ***Calculations based on element partitioning into by marine invertebrates with reference to phylogenetic similarities in calcification using two different values of the inorganic partition coefficient (α) for the calculation.*** Figure 10a presents a calculation of the empirical partition coefficient (D) (y-axis) versus the fraction of calcium remaining in the calcification reservoir after calcification (F) (x-axis) for strontium incorporation in all of the organisms that precipitate calcite studied by Ries et al. (2009) using the lowest reported inorganic partition coefficient of $\alpha = 0.020$ from Nehrke et al., 2007. Figure 10b presents a D versus F calculation for strontium incorporation in all of the calcitic organisms using the highest reported inorganic partition coefficient of $\alpha = 0.35$ from Gabitov and Watson, 2006. See Table 40 in the appendix for the tabulated data of the calculation presented here.

Table 16: ***Fraction of calcium remaining in the calcification reservoir (F) calculations using both the lowest and the highest reported inorganic partition coefficients for the range of empirical partition coefficients calculated for all of the elements and mineral polymorphs studied.***

Element in Polymorph [a]	D [b]	F (low α) [c]	F (high α) [d]
Strontium in calcite	0.1 < D < 0.75	Low α = 0.020	High α = 0.35
	0.1	0.0053	19
	0.75	8.00E-31	0.023
Magnesium in calcite	0.001 < D < 0.05	Low α = 0.0123	High α = 0.097
	0.001	50	940
	0.05	0.026	3.7
Barium in calcite	0.07 < D < 0.98	Low α = 0.015	High α = 0.1
	0.07	0.0057	2
	0.98	1.00E-110	1.00E-17
Manganese in calcite	1.3 < D < 2500	Low α = 8.5	High α = 30
	1.3	0.23	0.24
	2500	2.67	1.237
Boron in calcite	3.5E-5 < D < 0.013	Low α = 0.00127	High α = 2.0
	3.5E-5	193	unreal
	0.013	0.00003	unreal
Lithium in calcite	0.0022 < D < 0.022	Low α = 0.00025	High α = 3.82
	0.0022	0.00015	unreal
	0.022	1.00E-39	unreal
Cadmium in calcite	0.033 < D < 535	Low α = 7.0	High α = 110
	0.033	unreal	unreal
	535	2.63	1.024
Uranium in calcite	0.0014 < D < 0.13	Low α = 0.046	High α = 0.2
	0.0014	200	2750
	0.13	0.06	2.7
Strontium in aragonite	0.15 < D < 1.2	Low α = 1.133	High α = 1.24
	0.15	unreal	unreal
	1.2	2.2	0.8
Magnesium in aragonite	0.00012 < D < 0.005	Low α = 0.000275	High α = 0.00133
	0.00012	4.4	43
	0.005	0.00000001	0.025
Barium in aragonite	0.11 < D < 3.5	Low α = 1.521	High α = 2.817
	0.11	unreal	unreal
	3.5	9.5	1.25
Boron in aragonite	0.0003 < D < 0.016	Low α = 0.0016	High α = 0.981
	0.0003	16	unreal

	0.016	0.00004	unreal
Uranium in aragonite	0.003 < D < 7.5	Low α = 1.8	High α = 9.8
	0.003	unreal	unreal
	7.5	11.25	0.937

[a] the element and mineral polymorph for which the calculation was performed.
[b] the outlying empirical partition coefficients (D) for that element-polymorph combination.
[c] The fraction of calcium remaining in the calcification reservoir (F) value calculated for the associated D-value using the lowest reported inorganic partition coefficient.
[d] The fraction of calcium remaining in the calcification reservoir (F) value calculated for the associated D-value using the highest reported inorganic partition coefficient.

The grey shaded rows contain the element-polymorph combination, the range of D-values for that combination, the lowest reported inorganic partition coefficient (α) for that combination, and the highest reported inorganic partition coefficient (α) for that combination. The inorganic partition coefficients used here with their associated sources can be found in tabulated form in Table 8. It should be noted that the D-values reported here are averages, the F-values reported are approximations, and that extreme outlying D-values were eliminated from this analysis to provide a more accurate representation of the data.

Strontium incorporation in calcite

Figure 10 presents a comparison of the empirical partition coefficient (D) and the fraction of calcium remaining in the calcification reservoir after biomineralization has ended (F) for the incorporation of strontium across all of the calcitic organisms studied here. Figure 10a uses an inorganic partition coefficient of α = 0.020 (Nehrke et al., 2007) whereas Figure 10b uses α = 0.35 (Gabitov and Watson, 2006). The low inorganic partition coefficient produces F-values that are impossibly low and the high inorganic partition coefficient produces F-values that are impossibly high.

Magnesium incorporation in calcite

Table 16 presents a comparison of calculated F-values based on the lowest and highest reported inorganic partition coefficients for magnesium incorporation into calcite. All of the

inorganic partition coefficients reported in the literature for magnesium in calcite will produce impossibly high F-values.

Barium incorporation in calcite

Table 16 presents a comparison of calculated F-values based on the lowest and highest reported inorganic partition coefficients for barium incorporation into calcite. The lowest inorganic partition coefficient produces a broad range of F-values (0.7 – 0.98) that are possible, while the high inorganic partition coefficient produces F-values that are impossibly high.

Manganese incorporation in calcite

Table 16 presents a comparison of calculated F-values based on the lowest and highest reported inorganic partition coefficients for manganese incorporation into calcite. All of the inorganic partition coefficients reported in the literature for manganese in calcite will produce impossibly high F-values.

Boron incorporation in calcite

Table 16 presents a comparison of calculated F-values based on the lowest and highest reported inorganic partition coefficients for boron incorporation into calcite. The low inorganic partition coefficient produces F-values that are simultaneously impossibly low and high. The high inorganic partition coefficient produces only unreal numbers when calculating F.

Lithium incorporation in calcite

Table 16 presents a comparison of calculated F-values based on the lowest and highest reported inorganic partition coefficients for lithium incorporation into calcite. The low inorganic partition coefficient produces F-values that are impossibly low. The high inorganic partition coefficient produces only unreal numbers when calculating F.

Cadmium incorporation in calcite

Table 16 presents a comparison of calculated F-values based on the lowest and highest reported inorganic partition coefficients for cadmium incorporation into calcite. All of the inorganic partition coefficients reported in the literature for cadmium in calcite will produce impossibly high F-values for the highest D-values produced, and unreal numbers for the lowest D-values produced.

Uranium incorporation in calcite

Table 16 presents a comparison of calculated F-values based on the lowest and highest reported inorganic partition coefficients for uranium incorporation into calcite. All of the inorganic partition coefficients reported in the literature for uranium in calcite will produce impossibly high F-values.

Strontium incorporation in aragonite

Table 16 presents a comparison of calculated F-values based on the lowest and highest reported inorganic partition coefficients for strontium incorporation into aragonite. The low inorganic partition coefficient produces F-values that are either impossibly high or unreal. The

high inorganic partition coefficient produces F-values that are appropriate for the highest observed D-values, but that are unreal for the lowest observed D-values.

Magnesium incorporation in aragonite

Table 16 presents a comparison of calculated F-values based on the lowest and highest reported inorganic partition coefficients for magnesium incorporation into aragonite. The low inorganic partition coefficient produces F-values that are simultaneously impossibly low and high. The high inorganic partition coefficient produces F-values that are either appropriate or impossibly high.

Barium incorporation in aragonite

Table 16 presents a comparison of calculated F-values based on the lowest and highest reported inorganic partition coefficients for barium incorporation into aragonite. All of the inorganic partition coefficients reported in the literature for barium in aragonite will produce F-values that are either impossibly high or unreal.

Boron incorporation in aragonite

Table 14 presents a comparison of calculated F-values based on the lowest and highest reported inorganic partition coefficients for boron incorporation into aragonite. The low inorganic partition coefficient produces F-values that are simultaneously impossibly low and high. The high inorganic partition coefficient produces only unreal numbers when calculating F.

Uranium incorporation in aragonite

Table 16 presents a comparison of calculated F-values based on the lowest and highest reported inorganic partition coefficients for uranium incorporation into aragonite. The low inorganic partition coefficient produces F-values that are either impossibly high or unreal. The high inorganic partition coefficient produces F-values that are appropriate for the highest observed D-values, but that are unreal for the lowest observed D-values.

Discussion

Suitability of the Rayleigh model

The use of a Rayleigh model when considering the element-to-calcium ratios produced in the calcification of marine organisms makes physiological and biochemical sense, since it has been shown that many organisms use enclosed reservoirs from which they calcify. The Rayleigh model used in this study is a simple mathematical model that has one major known source of error, and one possible unknown source of error. The main source of error comes from uncertainties in the appropriate value for the inorganic partition coefficient used. As shown in Table 8, there is a considerable amount of variation in reported inorganic partition coefficients in the literature. As shown in Table 16 and Figure 10, the inorganic partition coefficient that is used for calculations with any given element will have a significant and direct effect on the F value that is calculated; however, this would not impact the grouping of taxa within their respective phyla since the comparisons are done for each element separately.

The use of a Rayleigh model is based on the condition that calcification occurs within an enclosed reservoir. Although a closed calcification reservoir has been suggested for several of the organisms studied here, definitive proof is still lacking for a few. There are two major concerns with the Rayleigh calculations presented in this thesis; unrealistic F values are calculated, and the F values of different elements within the same organisms do not match each other. An F value greater than 1 can generally be fixed by using a different inorganic partition coefficient in the calculation; however, as shown in Table 16, this will not work for all of the element-polymorph combinations studied here. Since the F-value is supposed to indicate the fraction of calcium remaining in the calcification reservoir when biomineralization is complete, it is expected that all of the elements within an organism will produce identical F-values. This is

not the case and indicates that there are still problems to be worked out with this model and the inorganic partition coefficients used.

Errors that could cause an F value greater than 1

The unknown source of error in this model is shown in the fact that a few organisms had F values above the value of 1, which is physically impossible since there can never be more than 100% calcium remaining in the calcification reservoir (F=1) unless the organisms have an open calcification reservoir and a fast flushing time. It is possible that the flushing time is fast enough that more calcium is being added to the reservoir while calcification is occurring through some combination of calcium ion channels, calcium pumps, and/or seawater leakage; for example, for F=2 the reservoir would have the all of calcium in the calcification reservoir replaced with new calcium twice during the time it took to finish one batch of calcification. However, it has been extensively shown that many calcifying organisms use a closed calcification reservoir (Borowitzka and Larkum, 1977, Rollion-Bard and Erez, 2010, de Nooijer et al., 2009, Erez et al., 2008, Erez, 2003, Bentov et al., 2009, Young and Henriksen, 2003, Paasche, 2002), and it is difficult to explain the extremely high F values. If these organisms do have an open, or even partially-open, calcification reservoir, it would preclude the use of a Rayleigh model to describe their calcification process.

There are at least two other possible explanations for F values above 1; the first possibility concerns the inorganic partition coefficient being used, the second concerns the mathematical model itself. As mentioned above, the inorganic partition coefficient used in the calculation can produce an error in the results of the model since a large range has been reported in the literature for many of the elements studied here. The collective coefficients for any one

element reported in the literature can range by several orders of magnitude (for example 0.0016 from Allison et al. (2010) and 0.981 from Hemming et al. (1995) are both reported inorganic partition coefficients reported for boron in aragonite); these studies do not compare their partition coefficients with those previously reported, nor do they discuss possible reasons for the large differences found. Additionally, in some cases, one reported inorganic coefficient is greater than 1 while others are less than 1 (for example 0.00025 from Elderfield et al. (1996) and 3.82 from Marriott et al. (2004a) are both reported inorganic partition coefficients reported for lithium in calcite); this produces a fundamental difference in the trends produced, as discussed in the breakdown of elemental groupings section below. Another possibility is that the Rayleigh model presented here is missing a factor, or that it is not accounting for some biological effect that is occurring within the calcification reservoir.

In the geochemistry of biologically-produced calcium carbonate, an organism with a more open calcification reservoir and a faster flushing time results in calcium carbonate may be more suited to use as a paleo-proxy, since any calcification produced may have a composition similar to that of inorganic calcification in the same ocean conditions. A major caveat to this is that there are still the biological effects, but an open calcification system is better for proxy development than a closed calcification system. For example, in the study of the macroinvertebrates cultured by Ries et al. (2009), the mollusks seem to have the most open calcification system (high F values, low D values) and the crustaceans seem to have the most closed calcification system (low F values, high D values). Contrary to what is expected, the coccolithophore and foraminifera samples that were studied here produced Rayleigh calculations similar to the mollusks, indicating that coccolithophores and foraminifera have a more open calcification reservoir when compared to crustaceans. Although there have been several

radioisotopic experiments performed on the flushing time of crustaceans in the past (especially the blue crab), it would be beneficial to culture and experiment with radioisotopes on the crustacean and mollusk species studied here to observe if this proposed trend is seen in radioisotopic experiments.

Breakdown of elemental groupings

There were a few trends produced by the Rayleigh calculations, all of which can be explained simply by the value of the inorganic partition coefficient; hence why the accuracy of the coefficients is so important for the use of this model.

Table 17: ***A comparison of the trends observed with the inorganic partition coefficients used.***

X [a]	Calcite [b]	α [c]	Aragonite [d]	α [e]
Sr	Negative, Exponential	0.12	Positive, Linear	1.193
Mg	Negative, Exponential	0.019	Negative, Exponential	0.001027
Ba	Negative, Exponential	0.08	Positive, Linear	2.11
Mn	Steep positive, Exponential	14.8	-	-
B	Negative, Exponential	0.0017	Negative, Exponential	0.0016
Li	Negative, Exponential	0.00195	-	-
Cd	Steep positive, Exponential	41	-	-
U	Negative, Exponential	0.123	Positive, Linear	5.8

[a] Element being examined in the element-to calcium ratio of interest.
[b] List of the trends seen for each element in calcite as shown in the plots above.
[c] The inorganic partition coefficient for that element in calcite.
[d] List of the trends seen for that element in aragonite as shown in the plots above.
[e] The inorganic partition coefficient for that element into aragonite.

The literature sources for the inorganic partition coefficients listed here can be found in Table 7 and will not be repeated here. A thorough search of the literature has failed to find inorganic partition coefficients for Mn, Li, or Cd in aragonite. The empirical partition coefficients for boron incorporation into calcite produced unreal F values.

Table 17 lists the trends observed in the calcite and aragonite for each element studied, as well as the inorganic partition coefficient used. There are five different qualities of the trends that can be broken down based on the coefficient used: negative or positive slope, exponential or linear trend, and whether or not the trend is steep. All of the trends that have negative slopes have an inorganic partition coefficient below the value of $\alpha=1$ and all of the positive slope trends have an inorganic partition coefficient above the value of $\alpha=1$. At the most basic level, an $\alpha>1$ results in a positive slope while an $\alpha<1$ results in a negative slope since the α is an exponent. Whether the trend produced is exponential or linear is a biological effect; if an organism creates calcium carbonate that with a uniform composition, then the trend will seem linear, if an organism's calcification does not have a uniform composition across all of the calcium carbonate produced the trend will seem exponential. All of these trends are exponential if there are enough data points to show the curve, but when a small enough sample is taken, the curve appears to be a straight line. A steep slope is produced when an inorganic partition coefficient is very large since α is an exponent in this equation; for example, the two steep slopes appear in Mn/Ca in calcite and Cd/Ca in calcite, which have α values of 14.8 and 41 respectively. The trends produced by this model can therefore be explained by simple mathematics. The question that needs to be answered by further experimentation is whether or not this mathematical model is directly relevant to the calcifying space of marine organisms.

Conclusions

One tool that could be used to better understand elemental partitioning into biologically precipitated carbonate minerals is a Rayleigh model. Such a model can be used to indicate how an organism treats its calcification reservoir during the precipitation of calcium carbonate. A clear separation has been seen between organisms in different phyla, indicating that these organisms are handling their calcification in a very similar way. For example, of the calcitic organisms studied here, the mollusk, coccolithophore, and foraminifera species appear to have a more open calcification system with faster flushing times than organisms in the Crustacea, Rhodophyta, and Echinodermata phyla. This knowledge can be used to create generalizations that may help constrain the elemental composition data within a wide range of organisms in an attempt to understand the conditions in which they were grown.

However, there are still problems and uncertainties with the model presented here that need to be worked out by further research before clear answers about the biological control of calcification can be drawn from this mathematical model. The first problem with the use of a Rayleigh model for element incorporation during calcification is the calculation of impossible F-values. An F-value greater than 1 is impossible since there can never be more than 100% calcium remaining in the calcification reservoir. A very small F-value (<10^-2) is also impossible since it is highly unlikely that calcification would proceed when there is so little calcium remaining within the calcification reservoir. The second problem with the use of a Rayleigh model in this context is the lack of correlation between F-values calculated by different elements for the same organism. Since the organism is calcifying at a certain fraction of calcium remaining in the calcification reservoir, every element should produce a similar F-value. The calculations presented here do not match between elements within the same organism. This

could be due to the use of inaccurate inorganic partition coefficients, or it could indicate that the Rayleigh model is not appropriate for use in the context of marine biomineralization.

No consistent discernable trends between elemental composition and the carbonate system could be found in the macroinvertebrates cultured in the Ries et al. (2009) study except for the nine element-organism combinations shown in Figures 3 and 6. This could be due to the macroscopic nature of these organisms, with the calcification that had already been laid down drowning out the elemental signal from the calcification that was formed during this short (sixty day) experiment. Alternatively it is possible that no relationship is discernible from the small population of individuals that were measured for this work. The foraminifera and coccolithophores studied here indicate potential for boron-to-calcium and magnesium-to-calcium ratios as proxies for both temperature and pH; however, since the elemental compositions vary with both temperature and pH, the proxies will be difficult to develop unless either temperature or pH conditions are constant between samples.

Appendix: Additional Figures

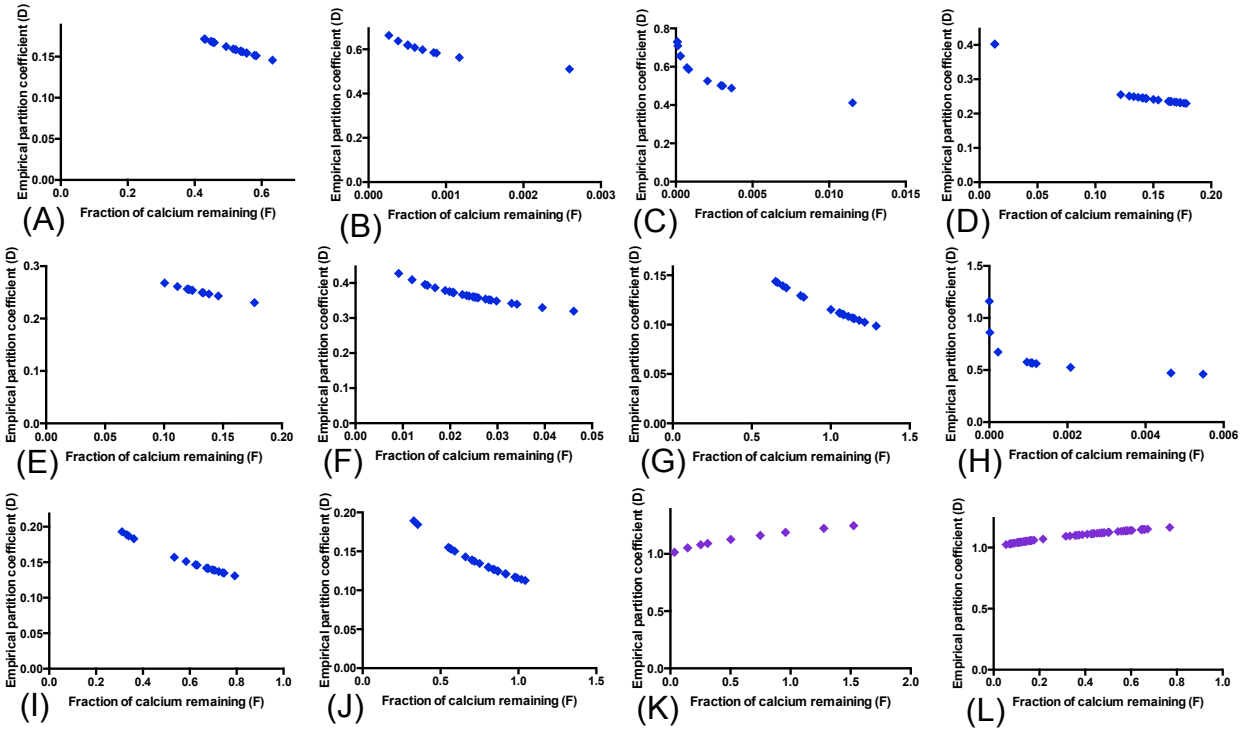

Figure 11: ***Plots of strontium incorporation into cultured calcitic and aragonitic organisms.*** These plots are of the empirical partition coefficient (D) (y-axis) versus the fraction of calcium remaining in the calcification reservoir after calcification (F) (x-axis) for strontium incorporation into both calcite and aragonite. These figures are for [A] bay scallop, [B] blue crab, [C] lobster, [D] purple urchin, [E] pencil urchin, [F] coralline red algae, [G] oyster, [H] shrimp, [I] blue mussel, [J] periwinkle, [K] halimeda, and [L] coral. In this figure, blue represents the calcitic organisms and purple represents the aragonitic organisms. Figure 1a is the representative figure that summarizes the calcitic organisms, and Figure 1b is the representative figure that summarizes the aragonitic organisms.

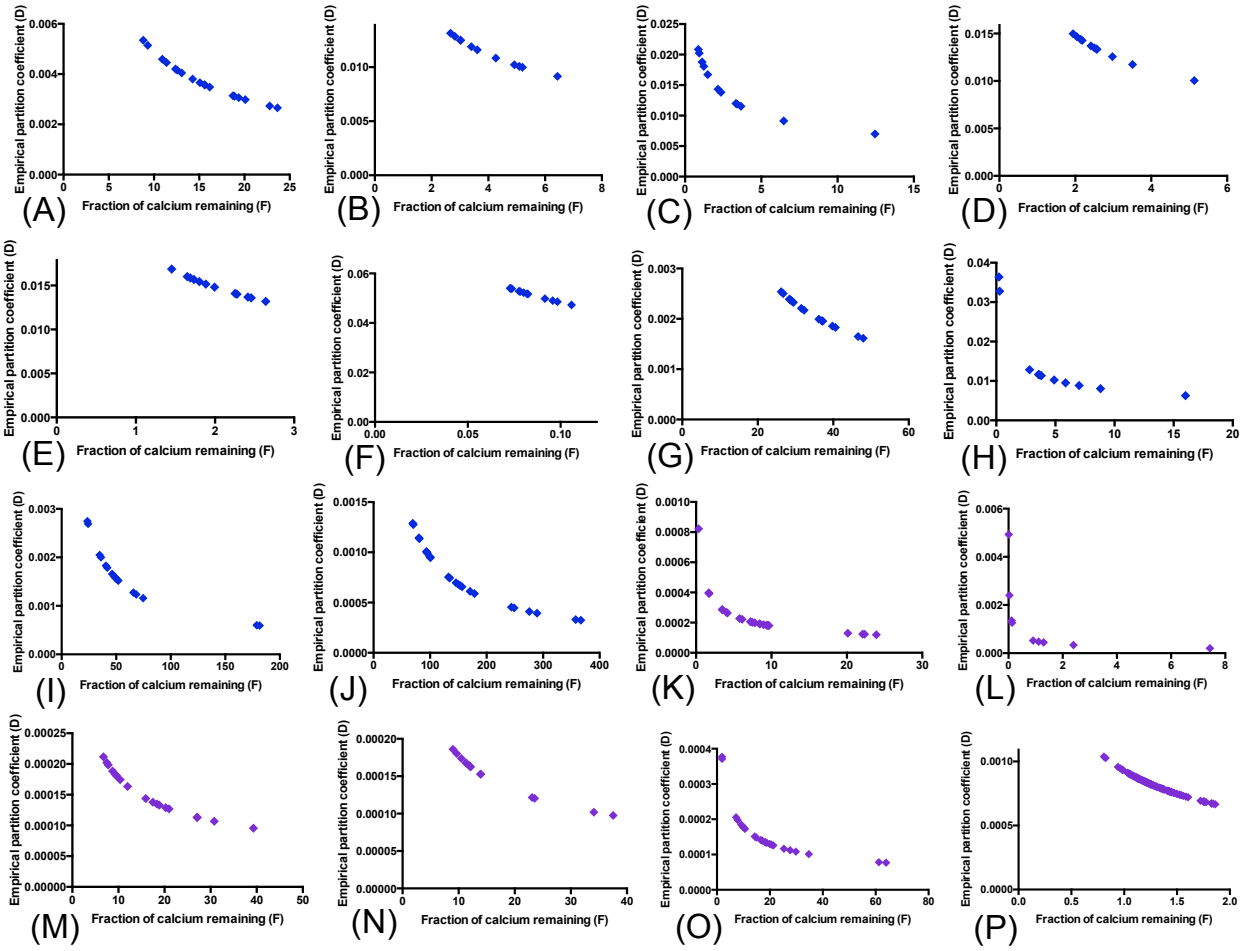

Figure 12: ***Plots of magnesium incorporation into cultured calcitic and aragonitic organisms.*** These plots are of the empirical partition coefficient (D) (y-axis) versus the fraction of calcium remaining in the calcification reservoir after calcification (F) (x-axis) for magnesium incorporation into both calcite and aragonite. These figures are for [A] bay scallop, [B] blue crab, [C] lobster, [D] purple urchin, [E] pencil urchin, [F] coralline red algae, [G] oyster, [H] shrimp, [I] blue mussel, [J] periwinkle, [K] limpet, [L] halimeda, [M] hard clam, [N] soft clam, [O] conch, and [P] coral. In this figure, blue represents the calcitic organisms and purple represents the aragonitic organisms. Figure 1c is the representative figure that summarizes the calcitic organisms, and Figure 1d is the representative figure that summarizes the aragonitic organisms.

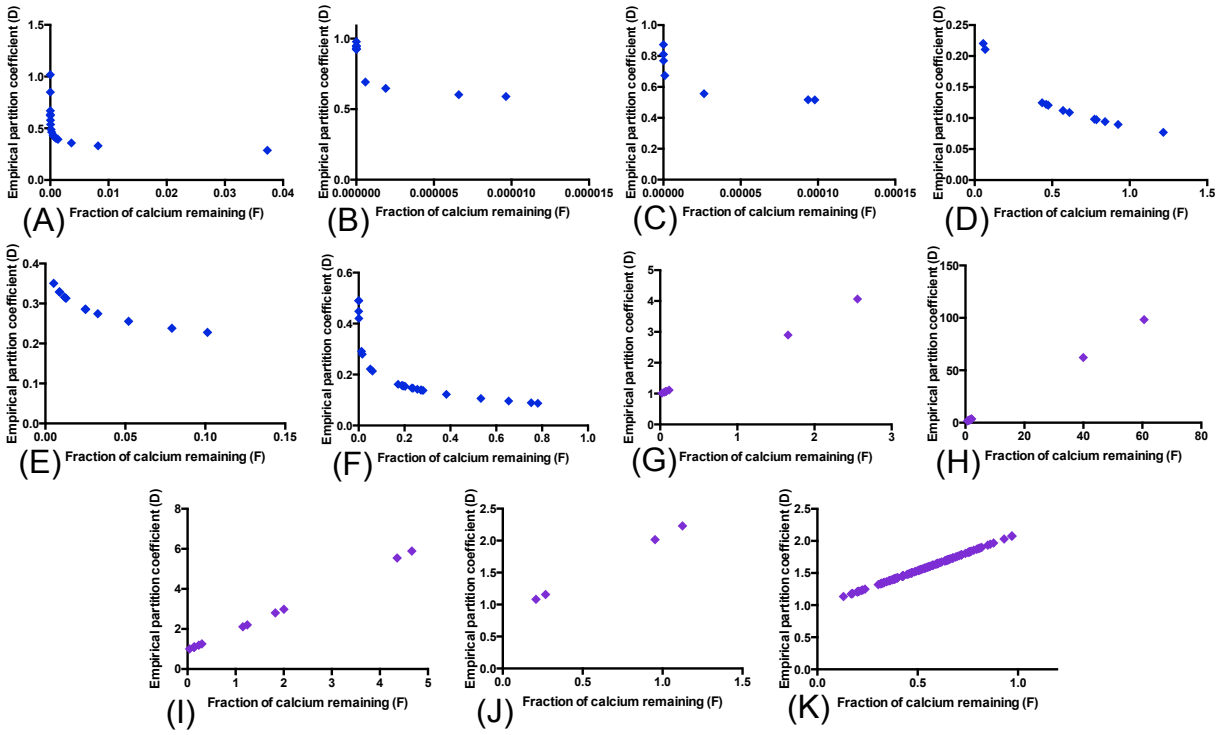

Figure 13: ***Plots of barium incorporation into cultured calcitic and aragonitic organisms.*** These plots are of the empirical partition coefficient (D) (y-axis) versus the fraction of calcium remaining in the calcification reservoir after calcification (F) (x-axis) for barium incorporation into both calcite and aragonite. These figures are for [A] bay scallop, [B] purple urchin, [C] pencil urchin, [D] oyster, [E] blue mussel, [F] periwinkle, [G] limpet, [H] halimeda, [I] hard clam, [J] soft clam, and [K] coral. In this figure, blue represents the calcitic organisms and purple represents the aragonitic organisms. Figure 1e is the representative figure that summarizes the calcitic organisms, and Figure 1f is the representative figure that summarizes the aragonitic organisms.

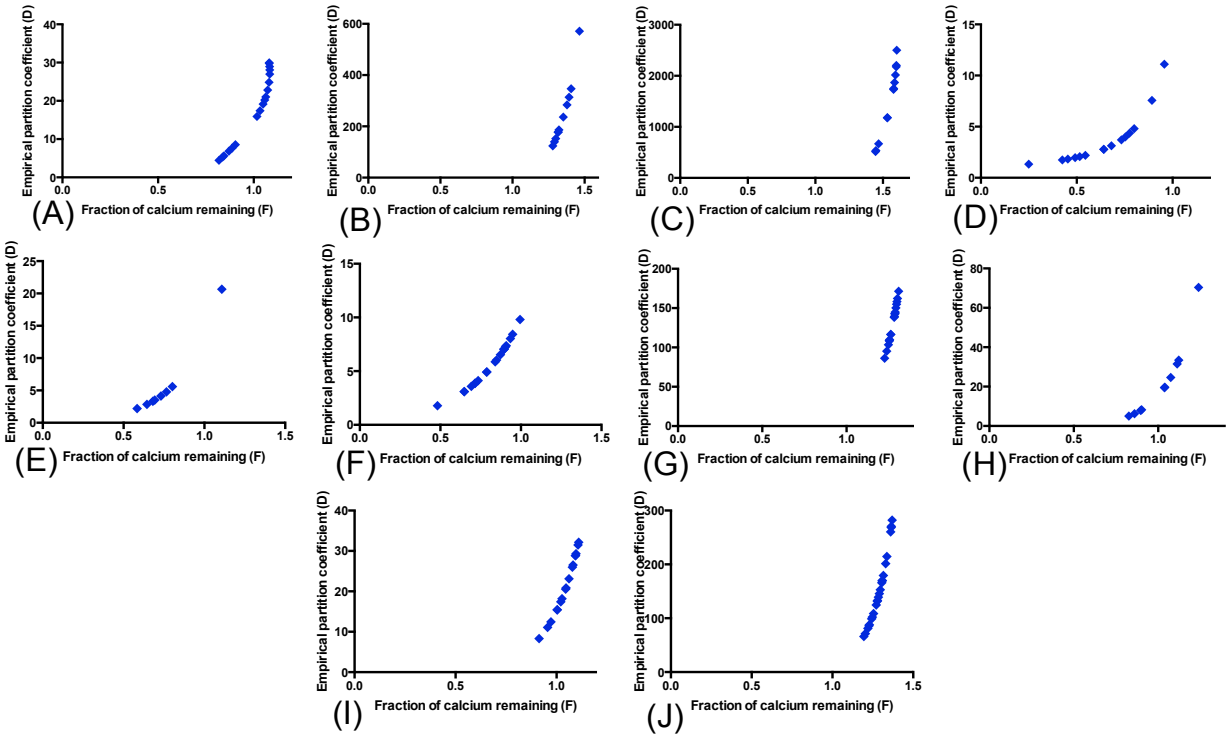

Figure 14: ***Plots of manganese incorporation into cultured calcitic organisms.*** These plots are of the empirical partition coefficient (D) (y-axis) versus the fraction of calcium remaining in the calcification reservoir after calcification (F) (x-axis) for manganese incorporation into calcite. These figures are for [A] bay scallop, [B] blue crab, [C] lobster, [D] purple urchin, [E] pencil urchin, [F] coralline red algae, [G] oyster, [H] shrimp, [I] blue mussel, and [J] periwinkle. Figure 1k was the representative figure chosen to summarize this group in the results section.

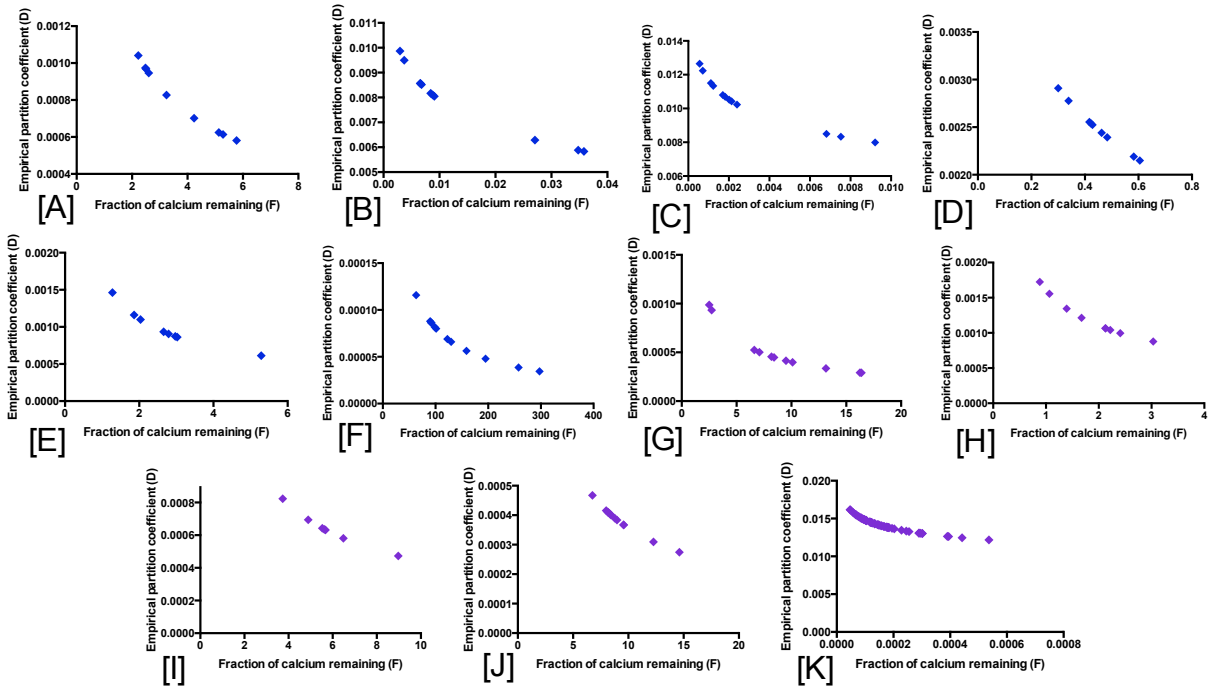

Figure 15: ***Plots of boron incorporation into cultured calcitic and aragonitic organisms.*** These plots are of the empirical partition coefficient (D) (y-axis) versus the fraction of calcium remaining in the calcification reservoir after calcification (F) (x-axis) for boron incorporation into both calcite and aragonite. These figures are for [A] bay scallop, [B] purple urchin, [C] coralline red algae, [D] oyster, [E] blue mussel, [F] periwinkle, [G] limpet, [H] hard clam, [I] soft clam, [J] conch, and [K] coral. Figure 1g is the representative figure that summarizes the calcitic organisms, and Figure 1h is the representative figure that summarizes the aragonitic organisms.

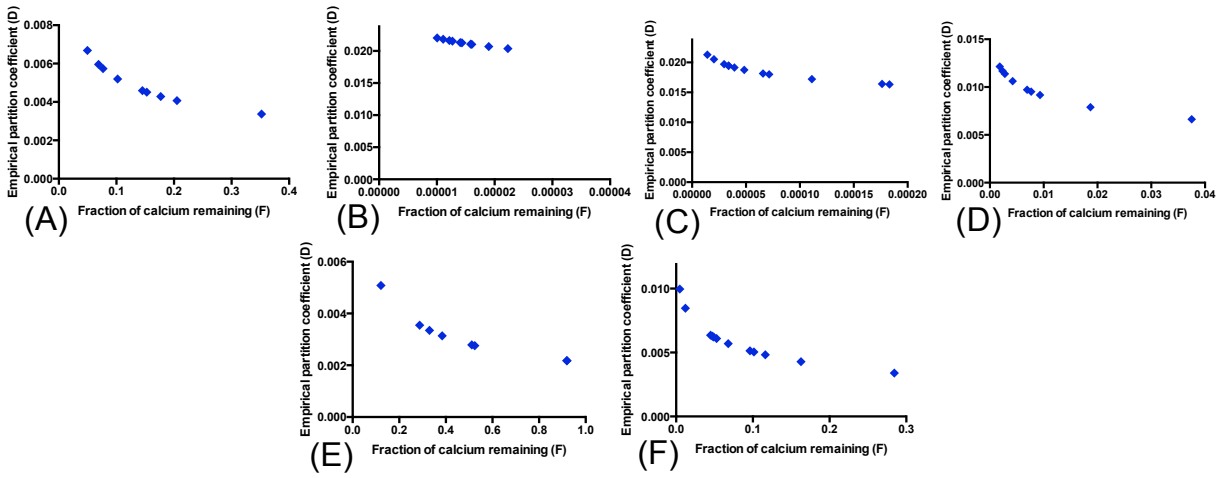

Figure 16: ***Plots of lithium incorporation into cultured calcitic organisms.*** These plots are of the empirical partition coefficient (D) (y-axis) versus the fraction of calcium remaining in the calcification reservoir after calcification (F) (x-axis) for lithium incorporation into calcite. These figures are for [A] bay scallop, [B] purple urchin, [C] coralline red algae, [D] oyster, [E] blue mussel, and [F] periwinkle. Figure 11 was the representative figure chosen to summarize this group in the results section.

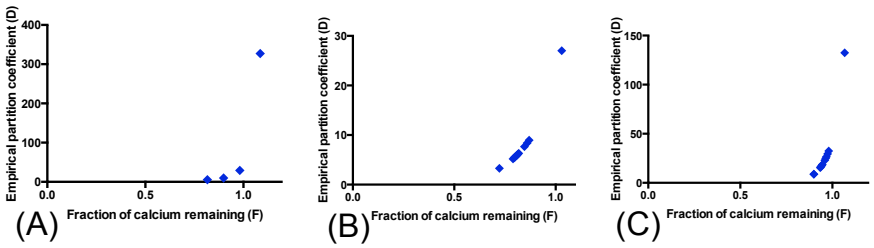

Figure 17: ***Plots of cadmium incorporation into cultured calcitic organisms.*** These plots are of the empirical partition coefficient (D) (y-axis) versus the fraction of calcium remaining in the calcification reservoir after calcification (F) (x-axis) for cadmium incorporation into calcite. These figures are for [A] bay scallop, [B] purple urchin, and [C] coralline red algae. Figure 1m was the representative figure chosen to summarize this group in the results section.

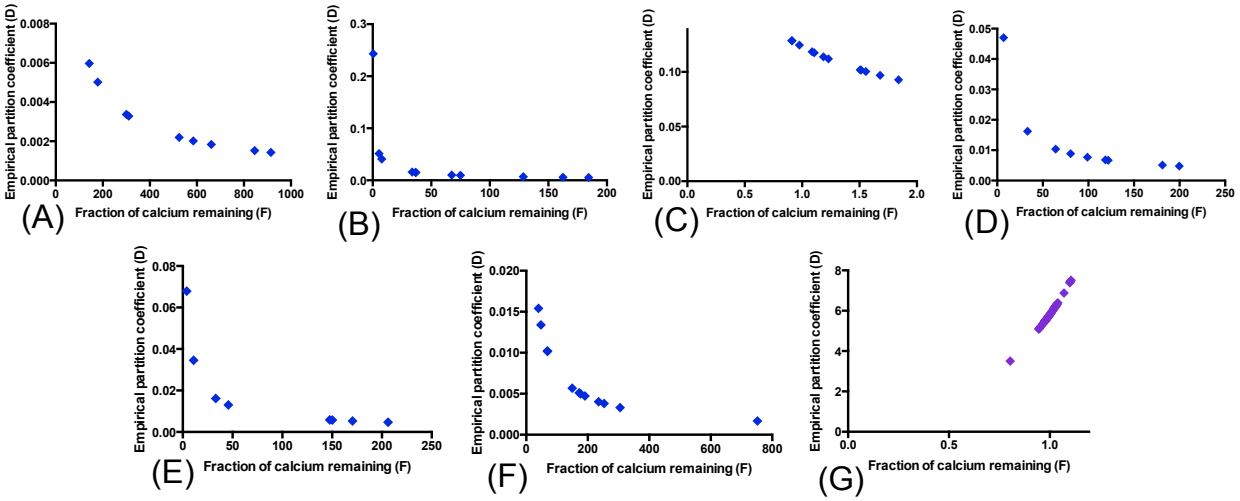

Figure 18: ***Plots of uranium incorporation into cultured calcitic and aragonitic organisms.*** These plots are of the empirical partition coefficient (D) (y-axis) versus the fraction of calcium remaining in the calcification reservoir after calcification (F) (x-axis) for uranium incorporation into both calcite and aragonite. These figures are for [A] bay scallop, [B] purple urchin, [C] coralline red algae, [D] oyster, [E] blue mussel, [F] periwinkle, and [G] coral. In this figure, blue represents the calcitic organisms and purple represents the aragonitic organisms. Figure 1i is the representative figure that summarizes the calcitic organisms, and Figure 1j is the representative figure that summarizes the aragonitic organisms.

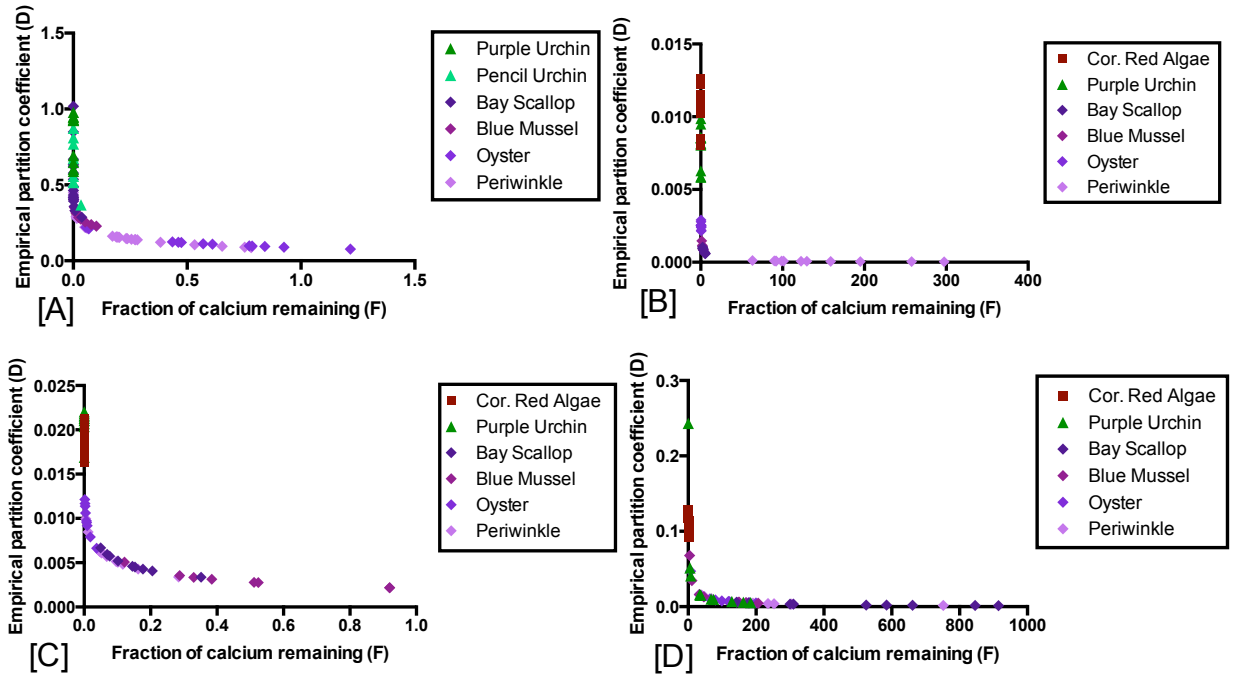

Figure 19: ***Calculations based on element partitioning into by marine invertebrates with reference to phylogenetic similarities in calcification.*** These figures present calculations of the empirical partition coefficient (D) (y-axis) versus the fraction of calcium remaining in the calcification reservoir after calcification (F) (x-axis) for the incorporation of [A] barium, [B] boron, [C] lithium, and [D] uranium in the cultured calcitic organisms.

Table 18: ***A compilation of the standard deviations and standard errors for the Sr/Ca ratios of the cultured samples at their respective pCO_2 treatment levels.***

Organism [a]	Standard Deviation [b]	Standard Error [c]
Lobster		
400 ppm	0.381	0.220
600 ppm	0.528	0.305
900 ppm	0.948	0.547
2850 ppm	0.523	0.302
Blue Crab		
400 ppm	0.466	0.330
600 ppm	0.292	0.169
900 ppm	0.243	0.140
2850 ppm	0.282	0.163
Shrimp		
400 ppm	3.38	1.95
600 ppm	0.0505	0.0357
900 ppm	1.47	0.846
2850 ppm	0.936	0.540
Bay Scallop		
400 ppm	0.0705	0.0352
600 ppm	0.0523	0.0214
900 ppm	0.0391	0.0196
2850 ppm	0.0289	0.0144
Oyster		
400 ppm	0.0267	0.0133
600 ppm	0.0526	0.0215
900 ppm	0.0216	0.0108
2850 ppm	0.100	0.0502
Blue Mussel		
400 ppm	0.0273	0.0137
600 ppm	0.206	0.0842
900 ppm	0.256	0.128
2850 ppm	0.0258	0.0129
Hard Clam		
400 ppm	0.255	0.128
600 ppm	0.263	0.107
900 ppm	0.218	0.109
2850 ppm	0.225	0.112
Soft Clam		
400 ppm	0.0352	0.0249
600 ppm	0.193	0.0967
900 ppm	0.0669	0.0335
2850 ppm	0.0919	0.0460

Conch		
400 ppm	0.147	0.0601
600 ppm	0.203	0.0831
900 ppm	0.0581	0.0237
2850 ppm	0.2481	0.101
Whelk		
400 ppm	0.219	0.0893
600 ppm	0.217	0.0887
900 ppm	0.0904	0.0369
2850 ppm	0.267	0.109
Periwinkle		
400 ppm	0.291	0.119
600 ppm	0.152	0.0621
900 ppm	0.0913	0.0373
2850 ppm	0.127	0.0520
Limpet		
400 ppm	0.102	0.0417
600 ppm	0.288	0.117
900 ppm	0.834	0.340
2850 ppm	0.117	0.0478
Serpulid Worm		
400 ppm	0.396	0.162
600 ppm	0.659	0.269
900 ppm	0.741	0.303
2850 ppm	0.490	0.200
Purple Urchin		
400 ppm	0.794	0.397
600 ppm	0.0179	0.00730
900 ppm	0.0479	0.0196
2850 ppm	0.0809	0.0330
Pencil Urchin		
400 ppm	0.114	0.0659
600 ppm	0.0710	0.0410
900 ppm	0.0527	0.0304
2850 ppm	0.0389	0.0224
Temperate Coral		
400 ppm	0.330	0.0915
600 ppm	0.403	0.0949
900 ppm	0.356	0.0919
2850 ppm	0.419	0.102
Coralline Red Algae		
400 ppm	0.0805	0.0328
600 ppm	0.158	0.0646
900 ppm	0.227	0.0927

2850 ppm	0.294	0.120
Halimeda		
400 ppm	0.386	0.223
600 ppm	0.175	0.101
2850 ppm	0.697	0.493

[a] The common name of the organism being studied.
[b] The standard deviation of the Sr/Ca ratios for the specified organism and pCO_2 treatment.
[c] The standard error of the Sr/Ca ratios for the specified organism and pCO_2 treatment.

Table 19: ***A compilation of the data for strontium incorporation in cultured organisms.***

Organism [a]	Sr/Ca (mmol/mol) [b]	D_{Sr} [c]	F_{Sr} [d]	pCO_2 [e]
Crustacea				
Lobster	6.45	0.73	9.4E-05	400
	6.43	0.73	9.7E-05	400
	5.78	0.66	2.9E-04	400
	4.41	0.50	3.1E-03	600
	3.63	0.41	1.2E-02	600
	4.64	0.53	2.1E-03	600
	5.80	0.66	2.9E-04	900
	6.25	0.71	1.3E-04	900
	4.43	0.50	2.9E-03	900
	5.26	0.60	7.2E-04	2850
	5.17	0.59	8.4E-04	2850
	4.31	0.49	3.6E-03	2850
Blue Crab	5.17	0.59	0.00084	400
	4.51	0.51	0.0026	400
	5.46	0.62	0.00051	600
	5.85	0.66	0.00026	600
	5.27	0.60	0.00070	600
	5.37	0.61	0.00060	900
	5.14	0.58	0.00088	900
	5.63	0.64	0.00038	900
	5.46	0.62	0.00051	2850
	5.46	0.62	0.00051	2850
	4.97	0.56	0.0012	2850
Shrimp	4.16	0.47	4.7E-03	400
	10.2	1.2	1.5E-07	400
	4.63	0.53	2.1E-03	400
	5.03	0.57	1.1E-03	600
	4.96	0.56	1.2E-03	600
	7.59	0.86	1.3E-05	900
	5.08	0.58	9.7E-04	900
	5.01	0.57	1.1E-03	900
	5.94	0.67	2.2E-04	2850
	4.07	0.46	5.5E-03	2850
	5.00	0.57	1.1E-03	2850
Mollusca				
Bay Scallop	1.48	0.17	0.45	400
	1.36	0.15	0.56	400
	1.51	0.17	0.43	400
	1.40	0.16	0.52	400
	1.47	0.17	0.46	600

	1.48	0.17	0.46	600
	1.38	0.16	0.54	600
	1.51	0.17	0.43	600
	1.49	0.17	0.45	600
	1.41	0.16	0.52	600
	1.29	0.15	0.63	900
	1.34	0.15	0.58	900
	1.33	0.15	0.58	900
	1.38	0.16	0.54	900
	1.36	0.15	0.55	2850
	1.38	0.16	0.54	2850
	1.40	0.16	0.52	2850
	1.43	0.16	0.49	2850
Oyster	1.21	0.14	0.72	400
	1.26	0.14	0.66	400
	1.23	0.14	0.70	400
	1.27	0.14	0.65	400
	0.921	0.10	1.2	600
	0.975	0.11	1.1	600
	0.869	0.10	1.3	600
	0.938	0.11	1.1	600
	1.02	0.12	1.0	600
	0.904	0.10	1.2	600
	0.936	0.11	1.1	900
	0.971	0.11	1.1	900
	0.956	0.11	1.1	900
	0.987	0.11	1.1	900
	0.943	0.11	1.1	2850
	1.13	0.13	0.83	2850
	0.984	0.11	1.1	2850
	1.14	0.13	0.81	2850
Blue Mussel	1.19	0.13	0.75	400
	1.15	0.13	0.79	400
	1.22	0.14	0.71	400
	1.19	0.14	0.74	400
	1.67	0.19	0.33	600
	1.33	0.15	0.58	600
	1.23	0.14	0.70	600
	1.70	0.19	0.31	600
	1.38	0.16	0.53	600
	1.25	0.14	0.67	600
	1.17	0.13	0.76	900
	1.61	0.18	0.36	900
	1.21	0.14	0.72	900
	1.65	0.19	0.34	900

	1.25	0.14	0.68	2850
	1.25	0.14	0.68	2850
	1.29	0.15	0.62	2850
	1.29	0.15	0.63	2850
Hard Clam	1.65	0.19	unreal	400
	2.12	0.24	unreal	400
	1.71	0.19	unreal	400
	2.12	0.24	unreal	400
	1.38	0.16	unreal	600
	1.93	0.22	unreal	600
	1.81	0.20	unreal	600
	1.41	0.16	unreal	600
	1.97	0.22	unreal	600
	1.82	0.21	unreal	600
	1.81	0.21	unreal	900
	2.16	0.25	unreal	900
	1.82	0.21	unreal	900
	2.22	0.25	unreal	900
	1.90	0.22	unreal	2850
	1.52	0.17	unreal	2850
	1.97	0.22	unreal	2850
	1.57	0.18	unreal	2850
Soft Clam	2.80	0.32	unreal	400
	2.75	0.31	unreal	400
	2.79	0.32	unreal	600
	2.46	0.28	unreal	600
	2.70	0.31	unreal	600
	2.38	0.27	unreal	600
	2.65	0.30	unreal	900
	2.74	0.31	unreal	900
	2.58	0.29	unreal	900
	2.61	0.30	unreal	900
	2.23	0.25	unreal	2850
	2.05	0.23	unreal	2850
	2.21	0.25	unreal	2850
	2.07	0.24	unreal	2850
Conch	1.55	0.18	unreal	400
	1.49	0.17	unreal	400
	1.25	0.14	unreal	400
	1.60	0.18	unreal	400
	1.52	0.17	unreal	400
	1.28	0.15	unreal	400
	1.81	0.20	unreal	600
	2.14	0.24	unreal	600

	2.27	0.26	unreal	600
	1.81	0.21	unreal	600
	2.09	0.24	unreal	600
	2.23	0.25	unreal	600
	1.86	0.21	unreal	900
	1.97	0.22	unreal	900
	1.85	0.21	unreal	900
	1.85	0.21	unreal	900
	1.95	0.22	unreal	900
	1.85	0.21	unreal	900
	1.48	0.17	unreal	2850
	1.95	0.22	unreal	2850
	1.99	0.23	unreal	2850
	1.51	0.17	unreal	2850
	1.94	0.22	unreal	2850
	2.01	0.23	unreal	2850
Periwinkle	1.12	0.13	0.84	400
	1.03	0.12	0.98	400
	1.63	0.18	0.35	400
	1.14	0.13	0.81	400
	1.07	0.12	0.92	400
	1.67	0.19	0.33	400
	1.33	0.15	0.59	600
	0.993	0.11	1.0	600
	1.22	0.14	0.70	600
	1.36	0.15	0.56	600
	1.03	0.12	0.98	600
	1.26	0.14	0.66	600
	1.10	0.12	0.87	900
	1.21	0.14	0.72	900
	1.01	0.11	1.0	900
	1.12	0.13	0.85	900
	1.22	0.14	0.70	900
	1.02	0.12	0.99	900
	1.07	0.12	0.92	2850
	1.14	0.13	0.81	2850
	1.35	0.15	0.57	2850
	1.10	0.12	0.87	2850
	1.19	0.13	0.75	2850
	1.37	0.16	0.55	2850
Limpet	1.82	0.21	unreal	400
	1.63	0.18	unreal	400
	1.61	0.18	unreal	400
	1.80	0.20	unreal	400
	1.61	0.18	unreal	400

	1.59	0.18	unreal	400
	1.47	0.17	unreal	600
	1.93	0.22	unreal	600
	1.33	0.15	unreal	600
	1.47	0.17	unreal	600
	1.96	0.22	unreal	600
	1.33	0.15	unreal	600
	3.24	0.37	unreal	900
	1.61	0.18	unreal	900
	1.57	0.18	unreal	900
	3.19	0.36	unreal	900
	1.64	0.19	unreal	900
	1.58	0.18	unreal	900
	1.43	0.16	unreal	2850
	1.37	0.16	unreal	2850
	1.66	0.19	unreal	2850
	1.45	0.16	unreal	2850
	1.38	0.16	unreal	2850
Echinodermata				
Purple Urchin	3.55	0.40	0.013	400
	2.15	0.24	0.14	400
	3.55	0.40	0.013	400
	2.20	0.25	0.13	400
	2.05	0.23	0.17	600
	2.05	0.23	0.17	600
	2.08	0.24	0.16	600
	2.03	0.23	0.18	600
	2.03	0.23	0.18	600
	2.06	0.23	0.17	600
	2.15	0.24	0.14	900
	2.18	0.25	0.14	900
	2.08	0.24	0.16	900
	2.17	0.25	0.14	900
	2.16	0.25	0.14	900
	2.07	0.23	0.17	900
	2.25	0.26	0.12	2850
	2.13	0.24	0.15	2850
	2.04	0.23	0.17	2850
	2.22	0.25	0.13	2850
	2.11	0.24	0.15	2850
	2.07	0.23	0.17	2850
Pencil Urchin	2.14	0.24	0.15	400
	2.03	0.23	0.18	400
	2.26	0.26	0.12	400

	2.36	0.27	0.10	600
	2.24	0.25	0.12	600
	2.24	0.25	0.12	600
	2.25	0.26	0.12	900
	2.20	0.25	0.13	900
	2.30	0.26	0.11	900
	2.18	0.25	0.14	2850
	2.25	0.26	0.12	2850
	2.20	0.25	0.13	2850
Cnidaria				
Temperate Coral	9.90	1.1	0.48	400
	10.1	1.1	0.60	400
	10.1	1.1	0.65	400
	9.66	1.1	0.33	400
	9.23	1.0	0.12	400
	9.85	1.1	0.45	400
	9.92	1.1	0.50	400
	9.93	1.1	0.50	400
	9.10	1.0	0.075	400
	9.26	1.0	0.13	400
	9.87	1.1	0.46	400
	9.89	1.1	0.48	400
	9.71	1.1	0.36	400
	10.1	1.1	0.60	600
	10.0	1.1	0.56	600
	10.0	1.1	0.58	600
	9.63	1.1	0.32	600
	9.83	1.1	0.44	600
	9.18	1.0	0.10	600
	10.3	1.2	0.77	600
	9.10	1.0	0.074	600
	10.0	1.1	0.58	600
	9.23	1.0	0.12	600
	9.19	1.0	0.11	600
	9.25	1.0	0.13	600
	9.19	1.0	0.11	600
	9.83	1.1	0.44	600
	9.99	1.1	0.54	600
	9.33	1.1	0.16	600
	9.31	1.1	0.16	600
	9.28	1.1	0.14	600
	9.93	1.1	0.50	900
	10.2	1.2	0.67	900
	10.0	1.1	0.57	900
	9.34	1.1	0.17	900

	9.82	1.1	0.43	900
	9.75	1.1	0.39	900
	9.79	1.1	0.41	900
	9.31	1.1	0.16	900
	9.36	1.1	0.18	900
	9.13	1.0	0.085	900
	9.20	1.0	0.11	900
	9.44	1.1	0.22	900
	10.0	1.1	0.58	900
	9.10	1.0	0.077	900
	9.73	1.1	0.37	900
	10.1	1.1	0.65	2850
	10.1	1.1	0.66	2850
	10.1	1.1	0.64	2850
	9.21	1.0	0.12	2850
	9.08	1.0	0.069	2850
	9.28	1.1	0.14	2850
	9.33	1.1	0.16	2850
	9.18	1.0	0.10	2850
	9.15	1.0	0.09	2850
	9.73	1.1	0.37	2850
	9.19	1.0	0.11	2850
	9.88	1.1	0.47	2850
	9.81	1.1	0.43	2850
	9.04	1.0	0.054	2850
	10.1	1.1	0.66	2850
	9.27	1.1	0.14	2850
	9.70	1.1	0.36	2850
Rhodophyta				
Coralline Red Algae	3.31	0.38	0.020	400
	3.29	0.37	0.021	400
	3.18	0.36	0.025	400
	3.18	0.36	0.025	400
	3.17	0.36	0.025	400
	3.10	0.35	0.029	400
	3.16	0.36	0.026	600
	3.47	0.39	0.015	600
	3.20	0.36	0.024	600
	3.02	0.34	0.033	600
	3.24	0.37	0.023	600
	3.08	0.35	0.030	600
	2.91	0.33	0.039	900
	3.21	0.36	0.023	900
	3.41	0.39	0.017	900
	2.82	0.32	0.046	900

	3.11	0.35	0.028	900
	3.29	0.37	0.021	900
	3.77	0.43	0.009	2850
	3.49	0.40	0.015	2850
	3.12	0.35	0.027	2850
	3.61	0.41	0.012	2850
	3.34	0.38	0.019	2850
	3.00	0.34	0.034	2850
Chlorophyte				
Halimeda	10.5	1.2	0.96	400
	11.0	1.2	1.5	400
	10.2	1.2	0.75	400
	9.29	1.1	0.14	600
	9.52	1.1	0.25	600
	9.63	1.1	0.31	600
	10.8	1.2	1.3	900
	9.93	1.1	0.50	2850
	8.95	1.0	0.03	2850

[a] Common name of the organisms with the phyla names in shaded gray.
[b] Strontium-to-Calcium ratio in units of milli-moles Sr / moles Ca.
[c] Empirical partition coefficient (D).
[d] Fraction of calcium remaining in the calcification reservoir after biomineralization (F).
[e] The pCO_2 treatment in which the organism was grown.

Table 20: ***A compilation of the standard deviations and standard errors for the Mg/Ca ratios of the cultured samples at their respective pCO_2 treatment levels.***

Organism [a]	Standard Deviation [b]	Standard Error [c]
Lobster		
400 ppm	15.3	8.81
600 ppm	11.7	6.77
900 ppm	23.6	13.6
2850 ppm	18.0	10.4
Blue Crab		
400 ppm	11.1	7.86
600 ppm	6.53	3.77
900 ppm	8.74	5.04
2850 ppm	5.15	2.98
Shrimp		
400 ppm	72.3	41.7
600 ppm	5.16	3.65
900 ppm	77.2	44.5
2850 ppm	17.8	10.3
Bay Scallop		
400 ppm	3.44	1.72
600 ppm	4.17	1.70
900 ppm	2.73	1.36
2850 ppm	4.16	2.08
Oyster		
400 ppm	0.506	0.253
600 ppm	1.75	0.713
900 ppm	0.699	0.349
2850 ppm	1.53	0.763
Blue Mussel		
400 ppm	1.13	0.565
600 ppm	1.15	0.470
900 ppm	1.67	0.830
2850 ppm	3.39	1.70
Hard Clam		
400 ppm	0.214	0.107
600 ppm	0.258	0.105
900 ppm	0.111	0.0554
2850 ppm	0.0188	0.00938
Soft Clam		
400 ppm	0.0214	0.0151
600 ppm	0.175	0.0874
900 ppm	0.0540	0.0270
2850 ppm	0.110	0.0552

Conch		
400 ppm	0.730	0.298
600 ppm	0.0670	0.0273
900 ppm	0.0626	0.0256
2850 ppm	0.105	0.0430
Whelk		
400 ppm	0.324	0.132
600 ppm	0.371	0.151
900 ppm	0.6322	0.258
2850 ppm	0.0765	0.0312
Periwinkle		
400 ppm	1.78	0.726
600 ppm	0.866	0.356
900 ppm	0.6219	0.254
2850 ppm	1.99	0.811
Limpet		
400 ppm	0.332	0.136
600 ppm	0.369	0.150
900 ppm	0.485	0.198
2850 ppm	1.32	0.540
Serpulid Worm		
400 ppm	3.80	2.19
600 ppm	9.32	5.38
900 ppm	10.8	6.23
2850 ppm	14.0	8.11
Purple Urchin		
400 ppm	16.8	11.9
600 ppm	4.64	2.68
900 ppm	1.92	1.11
2850 ppm	4.18	2.41
Pencil Urchin		
400 ppm	3.63	2.10
600 ppm	10.2	5.91
900 ppm	6.13	3.54
2850 ppm	2.22	1.28
Temperate Coral		
400 ppm	0.294	0.0578
600 ppm	0.677	0.113
900 ppm	0.338	0.0617
2850 ppm	0.373	0.0641
Coralline Red Algae		
400 ppm	14.6	8.45
600 ppm	5.04	2.91
900 ppm	7.54	4.35

2850 ppm	11.4	6.57
Halimeda		
400 ppm	2.57	1.48
600 ppm	5.93	3.42
2850 ppm	16.0	11.3

[a] The common name of the organism being studied.
[b] The standard deviation of the Mg/Ca ratios for the specified organism and pCO_2 treatment.
[c] The standard error of the Mg/Ca ratios for the specified organism and pCO_2 treatment.

Table 21: ***A compilation of the data for magnesium incorporation in cultured organisms.***

Organism [a]	Mg/Ca (mmol/mol) [b]	D_{Mg} [c]	F_{Mg} [d]	pCO_2 [e]
Crustacea				
Lobster	104	0.020	0.93	400
	85.9	0.017	1.5	400
	73.6	0.014	2.2	400
	46.9	0.0091	6.5	600
	35.9	0.0070	12	600
	59.3	0.012	3.7	600
	92.8	0.018	1.2	900
	107	0.021	0.87	900
	61.0	0.012	3.4	900
	96.4	0.019	1.1	2850
	71.0	0.014	2.4	2850
	61.6	0.012	3.3	2850
Blue Crab	67.5	0.013	2.7	400
	51.8	0.010	5.1	400
	64.2	0.012	3.0	600
	59.6	0.012	3.6	600
	51.3	0.010	5.2	600
	64.1	0.012	3.0	900
	47.0	0.0092	6.4	900
	52.5	0.010	4.9	900
	55.7	0.011	4.3	2850
	61.1	0.012	3.4	2850
	66.0	0.013	2.8	2850
Shrimp	45.4	0.0088	7.0	400
	168	0.033	0.29	400
	41.3	0.0080	8.8	400
	59.9	0.012	3.6	600
	52.6	0.010	4.9	600
	187	0.036	0.22	900
	58.3	0.011	3.8	900
	48.9	0.0095	5.9	900
	59.3	0.012	3.7	2850
	32.3	0.0063	16	2850
	66.0	0.013	2.8	2850
Mollusca				
Bay Scallop	21.6	0.0042	12	400
	15.7	0.0031	19	400
	21.4	0.0042	13	400
	15.3	0.0030	20	400
	18.3	0.0036	16	600

	27.5	0.0053	8.8	600
	20.8	0.0040	13	600
	17.9	0.0035	16	600
	26.4	0.0051	9.3	600
	19.5	0.0038	14	600
	14.0	0.0027	23	900
	18.8	0.0037	15	900
	13.7	0.0027	24	900
	18.3	0.0036	16	900
	23.6	0.0046	11	2850
	16.1	0.0031	19	2850
	22.9	0.0045	11	2850
	16.0	0.0031	19	2850
Oyster	13.0	0.0025	26	400
	12.1	0.0024	29	400
	12.8	0.0025	27	400
	12.0	0.0023	29	400
	10.2	0.0020	36	600
	12.3	0.0024	28	600
	8.29	0.0016	48	600
	10.1	0.0020	37	600
	12.3	0.0024	28	600
	8.47	0.0016	47	600
	10.0	0.0020	37	900
	11.3	0.0022	32	900
	10.1	0.0020	37	900
	11.2	0.0022	32	900
	9.54	0.0019	40	2850
	12.2	0.0024	29	2850
	9.40	0.0018	41	2850
	12.0	0.0023	29	2850
Blue Mussel	6.54	0.0013	66	400
	8.52	0.0017	46	400
	6.35	0.0012	68	400
	8.27	0.0016	48	400
	9.40	0.0018	41	600
	10.5	0.0020	35	600
	7.89	0.0015	51	600
	9.18	0.0018	42	600
	10.3	0.0020	36	600
	7.81	0.0015	52	600
	5.97	0.0012	74	900
	3.06	0.0006	180	900
	5.95	0.0012	75	900
	3.09	0.0006	180	900

	14.1	0.0027	24	2850
	8.09	0.0016	50	2850
	13.8	0.0027	24	2850
	8.09	0.0016	50	2850
Hard Clam	0.581	0.00011	27	400
	1.02	0.00020	7.8	400
	0.581	0.00011	27	400
	0.840	0.00016	12	400
	0.548	0.00011	31	600
	1.04	0.00020	7.5	600
	0.942	0.00018	9.3	600
	0.491	0.00010	39	600
	1.09	0.00021	6.8	600
	0.968	0.00019	8.7	600
	0.897	0.00017	10	900
	0.708	0.00014	17	900
	0.928	0.00018	10	900
	0.739	0.00014	16	900
	0.684	0.00013	19	2850
	0.652	0.00013	21	2850
	0.693	0.00013	18	2850
	0.662	0.00013	20	2850
Soft Clam	0.862	0.00017	11	400
	0.892	0.00017	10	400
	0.785	0.00015	14	600
	0.501	0.00010	38	600
	0.839	0.00016	12	600
	0.524	0.00010	34	600
	0.956	0.00019	9.0	900
	0.842	0.00016	12	900
	0.926	0.00018	10	900
	0.860	0.00017	11	900
	0.624	0.00012	23	2850
	0.835	0.00016	12	2850
	0.619	0.00012	24	2850
	0.784	0.00015	14	2850
Conch	1.91	0.00037	2.0	400
	0.647	0.00013	21	400
	0.394	0.000077	64	400
	1.94	0.00038	1.9	400
	0.658	0.00013	21	400
	0.402	0.00008	61	400
	0.887	0.00017	11	600
	0.915	0.00018	9.9	600

	1.02	0.00020	7.8	600
	0.910	0.00018	10	600
	0.947	0.00018	9.2	600
	1.06	0.00021	7.2	600
	0.694	0.00014	18	900
	0.575	0.00011	28	900
	0.685	0.00013	19	900
	0.714	0.00014	17	900
	0.599	0.00012	25	900
	0.725	0.00014	17	900
	0.519	0.00010	35	2850
	0.761	0.00015	15	2850
	0.667	0.00013	20	2850
	0.556	0.00011	30	2850
	0.776	0.00015	14	2850
	0.694	0.00014	18	2850
Periwinkle	5.83	0.0011	81	400
	4.92	0.0010	99	400
	2.03	0.00039	290	400
	5.88	0.0011	80	400
	5.10	0.0010	95	400
	2.11	0.00041	280	400
	3.03	0.00059	180	600
	3.49	0.00068	150	600
	1.66	0.00032	370	600
	3.14	0.00061	170	600
	3.58	0.00070	150	600
	1.70	0.00033	360	600
	3.87	0.00075	130	900
	4.86	0.00095	1.0E2	900
	5.17	0.0010	94	900
	3.82	0.00074	140	900
	4.90	0.0010	1.0E2	900
	5.17	0.0010	94	900
	3.37	0.00066	160	2850
	6.56	0.0013	70.	2850
	2.30	0.00045	250	2850
	3.44	0.00067	150	2850
	6.63	0.0013	69	2850
	2.34	0.00045	240	2850
Limpet	1.37	0.00027	4.0	400
	0.933	0.00018	9.5	400
	0.615	0.00012	24	400
	1.36	0.00026	4.2	400
	0.925	0.00018	9.7	400

	0.637	0.00012	22	400
	0.634	0.00012	22	600
	1.47	0.00029	3.5	600
	0.982	0.00019	8.5	600
	0.664	0.00013	20	600
	1.46	0.00028	3.5	600
	0.986	0.00019	8.4	600
	2.01	0.00039	1.7	900
	1.14	0.00022	6.1	900
	1.02	0.00020	7.8	900
	2.04	0.00040	1.7	900
	1.17	0.00023	5.8	900
	1.05	0.00021	7.2	900
	1.04	0.00020	7.5	2850
	0.930	0.00018	9.6	2850
	0.941	0.00018	9.3	2850
	1.06	0.00021	7.2	2850
	0.959	0.00019	8.9	2850
	4.22	0.00082	0.34	2850
Echinodermata				
Purple Urchin	51.6	0.010	5.1	400
	75.4	0.015	2.0	400
	69.3	0.013	2.5	600
	68.5	0.013	2.6	600
	76.9	0.015	1.9	600
	73.3	0.014	2.2	900
	73.9	0.014	2.1	900
	70.4	0.014	2.4	900
	60.3	0.012	3.5	2850
	68.7	0.013	2.6	2850
	64.5	0.013	3.0	2850
Pencil Urchin	76.1	0.015	2.0	400
	72.0	0.014	2.3	400
	79.3	0.015	1.8	400
	67.8	0.013	2.6	600
	70.3	0.014	2.4	600
	86.7	0.017	1.5	600
	72.4	0.014	2.3	900
	69.8	0.014	2.5	900
	81.5	0.016	1.7	900
	80.6	0.016	1.7	2850
	77.9	0.015	1.9	2850
	82.3	0.016	1.6	2850
Cnidaria				

Temperate Coral	3.92	0.00076	1.4	400
	4.03	0.00078	1.4	400
	4.03	0.00078	1.4	400
	4.64	0.00090	1.0	400
	3.53	0.00069	1.8	400
	4.68	0.00091	1.0	400
	3.94	0.00077	1.4	400
	4.24	0.00083	1.2	400
	4.16	0.00081	1.3	400
	4.22	0.00082	1.3	400
	4.02	0.00078	1.4	400
	4.06	0.00079	1.3	400
	4.36	0.00085	1.2	400
	3.91	0.00076	1.4	400
	3.96	0.00077	1.4	400
	3.94	0.00077	1.4	400
	4.54	0.00088	1.1	400
	3.45	0.00067	1.8	400
	4.56	0.00089	1.1	400
	3.87	0.00075	1.5	400
	4.12	0.00080	1.3	400
	4.07	0.00079	1.3	400
	4.08	0.00079	1.3	400
	4.01	0.00078	1.4	400
	3.97	0.00077	1.4	400
	4.31	0.00084	1.2	400
	4.47	0.00087	1.1	600
	4.29	0.00084	1.2	600
	4.13	0.00080	1.3	600
	4.92	0.00096	0.94	600
	4.52	0.00088	1.1	600
	4.30	0.00084	1.2	600
	3.56	0.00069	1.7	600
	4.50	0.00088	1.1	600
	4.45	0.00087	1.1	600
	4.81	0.00094	1.0	600
	4.47	0.00087	1.1	600
	4.48	0.00087	1.1	600
	4.48	0.00087	1.1	600
	4.29	0.00084	1.2	600
	3.94	0.00077	1.4	600
	4.30	0.00084	1.2	600
	5.33	0.0010	0.81	600
	4.14	0.00081	1.3	600
	4.44	0.00086	1.1	600

	4.07	0.00079	1.3	600
	4.86	0.00095	1.0	600
	0.97	0.00019	unreal	600
	4.46	0.00087	1.1	600
	4.27	0.00083	1.2	600
	3.52	0.00069	1.8	600
	4.44	0.00086	1.1	600
	4.40	0.00086	1.2	600
	4.66	0.00091	1.0	600
	4.34	0.00085	1.2	600
	4.34	0.00084	1.2	600
	4.35	0.00085	1.2	600
	4.24	0.00083	1.2	600
	3.96	0.00077	1.4	600
	4.29	0.00084	1.2	600
	5.28	0.0010	0.79	600
	4.08	0.00079	1.3	600
	4.05	0.00079	1.4	900
	3.46	0.00067	1.8	900
	3.83	0.00075	1.5	900
	3.73	0.00073	1.6	900
	4.24	0.00082	1.2	900
	4.47	0.00087	1.1	900
	4.18	0.00081	1.3	900
	4.60	0.00090	1.1	900
	4.37	0.00085	1.2	900
	4.33	0.00084	1.2	900
	3.92	0.00076	1.4	900
	4.43	0.00086	1.1	900
	4.23	0.00082	1.2	900
	4.61	0.00090	1.1	900
	4.55	0.00089	1.1	900
	4.04	0.00079	1.4	900
	3.42	0.00067	1.9	900
	3.85	0.00075	1.5	900
	3.70	0.00072	1.6	900
	4.24	0.00082	1.2	900
	4.43	0.00086	1.1	900
	4.12	0.00080	1.3	900
	4.52	0.00088	1.1	900
	4.32	0.00084	1.2	900
	4.28	0.00083	1.2	900
	3.91	0.00076	1.4	900
	4.41	0.00086	1.2	900
	4.18	0.00081	1.3	900

	4.64	0.00090	1.0	900
	4.59	0.00089	1.1	900
	3.44	0.00067	1.8	2850
	3.80	0.00074	1.5	2850
	3.53	0.00069	1.8	2850
	4.33	0.00084	1.2	2850
	3.94	0.00077	1.4	2850
	4.25	0.00083	1.2	2850
	4.80	0.00093	1.0	2850
	4.59	0.00089	1.1	2850
	4.49	0.00087	1.1	2850
	4.44	0.00086	1.1	2850
	4.37	0.00085	1.2	2850
	4.32	0.00084	1.2	2850
	4.27	0.00083	1.2	2850
	4.26	0.00083	1.2	2850
	3.78	0.00074	1.5	2850
	4.63	0.00090	1.1	2850
	4.21	0.00082	1.3	2850
	3.51	0.00068	1.8	2850
	3.76	0.00073	1.6	2850
	3.53	0.00069	1.8	2850
	4.21	0.00082	1.3	2850
	3.88	0.00076	1.5	2850
	4.31	0.00084	1.2	2850
	4.79	0.00093	1.0	2850
	4.55	0.00089	1.1	2850
	4.48	0.00087	1.1	2850
	4.49	0.00087	1.1	2850
	4.38	0.00085	1.2	2850
	4.30	0.00084	1.2	2850
	4.23	0.00082	1.3	2850
	4.19	0.00082	1.3	2850
	3.80	0.00074	1.5	2850
	4.64	0.00090	1.0	2850
	4.22	0.00082	1.3	2850
Rhodophyta				
Coralline Red Algae	277	0.054	0.073	400
	249	0.049	0.098	400
	271	0.053	0.078	400
	268	0.052	0.080	600
	278	0.054	0.073	600
	276	0.054	0.074	600
	271	0.053	0.078	900
	256	0.050	0.092	900

	266	0.052	0.082	900
	252	0.049	0.096	2850
	266	0.052	0.082	2850
	243	0.047	0.11	2850
Chlorophyte				
Halimeda	6.95	0.0014	0.11	400
	2.30	0.00045	1.3	400
	6.50	0.0013	0.13	400
	12.3	0.0024	0.031	600
	2.46	0.00048	1.1	600
	1.74	0.00034	2.4	600
	1.04	0.00020	7.4	900
	2.69	0.00052	0.91	2850
	25.3	0.0049	0.0064	2850

[a] Common name of the organisms with the phyla names in shaded gray.
[b] Magnesium-to-Calcium ratio in units of milli-moles Mg / moles Ca.
[c] Empirical partition coefficient (D).
[d] Fraction of calcium remaining in the calcification reservoir after biomineralization (F).
[e] The pCO_2 treatment in which the organism was grown.

Table 22: ***A compilation of the standard deviations and standard errors for the Ba/Ca ratios of the cultured samples at their respective pCO_2 treatment levels.***

Organism [a]	Standard Deviation [b]	Standard Error [c]
Lobster		
400 ppm	12.6	7.29
600 ppm	457	264
900 ppm	37.4	21.6
2850 ppm	12.6	7.30
Blue Crab		
400 ppm	7.03	4.97
600 ppm	268	155
900 ppm	42.9	24.8
2850 ppm	14.2	8.20
Shrimp		
400 ppm	79.9	46.1
900 ppm	40.6	23.5
2850 ppm	20.2	11.6
Bay Scallop		
400 ppm	0.907	0.454
600 ppm	2.21	0.902
900 ppm	1.24	0.619
2850 ppm	0.995	0.498
Oyster		
400 ppm	0.521	0.261
600 ppm	6.86	2.80
900 ppm	0.0990	0.0495
2850 ppm	0.0889	0.0444
Blue Mussel		
400 ppm	0.540	0.270
600 ppm	6.50	2.65
900 ppm	0.472	0.236
2850 ppm	0.208	0.104
Hard Clam		
400 ppm	1.42	0.709
600 ppm	16.4	6.68
900 ppm	1.08	0.541
2850 ppm	0.232	0.116
Soft Clam		
400 ppm	0.879	0.621
600 ppm	5.70	2.85
900 ppm	1.38	0.688
2850 ppm	1.23	0.615
Conch		

400 ppm	0.866	0.353
600 ppm	1.32	0.538
900 ppm	0.989	0.404
2850 ppm	0.718	0.293
Whelk		
400 ppm	0.860	0.351
600 ppm	8.17	3.33
900 ppm	1.20	0.489
2850 ppm	0.868	0.355
Periwinkle		
400 ppm	0.280	0.114
600 ppm	1.25	0.511
900 ppm	0.249	0.102
2850 ppm	0.671	0.274
Limpet		
400 ppm	0.466	0.190
600 ppm	3.62	1.48
900 ppm	15.7	6.42
2850 ppm	2.78	1.13
Serpulid Worm		
400 ppm	24.5	9.99
600 ppm	111	45.3
900 ppm	39.4	16.1
2850 ppm	59.9	24.4
Purple Urchin		
400 ppm	0.455	0.228
600 ppm	1.09	0.446
900 ppm	1.67	0.684
2850 ppm	0.996	0.407
Pencil Urchin		
400 ppm	0.791	0.457
600 ppm	2.88	1.66
900 ppm	3.44	1.99
2850 ppm	1.15	0.663
Temperate Coral		
400 ppm	1.52	0.298
600 ppm	1	0.457
900 ppm	2.10	0.383
2850 ppm	2.24	0.383
Coralline Red Algae		
400 ppm	5.67	2.31
600 ppm	6.44	2.63
900 ppm	7.35	3.00
2850 ppm	1.76	0.720

Halimeda		
400 ppm	7.58	4.38
600 ppm	248	175
2850 ppm	12.1	8.55

[a] The common name of the organism being studied.
[b] The standard deviation of the Ba/Ca ratios for the specified organism and pCO_2 treatment.
[c] The standard error of the Ba/Ca ratios for the specified organism and pCO_2 treatment.

Table 23: ***A compilation of the data for barium incorporation in cultured organisms.***

Organism [a]	Ba/Ca (µmol/mol) [b]	D_{Ba} [c]	F_{Ba} [d]	pCO_2 [e]
Crustacea				
Lobster	156	16.1	unreal	400
	150	15.4	unreal	400
	174	17.9	unreal	400
	4684	482	unreal	600
	5291	545	unreal	600
	4396	453	unreal	600
	180	18.5	unreal	900
	155	15.9	unreal	900
	106	10.9	unreal	900
	64.6	6.65	unreal	2850
	52.6	5.42	unreal	2850
	77.9	8.02	unreal	2850
Blue Crab	39.4	4.05	unreal	400
	29.4	3.03	unreal	400
	912	93.9	unreal	600
	1418	146	unreal	600
	1319	136	unreal	600
	108	11.1	unreal	900
	48.1	4.96	unreal	900
	24.9	2.57	unreal	900
	23.6	2.43	unreal	2850
	50.6	5.21	unreal	2850
	29.4	3.02	unreal	2850
Shrimp	50.4	5.19	unreal	400
	183	18.8	unreal	400
	39.6	4.07	unreal	400
		6.51	unreal	900
		4.04	unreal	900
	63.2	12.2	unreal	900
	39.2	6.94	unreal	2850
	118	4.86	unreal	2850
	67.3	2.78	unreal	2850
Mollusca				
Bay Scallop	4.07	0.419	0.000677	400
	3.47	0.358	0.00362	400
	5.62	0.579	0.0000227	400
	4.21	0.433	0.000480	400
	3.93	0.405	0.000990	600
	6.50	0.670	0.00000484	600
	6.05	0.624	0.0000103	600

	4.73	0.488	0.000137	600
	9.89	1.02	5.784E-08	600
	8.25	0.850	3.912E-07	600
	3.21	0.331	0.00821	900
	4.02	0.414	0.000778	900
	4.49	0.463	0.000240	900
	6.15	0.633	0.000009	900
	3.92	0.404	0.00101	2850
	2.79	0.287	0.0373	2850
	5.21	0.537	0.0000497	2850
	3.82	0.393	0.00133	2850
Oyster	1.21	0.125	0.436	400
	2.05	0.211	0.0683	400
	1.17	0.121	0.474	400
	2.14	0.220	0.0557	400
	12.4	1.28	unreal	600
	12.6	1.30	unreal	600
	25.1	2.59	unreal	600
	13.0	1.34	unreal	600
	13.5	1.39	unreal	600
	27.1	2.79	unreal	600
	1.09	0.112	0.570	900
	1.19	0.122	0.461	900
	0.946	0.0974	0.785	900
	1.06	0.109	0.612	900
	0.872	0.0898	0.926	2850
	0.953	0.0981	0.773	2850
	0.748	0.0771	1.22	2850
	0.915	0.0942	0.841	2850
Blue Mussel	2.21	0.228	0.101	400
	2.67	0.275	0.0328	400
	2.31	0.238	0.0792	400
	3.40	0.351	0.00525	400
	25.0	2.58	unreal	600
	15.1	1.55	unreal	600
	12.2	1.26	unreal	600
	28.1	2.89	unreal	600
	17.4	1.79	unreal	600
	13.5	1.39	unreal	600
	2.21	0.227	0.103	900
	3.07	0.316	0.0120	900
	2.48	0.256	0.0521	900
	3.20	0.329	0.00879	900
	2.78	0.286	0.0250	2850
	2.77	0.286	0.0252	2850

	3.04	0.313	0.0129	2850
	3.19	0.329	0.00884	2850
Hard Clam	8.07	0.832	unreal	400
	10.6	1.09	0.134	400
	8.36	0.861	unreal	400
	10.7	1.10	0.144	400
	20.5	2.11	1.15	600
	27.2	2.80	1.83	600
	53.8	5.54	4.36	600
	21.4	2.20	1.24	600
	29.0	2.98	2.00	600
	57.2	5.89	4.66	600
	11.6	1.19	0.234	900
	9.74	1.00	0.0420	900
	12.2	1.26	0.299	900
	10.6	1.09	0.131	900
	6.29	0.648	unreal	2850
	6.06	0.624	unreal	2850
	6.61	0.681	unreal	2850
	6.40	0.659	unreal	2850
Soft Clam	5.92	0.610	unreal	400
	7.17	0.738	unreal	400
	19.6	2.02	0.953	600
	10.5	1.08	0.208	600
	21.7	2.23	1.12	600
	11.2	1.16	0.268	600
	4.04	0.416	unreal	900
	5.40	0.556	unreal	900
	4.28	0.441	unreal	900
	7.06	0.727	unreal	900
	5.13	0.528	unreal	2850
	3.19	0.328	unreal	2850
	5.23	0.539	unreal	2850
	2.93	0.302	unreal	2850
Conch	2.74	0.282	unreal	400
	2.26	0.233	unreal	400
	1.10	0.113	unreal	400
	2.96	0.305	unreal	400
	2.48	0.256	unreal	400
	0.907	0.093	unreal	400
	6.69	0.689	unreal	600
	7.52	0.774	unreal	600
	9.01	0.928	unreal	600
	7.77	0.801	unreal	600

	8.01	0.825	unreal	600
	10.5	1.08	unreal	600
	3.56	0.367	unreal	900
	3.53	0.364	unreal	900
	5.08	0.523	unreal	900
	3.54	0.364	unreal	900
	4.06	0.418	unreal	900
	5.89	0.606	unreal	900
	2.27	0.234	unreal	2850
	3.74	0.385	unreal	2850
	2.94	0.303	unreal	2850
	2.43	0.251	unreal	2850
	4.11	0.423	unreal	2850
	3.16	0.326	unreal	2850
Periwinkle	1.35	0.139	0.272	400
	0.865	0.0891	0.753	400
	1.42	0.146	0.237	400
	1.38	0.142	0.256	400
	0.85	0.087	0.781	400
	1.428	0.147	0.232	400
	4.08	0.420	0.000916	600
	2.08	0.214	0.0600	600
	4.35	0.448	0.000516	600
	4.76	0.490	0.000222	600
	2.16	0.222	0.0508	600
	4.76	0.490	0.000220	600
	1.53	0.157	0.188	900
	1.03	0.106	0.533	900
	1.34	0.138	0.281	900
	1.52	0.156	0.192	900
	0.932	0.0960	0.654	900
	1.19	0.122	0.383	900
	1.51	0.155	0.196	2850
	1.35	0.139	0.271	2850
	2.72	0.280	0.0157	2850
	1.49	0.154	0.202	2850
	1.57	0.162	0.172	2850
	2.83	0.291	0.0125	2850
Limpet	4.74	0.488	unreal	400
	4.58	0.471	unreal	400
	5.20	0.536	unreal	400
	5.78	0.595	unreal	400
	4.90	0.505	unreal	400
	5.51	0.568	unreal	400
	9.87	1.02	0.0245	600

	10.2	1.05	0.0543	600
	3.35	0.345	unreal	600
	10.4	1.07	0.0768	600
	10.8	1.11	0.115	600
	3.34	0.344	unreal	600
	28.1	2.90	1.66	900
	4.15	0.427	unreal	900
	3.78	0.389	unreal	900
	39.4	4.06	2.56	900
	4.80	0.495	unreal	900
	3.82	0.393	unreal	900
	3.20	0.329	unreal	2850
	3.81	0.392	unreal	2850
	3.69	0.380	unreal	2850
	3.51	0.362	unreal	2850
	3.77	0.388	unreal	2850
	10.4	1.07	0.0736	2850
Echinodermata				
Purple Urchin	6.73	0.693	5.86E-07	400
	5.85	0.603	6.60E-06	400
	6.29	0.648	1.89E-06	400
	5.73	0.590	9.64E-06	400
	9.50	0.979	1.46E-09	600
	10.1	1.04	unreal	600
	11.8	1.21	unreal	600
	9.22	0.950	2.44E-09	600
	10.2	1.05	unreal	600
	11.7	1.21	unreal	600
	15.3	1.57	unreal	900
	16.4	1.69	unreal	900
	12.5	1.29	unreal	900
	14.6	1.51	unreal	900
	15.9	1.64	unreal	900
	12.5	1.29	unreal	900
	11.0	1.13	unreal	2850
	9.17	0.944	2.71E-09	2850
	8.98	0.924	3.91E-09	2850
	11.0	1.13	unreal	2850
	9.05	0.932	3.41E-09	2850
	8.99	0.926	3.82E-09	2850
Pencil Urchin	6.54	0.674	9.49E-07	400
	5.40	0.557	2.63E-05	400
	5.02	0.517	9.37E-05	400
	5.01	0.516	9.80E-05	600

	7.87	0.810	3.85E-08	600
	10.8	1.11	unreal	600
	7.47	0.770	9.43E-08	900
	3.58	0.368	3.42E-02	900
	10.4	1.08	unreal	900
	8.48	0.874	1.04E-08	2850
	10.6	1.09	unreal	2850
	10.3	1.07	unreal	2850
Cnidaria				
Temperate Coral	16.5	1.70	0.643	400
	16.7	1.72	0.659	400
	14.1	1.45	0.423	400
	16.9	1.74	0.677	400
	13.4	1.38	0.356	400
	17.3	1.78	0.717	400
	15.4	1.59	0.548	400
	18.8	1.93	0.849	400
	18.0	1.85	0.780	400
	18.3	1.88	0.802	400
	15.6	1.61	0.562	400
	17.7	1.82	0.751	400
	15.1	1.56	0.517	400
	16.0	1.65	0.601	400
	16.6	1.71	0.653	400
	13.8	1.43	0.400	400
	16.7	1.72	0.664	400
	13.7	1.41	0.390	400
	16.2	1.67	0.620	400
	14.5	1.49	0.461	400
	18.2	1.87	0.794	400
	17.7	1.83	0.756	400
	17.3	1.78	0.719	400
	15.6	1.60	0.558	400
	17.3	1.78	0.719	400
	15.3	1.58	0.538	400
	13.7	1.41	0.383	600
	11.0	1.13	0.130	600
	16.1	1.66	0.611	600
	6.61	0.681	unreal	600
	11.9	1.23	0.220	600
	15.0	1.54	0.504	600
	16.0	1.65	0.602	600
	16.0	1.65	0.600	600
	15.7	1.62	0.574	600
	17.8	1.83	0.760	600

	13.7	1.41	0.386	600
	14.1	1.45	0.424	600
	14.1	1.46	0.427	600
	13.1	1.35	0.333	600
	15.3	1.58	0.536	600
	6.29	0.648	unreal	600
	11.7	1.21	0.199	600
	12.0	1.24	0.226	600
	14.6	1.50	0.469	600
	15.2	1.56	0.525	600
	14.6	1.50	0.470	600
	13.0	1.34	0.319	600
	11.7	1.21	0.199	600
	15.1	1.55	0.515	600
	14.3	1.48	0.447	600
	14.8	1.52	0.485	600
	16.0	1.64	0.596	600
	13.5	1.40	0.372	600
	13.6	1.40	0.376	600
	14.2	1.46	0.429	600
	14.8	1.53	0.492	600
	13.7	1.41	0.386	900
	20.2	2.08	0.970	900
	13.1	1.35	0.330	900
	12.1	1.25	0.238	900
	15.7	1.62	0.572	900
	17.5	1.81	0.738	900
	18.9	1.95	0.862	900
	15.7	1.62	0.574	900
	16.8	1.73	0.673	900
	17.7	1.83	0.756	900
	19.1	1.97	0.878	900
	15.4	1.59	0.545	900
	16.5	1.70	0.647	900
	16.6	1.71	0.650	900
	13.7	1.42	0.390	900
	13.4	1.38	0.363	900
	18.3	1.88	0.806	900
	13.7	1.41	0.383	900
	11.8	1.21	0.205	900
	14.9	1.54	0.503	900
	15.8	1.62	0.579	900
	17.8	1.83	0.762	900
	16.0	1.64	0.596	900
	16.4	1.69	0.635	900

	17.0	1.75	0.689	900
	18.4	1.89	0.811	900
	14.6	1.50	0.471	900
	16.6	1.71	0.653	900
	17.1	1.76	0.697	900
	13.3	1.37	0.345	900
	17.2	1.77	0.707	2850
	14.6	1.50	0.470	2850
	13.7	1.41	0.384	2850
	11.4	1.17	0.169	2850
	14.1	1.45	0.424	2850
	16.8	1.73	0.674	2850
	13.8	1.43	0.399	2850
	13.1	1.35	0.331	2850
	19.7	2.03	0.931	2850
	11.5	1.18	0.175	2850
	16.5	1.70	0.648	2850
	16.5	1.69	0.641	2850
	14.1	1.45	0.424	2850
	13.0	1.34	0.321	2850
	20.2	2.08	0.970	2850
	15.0	1.55	0.509	2850
	12.8	1.32	0.303	2850
	15.9	1.64	0.589	2850
	13.8	1.43	0.400	2850
	14.1	1.46	0.428	2850
	11.5	1.18	0.175	2850
	14.4	1.49	0.454	2850
	16.4	1.69	0.637	2850
	13.4	1.38	0.362	2850
	13.0	1.34	0.321	2850
	17.9	1.84	0.767	2850
	11.8	1.22	0.207	2850
	15.5	1.60	0.554	2850
	15.3	1.57	0.532	2850
	13.7	1.41	0.388	2850
	12.9	1.33	0.314	2850
	18.4	1.90	0.819	2850
	14.6	1.51	0.472	2850
Rhodophyta				
Coralline Red Algae	21.6	2.22	unreal	400
	26.6	2.74	unreal	400
	17.2	1.77	unreal	400
	27.2	2.80	unreal	400
	33.0	3.40	unreal	400

	20.5	2.12	unreal	400
	223	22.9	unreal	600
	215	22.2	unreal	600
	211	21.8	unreal	600
	222	22.9	unreal	600
	221	22.8	unreal	600
	207	21.3	unreal	600
	17.6	1.82	unreal	900
	29.0	2.99	unreal	900
	24.4	2.52	unreal	900
	21.9	2.25	unreal	900
	38.3	3.95	unreal	900
	31.2	3.21	unreal	900
	22.6	2.32	unreal	2850
	20.7	2.14	unreal	2850
	20.4	2.10	unreal	2850
	23.9	2.47	unreal	2850
	24.0	2.47	unreal	2850
	20.1	2.07	unreal	2850
Chlorophyte				
Halimeda	1.33	2.57	1.33	400
	1.05	2.17	1.05	400
	2.10	3.68	2.10	400
	60.6	98.3	60.6	600
	40.0	62.2	40.0	600
	1.61	2.98	1.61	900
	1.94	3.45	1.94	2850
	0.715	1.69	0.715	2850

[a] Common name of the organisms with the phyla names in shaded gray.
[b] Barium-to-Calcium ratio in units of micro-moles Ba / moles Ca.
[c] Empirical partition coefficient (D).
[d] Fraction of calcium remaining in the calcification reservoir after biomineralization (F).
[e] The pCO_2 treatment in which the organism was grown.

Table 24: ***A compilation of the standard deviations and standard errors for the Mn/Ca ratios of the cultured samples at their respective pCO_2 treatment levels.***

Organism [a]	Standard Deviation [b]	Standard Error [c]
Lobster		
400 ppm	109	62.7
600 ppm	287	166
900 ppm	196	113
2850 ppm	40.0	23.1
Blue Crab		
400 ppm	49.4	35.0
600 ppm	95.9	55.4
900 ppm	42.1	24.3
2850 ppm	27.4	15.8
Shrimp		
400 ppm	15.3	8.84
900 ppm	3.72	2.15
2850 ppm	7.05	4.07
Bay Scallop		
400 ppm	2.25	1.12
600 ppm	3.90	1.59
900 ppm	3.15	1.58
2850 ppm	0.661	0.331
Oyster		
400 ppm	9.80	4.90
600 ppm	16.8	6.84
900 ppm	9.64	4.82
2850 ppm	4.93	2.46
Blue Mussel		
400 ppm	1.10	0.549
600 ppm	3.48	1.42
900 ppm	3.66	1.45
2850 ppm	1.09	0.544
Hard Clam		
400 ppm	3.02	1.74
600 ppm	0.540	0.242
900 ppm	2.33	1.16
2850 ppm	0.522	0.369
Soft Clam		
400 ppm	0.873	0.617
600 ppm	1.27	0.633
900 ppm	8.04	4.02
2850 ppm	6.09	3.04
Conch		

400 ppm	1.89	0.772
600 ppm	1.18	0.481
900 ppm	10.4	4.25
2850 ppm	2.00	0.810
Periwinkle		
400 ppm	43.0	17.5
600 ppm	13.3	5.43
900 ppm	32.2	13.1
2850 ppm	13.1	5.33
Limpet		
400 ppm	4.76	1.94
600 ppm	6.16	2.52
900 ppm	1.17	0.480
2850 ppm	4.16	1.70
Purple Urchin		
400 ppm	2.24	1.29
600 ppm	0.546	0.273
900 ppm	0.184	0.0918
2850 ppm	0.642	0.321
Pencil Urchin		
400 ppm	5.17	3.66
600 ppm	0.165	0.117
2850 ppm	0.653	0.377
Temperate Coral		
400 ppm	0.976	0.195
600 ppm	2.34	0.427
900 ppm	1.06	0.194
2850 ppm	0.762	0.131
Coralline Red Algae		
400 ppm	0.946	0.423
600 ppm	0.859	0.384
900 ppm	0.734	0.300
2850 ppm	1.21	0.605
Halimeda		
400 ppm	62.2	35.9

[a] The common name of the organism being studied.
[b] The standard deviation of the Mn/Ca ratios for the specified organism and pCO_2 treatment.
[c] The standard error of the Mn/Ca ratios for the specified organism and pCO_2 treatment.

Table 25: ***A compilation of the data for manganese incorporation in cultured organisms.***

Organism [a]	Mn/Ca (µmol/mol) [b]	D_{Mn} [c]	F_{Mn} [d]	pCO_2 [e]
Crustacea				
Lobster	979	2.0E3	1.6	400
	842	1700	1.6	400
	1060	2200	1.6	400
	571	1200	1.5	600
	1070	2200	1.6	600
	573	1200	1.5	600
	1210	2500	1.6	900
	907	1600	1.6	900
	850	1800	1.6	900
	325	670	1.5	2850
	251	520	1.4	2850
	260	540	1.4	2850
Blue Crab	138	290	1.4	400
	68.0	140	1.3	400
	168	350	1.4	600
	277	570	1.5	600
	85.9	180	1.3	600
	152	310	1.4	900
	74.0	150	1.3	900
	86.2	180	1.3	900
	60.0	120	1.3	2850
	90.4	190	1.3	2850
	115	240	1.4	2850
Shrimp	34.2	70	1.2	400
	15.3	32	1.1	400
	3.84	7.9	0.90	400
	3.98	8.2	0.90	600
	9.55	20	1.0	900
	3.04	6.3	0.86	900
	9.42	19	1.0	900
	12.0	25	1.1	2850
	16.2	33	1.1	2850
	2.46	5.1	0.83	2850
Mollusca				
Bay Scallop	8.45	17	1.0	400
	12.1	25	1.1	400
	10.2	21	1.1	400
	13.6	28	1.1	400
	9.82	20	1.1	600
	3.32	6.8	0.87	600

	2.16	4.5	0.82	600
	11.1	23	1.1	600
	4.15	8.6	0.90	600
	2.58	5.3	0.84	600
	7.73	16	1.0	900
	2.73	5.6	0.84	900
	9.29	19	1.0	900
	3.69	7.6	0.89	900
	14.1	29	1.1	2850
	13.1	27	1.1	2850
	14.5	30	1.1	2850
	14.5	30	1.1	2850
Oyster	52.6	110	1.3	400
	69.3	140	1.3	400
	56.6	120	1.3	400
	72.9	150	1.3	400
	52.7	110	1.3	600
	41.9	86	1.2	600
	76.8	160	1.3	600
	56.5	120	1.3	600
	46.2	95	1.2	600
	83.2	170	1.3	600
	50.2	100	1.2	900
	67.1	140	1.3	900
	53.3	110	1.3	900
	69.4	140	1.3	900
	75.2	160	1.3	2850
	67.7	140	1.3	2850
	78.7	160	1.3	2850
	70.3	150	1.3	2850
Blue Mussel	14.0	29	1.1	400
	12.6	26	1.1	400
	15.3	31	1.1	400
	14.2	29	1.1	400
	11.2	23	1.1	600
	4.03	8.3	0.91	600
	6.04	12	1.0	600
	12.9	27	1.1	600
	5.39	11	1.0	600
	7.48	15	1.0	600
	7.63	16	1.0	900
	14.0	29	1.1	900
	9.98	21	1.0	900
	15.6	32	1.1	900
	8.82	18	1.0	2850

	7.50	15	1.0	2850
	10.1	21	1.0	2850
	8.45	17	1.0	2850
Periwinkle	126	260	1.4	400
	49.5	100	1.2	400
	39.3	81	1.2	400
	130	270	1.4	400
	52.7	110	1.3	400
	41.7	86	1.2	400
	42.7	88	1.2	600
	60.6	130	1.3	600
	32.0	66	1.2	600
	48.0	99	1.2	600
	64.5	130	1.3	600
	34.7	71	1.2	600
	80.5	170	1.3	900
	63.8	130	1.3	900
	131	270	1.4	900
	82.3	170	1.3	900
	67.5	140	1.3	900
	137	280	1.4	900
	82.6	170	1.3	2850
	97.8	200	1.3	2850
	70.7	150	1.3	2850
	87.1	180	1.3	2850
	104	220	1.3	2850
	74.2	150	1.3	2850
Echinodermata				
Purple Urchin	3.68	7.6	0.89	400
	0.955	2.0	0.49	400
	5.39	11	0.96	400
	0.647	1.3	0.25	600
	1.52	3.1	0.68	600
	0.845	1.7	0.43	600
	1.80	3.7	0.73	600
	1.07	2.2	0.55	900
	1.35	2.8	0.64	900
	1.35	2.8	0.64	900
	1.00	2.1	0.52	900
	0.889	1.8	0.45	2850
	1.94	4.0	0.75	2850
	2.33	4.8	0.80	2850
	2.12	4.4	0.78	400
Pencil Urchin	10.0	21	1.1	400

	2.71	5.6	0.80	400
	1.38	2.9	0.64	600
	1.62	3.3	0.68	600
	1.70	3.5	0.69	900
	2.32	4.8	0.77	2850
	1.06	2.2	0.58	2850
	2.00	4.1	0.73	2850
Rhodophyta				
Coralline Red Algae	1.88	3.9	0.72	400
	0.863	1.8	0.48	400
	3.42	7.1	0.90	400
	1.50	3.1	0.65	400
	1.74	3.6	0.69	400
	3.58	7.4	0.91	600
	3.17	6.5	0.87	600
	4.76	9.8	0.99	600
	3.41	7.0	0.89	600
	2.38	4.9	0.79	600
	2.40	4.9	0.79	900
	2.93	6.0	0.85	900
	1.88	3.9	0.72	900
	3.53	7.3	0.90	900
	3.90	8.0	0.93	900
	2.85	5.9	0.84	900
	1.50	3.1	0.65	2850
	4.09	8.4	0.95	2850
	2.00	4.1	0.73	2850
	3.43	7.1	0.90	2850

[a] Common name of the organisms with the phyla names in shaded gray.
[b] Manganese-to-Calcium ratio in units of micro-moles Mn / moles Ca.
[c] Empirical partition coefficient (D).
[d] Fraction of calcium remaining in the calcification reservoir after biomineralization (F).
[e] The pCO_2 treatment in which the organism was grown.

Table 26: ***A compilation of the standard deviations and standard errors for the B/Ca ratios of the cultured samples at their respective pCO_2 treatment levels.***

Organism [a]	Standard Deviation [b]	Standard Error [c]
Bay Scallop		
400 ppm	2.74	1.94
600 ppm	7.05	4.07
900 ppm	10.4	7.35
2850 ppm	3.48	2.46
Oyster		
400 ppm	0.458	0.324
600 ppm	15.6	9.00
900 ppm	1.36	0.959
2850 ppm	10.8	7.65
Blue Mussel		
400 ppm	5.58	3.94
600 ppm	6.21	3.59
2850 ppm	17.3	12.2
Hard Clam		
400 ppm	14.1	9.98
600 ppm	9.81	5.67
900 ppm	19.7	13.9
2850 ppm	2.00	1.41
Soft Clam		
600 ppm	3.11	2.20
900 ppm	1.69	1.19
2850 ppm	5.22	3.69
Conch		
400 ppm	1.83	1.06
600 ppm	2.03	1.17
900 ppm	3.07	1.77
2850 ppm	0.964	0.557
Whelk		
400 ppm	2.80	1.62
600 ppm	1.30	0.752
900 ppm	1.48	0.854
2850 ppm	0.697	0.403
Periwinkle		
400 ppm	0.567	0.327
600 ppm	0.693	0.400
900 ppm	1.68	0.971
2850 ppm	0.168	0.0969
Limpet		
400 ppm	2.58	1.49

600 ppm	12.1	6.98
900 ppm	13.2	7.65
2850 ppm	334	193
Serpulid Worm		
400 ppm	58.3	33.6
600 ppm	48.7	28.1
900 ppm	43.9	25.4
2850 ppm	39.8	23.0
Purple Urchin		
400 ppm	10.8	7.62
600 ppm	9.08	5.24
900 ppm	12.2	7.07
2850 ppm	10.1	5.85
Temperate Coral		
400 ppm	34.7	9.61
600 ppm	138	32.6
900 ppm	41.2	10.6
2850 ppm	35.5	8.62
Coralline Red Algae		
400 ppm	40.0	23.1
600 ppm	20.7	12.0
900 ppm	49.4	28.5
2850 ppm	10.4	6.01

[a] The common name of the organism being studied.
[b] The standard deviation of the B/Ca ratios for the specified organism and pCO_2 treatment.
[c] The standard error of the B/Ca ratios for the specified organism and pCO_2 treatment.

Table 27: ***A compilation of the data for boron incorporation in cultured organisms.***

Organism [a]	B/Ca (µmol/mol) [b]	D_B [c]	F_B [d]	pCO_2 [e]
Mollusca				
Bay Scallop	42.5	0.0010	2.2	400
	38.6	0.00095	2.6	400
	33.7	0.00083	3.2	600
	39.5	0.00097	2.5	600
	25.5	0.00062	5.1	600
	25.0	0.00061	5.3	900
	39.7	0.00097	2.5	900
	28.6	0.00070	4.2	2850
	23.7	0.00058	5.8	2850
Oyster	104	0.0025	0.42	400
	104	0.0026	0.42	400
	119	0.0029	0.30	600
	89.3	0.0022	0.58	600
	113	0.0028	0.34	600
	97.6	0.0024	0.48	900
	100	0.0024	0.46	900
	103	0.0025	0.43	2850
	87.7	0.0021	0.61	2850
Blue Mussel	36.9	0.00091	2.8	400
	44.8	0.0011	2.0	400
	38.1	0.00093	2.7	600
	35.6	0.00087	3.0	600
	47.4	0.0012	1.9	600
	25.0	0.00061	5.3	900
	59.7	0.0015	1.3	900
	35.2	0.00086	3.0	2850
	36.9	0.00091	2.8	2850
Hard Clam	43.5	0.0011	2.1	400
	63.4	0.0016	1.1	400
	35.8	0.00088	3.0	600
	54.8	0.0013	1.4	600
	49.5	0.0012	1.7	600
	42.5	0.0010	2.2	900
	70.3	0.0017	0.88	900
	43.4	0.0011	2.1	2850
	40.6	0.0010	2.4	2850
Soft Clam	25.8	0.00063	5.7	400
	23.7	0.00058	6.5	600
	19.3	0.00047	9.0	600
	25.9	0.00064	5.6	900

	28.3	0.00069	4.9	900
	26.2	0.00064	5.5	2850
	33.6	0.00082	3.7	2850
Conch	15.6	0.00038	9.0	400
	15.9	0.00039	8.8	400
	12.6	0.00031	12	400
	15.0	0.00037	9.6	600
	16.9	0.00042	8.0	600
	19.0	0.00047	6.8	600
	16.7	0.00041	8.2	900
	16.3	0.00040	8.4	900
	11.2	0.00027	15	900
	16.7	0.00041	8.1	2850
	16.5	0.00040	8.3	2850
	15.0	0.00037	9.6	2850
Periwinkle	2.69	6.6E-05	130	400
	1.57	3.9E-05	260	400
	2.29	5.6E-05	160	400
	3.33	8.2E-05	99	600
	1.95	4.8E-05	200	600
	2.81	6.9E-05	120	600
	3.53	8.6E-05	92	900
	4.72	1.2E-04	63	900
	1.40	3.4E-05	300	900
	3.27	8.0E-05	100	2850
	3.51	8.6E-05	92	2850
	3.59	8.8E-05	90	2850
Limpet	18.6	0.00046	8.2	400
	16.2	0.00040	10	400
	21.4	0.00052	6.6	400
	18.3	0.00045	8.4	600
	40.2	0.00099	2.5	600
	20.4	0.00050	7.1	600
	38.0	0.00093	2.7	900
	13.7	0.00034	13	900
	16.9	0.00041	9.5	900
	11.9	0.00029	16	2850
	11.8	0.00029	16	2850
	590	0.014	0.040	2850
Echinodermata				
Purple Urchin	402	0.0099	0.0029	400
	387	0.0095	0.0037	400
	347	0.0085	0.0068	600
	330	0.0081	0.0088	600

	333	0.0082	0.0084	600
	328	0.0080	0.0091	900
	349	0.0086	0.0066	900
	349	0.0086	0.0066	900
	240	0.0059	0.035	2850
	256	0.0063	0.027	2850
	238	0.0058	0.036	2850
Cnidaria				
Temperate Coral	563	0.014	1.8E-04	400
	587	0.014	1.3E-04	400
	610	0.015	9.2E-05	400
	515	0.013	3.9E-04	400
	601	0.015	1.0E-04	400
	515	0.013	3.9E-04	400
	572	0.014	1.6E-04	400
	564	0.014	1.8E-04	400
	565	0.014	1.8E-04	400
	578	0.014	1.5E-04	400
	562	0.014	1.8E-04	400
	591	0.015	1.2E-04	400
	496	0.012	5.4E-04	400
	566	0.014	1.8E-04	600
	615	0.015	8.6E-05	600
	590	0.014	1.2E-04	600
	19.0	0.000	7.6E+08	600
	593	0.015	1.2E-04	600
	589	0.014	1.2E-04	600
	660	0.016	4.7E-05	600
	584	0.014	1.3E-04	600
	533	0.013	2.9E-04	600
	579	0.014	1.4E-04	600
	616	0.015	8.4E-05	600
	556	0.014	2.0E-04	600
	559	0.014	1.9E-04	600
	601	0.015	1.0E-04	600
	632	0.016	6.7E-05	600
	563	0.014	1.8E-04	600
	574	0.014	1.6E-04	600
	630	0.015	7.0E-05	600
	632	0.016	6.8E-05	900
	645	0.016	5.7E-05	900
	583	0.014	1.3E-04	900
	657	0.016	4.9E-05	900
	568	0.014	1.7E-04	900
	532	0.013	3.0E-04	900

	549	0.013	2.3E-04	900
	576	0.014	1.5E-04	900
	564	0.014	1.8E-04	900
	624	0.015	7.6E-05	900
	602	0.015	1.0E-04	900
	584	0.014	1.3E-04	900
	606	0.015	9.7E-05	900
	531	0.013	3.0E-04	900
	533	0.013	2.9E-04	900
	602	0.015	1.0E-04	2850
	613	0.015	8.7E-05	2850
	607	0.015	9.6E-05	2850
	637	0.016	6.3E-05	2850
	600	0.015	1.1E-04	2850
	614	0.015	8.7E-05	2850
	541	0.013	2.5E-04	2850
	591	0.014	1.2E-04	2850
	607	0.015	9.6E-05	2850
	531	0.013	3.0E-04	2850
	544	0.013	2.4E-04	2850
	570	0.014	1.7E-04	2850
	593	0.015	1.2E-04	2850
	603	0.015	1.0E-04	2850
	620	0.015	7.9E-05	2850
	508	0.012	4.4E-04	2850
	577	0.014	1.5E-04	2850
Rhodophyta				
Coralline Red Algae	499	0.012	0.00071	400
	436	0.011	0.0018	400
	425	0.010	0.0021	400
	440	0.011	0.0017	600
	469	0.012	0.0011	600
	429	0.011	0.0020	600
	516	0.013	0.00056	900
	417	0.010	0.0024	900
	462	0.011	0.0012	900
	346	0.0085	0.0068	2850
	326	0.0080	0.0092	2850
	340	0.0083	0.0075	2850

[a] Common name of the organisms with the phyla names in shaded gray.
[b] Boron-to-Calcium ratio in units of micro-moles B / moles Ca.
[c] Empirical partition coefficient (D).
[d] Fraction of calcium remaining in the calcification reservoir after biomineralization (F).
[e] The pCO_2 treatment in which the organism was grown.

Table 28: ***A compilation of the standard deviations and standard errors for the Li/Ca ratios of the cultured samples at their respective pCO_2 treatment levels.***

Organism [a]	Standard Deviation [b]	Standard Error [c]
Bay Scallop		
400 ppm	2.48	1.75
600 ppm	4.07	2.35
900 ppm	0.370	0.262
2850 ppm	0.935	0.661
Oyster		
400 ppm	1.30	0.919
600 ppm	1.42	0.819
900 ppm	2.18	1.54
2850 ppm	8.68	6.14
Blue Mussel		
400 ppm	2.34	1.66
600 ppm	1.18	0.680
2850 ppm	3.99	2.82
Hard Clam		
400 ppm	0.683	0.483
600 ppm	1.41	0.811
900 ppm	1.00	0.710
2850 ppm	0.256	0.181
Soft Clam		
600 ppm	0.211	0.149
900 ppm	0.245	0.173
2850 ppm	1.13	0.798
Conch		
400 ppm	0.109	0.0627
600 ppm	0.554	0.320
900 ppm	0.346	0.200
2850 ppm	0.748	0.432
Periwinkle		
400 ppm	3.02	1.74
600 ppm	2.01	1.16
900 ppm	6.16	3.55
2850 ppm	1.57	0.909
Limpet		
400 ppm	0.0326	0.0188
600 ppm	0.468	0.270
900 ppm	1.34	0.775
2850 ppm	1.83	1.06
Purple Urchin		
400 ppm	7.53	5.32

600 ppm	1.08	0.625
900 ppm	2.08	1.20
2850 ppm	1.16	0.667
Temperate Coral		
400 ppm	0.520	0.144
600 ppm	1.10	0.259
900 ppm	0.667	0.172
2850 ppm	0.551	0.134
Coralline Red Algae		
400 ppm	2.37	1.37
600 ppm	3.12	1.80
900 ppm	6.00	3.46
2850 ppm	3.96	2.29

[a] The common name of the organism being studied.
[b] The standard deviation of the Li/Ca ratios for the specified organism and pCO_2 treatment.
[c] The standard error of the Li/Ca ratios for the specified organism and pCO_2 treatment.

Table 29: ***A compilation of the data for lithium incorporation in cultured organisms.***

Organism [a]	Li/Ca (µmol/mol) [b]	D_{Li} [c]	F_{Li} [d]	pCO_2 [e]
Mollusca				
Bay Scallop	10.9	0.0045	0.15	400
	14.5	0.0060	0.069	400
	16.2	0.0067	0.050	600
	11.1	0.0046	0.15	600
	8.17	0.0034	0.35	600
	9.87	0.0041	0.21	900
	10.4	0.0043	0.18	900
	12.6	0.0052	0.10	2850
	13.9	0.0057	0.077	2850
Oyster	27.6	0.011	0.0028	400
	29.5	0.012	0.0018	400
	25.8	0.011	0.0042	600
	23.1	0.010	0.0077	600
	23.6	0.010	0.0069	600
	19.2	0.0079	0.019	900
	22.3	0.0092	0.0093	900
	16.1	0.0066	0.038	2850
	28.4	0.012	0.0024	2850
Blue Mussel	8.60	0.0035	0.29	400
	5.29	0.0022	0.92	400
	7.62	0.0031	0.38	600
	5.29	0.0022	0.92	600
	6.76	0.0028	0.51	600
	8.12	0.0033	0.33	900
	12.3	0.0051	0.12	900
	6.69	0.0028	0.52	2850
Periwinkle	20.6	0.0085	0.012	400
	15.2	0.0063	0.047	400
	15.4	0.0064	0.045	400
	10.4	0.0043	0.16	600
	12.3	0.0050	0.10	600
	8.23	0.0034	0.28	600
	15.1	0.0062	0.049	900
	12.5	0.0051	0.096	900
	24.2	0.010	0.0047	900
	14.8	0.0061	0.053	2850
	13.8	0.0057	0.068	2850
	11.7	0.0048	0.12	2850
Echinodermata				
Purple Urchin	41.0	0.017	1.5E-04	400

	51.6	0.021	1.4E-05	400
	51.1	0.021	1.6E-05	600
	51.1	0.021	1.6E-05	600
	53.0	0.022	1.1E-05	600
	49.4	0.020	2.2E-05	900
	53.5	0.022	1.0E-05	900
	52.3	0.022	1.3E-05	900
	51.7	0.021	1.4E-05	2850
	52.5	0.022	1.2E-05	2850
	50.2	0.021	1.9E-05	2850
Rhodophyta				
Coralline Red Algae	46.5	0.019	3.9E-05	400
	44.1	0.018	6.6E-05	400
	41.8	0.017	1.1E-04	400
	43.7	0.018	7.1E-05	600
	49.8	0.021	2.0E-05	600
	47.9	0.020	3.0E-05	600
	39.8	0.016	1.8E-04	900
	47.2	0.019	3.4E-05	900
	51.7	0.021	1.4E-05	900
	45.5	0.019	4.8E-05	2850
	47.2	0.019	3.4E-05	2850
	39.6	0.016	1.8E-04	2850

[a] Common name of the organisms with the phyla names in shaded gray.
[b] Lithium-to-Calcium ratio in units of micro-moles Li / moles Ca.
[c] Empirical partition coefficient (D).
[d] Fraction of calcium remaining in the calcification reservoir after biomineralization (F).
[e] The pCO_2 treatment in which the organism was grown.

Table 30: ***A compilation of the standard deviations and standard errors for the Cd/Ca ratios of the cultured samples at their respective pCO_2 treatment levels.***

Organism [a]	Standard Deviation [b]	Standard Error [c]
Bay Scallop		
400 ppm	0.45	0.32
600 ppm	0.00075	0.00043
900 ppm	1.1	0.80
2850 ppm	16	11
Oyster		
400 ppm	0.97	0.69
600 ppm	0.011	0.0061
900 ppm	5.0	3.5
2850 ppm	0.011	0.0061
Blue Mussel		
400 ppm	270	190
600 ppm	0.0071	0.0041
2850 ppm	3.9	2.7
Hard Clam		
400 ppm	0.017	0.012
600 ppm	0.0027	0.0016
900 ppm	0.0022	0.0015
2850 ppm	1.1	0.75
Soft Clam		
600 ppm	0.016	0.011
900 ppm	0.0017	0.0012
2850 ppm	0.066	0.047
Conch		
400 ppm	0.011	0.0061
600 ppm	0.00092	0.00065
900 ppm	0.0071	0.0041
2850 ppm	0.11	0.062
Periwinkle		
400 ppm	0.0014	0.00079
600 ppm	0.0030	0.0017
900 ppm	0.043	0.025
2850 ppm	0.0050	0.0029
Limpet		
400 ppm	0.0034	0.0019
600 ppm	0.011	0.0065
900 ppm	0.0078	0.0045
2850 ppm	0.016	0.0095
Purple Urchin		
400 ppm	1.1	0.81

600 ppm	0.10	0.059
900 ppm	0.13	0.076
2850 ppm	0.080	0.046
Temperate Coral		
400 ppm	1.0	0.29
600 ppm	2.7	0.63
900 ppm	1.0	0.26
2850 ppm	0.54	0.13
Coralline Red Algae		
400 ppm	4.7	2.7
600 ppm	0.20	0.12
900 ppm	0.36	0.21
2850 ppm	0.34	0.20

[a] The common name of the organism being studied.
[b] The standard deviation of the Cd/Ca ratios for the specified organism and pCO_2 treatment.
[c] The standard error of the Cd/Ca ratios for the specified organism and pCO_2 treatment.

Table 31: ***A compilation of the data for cadmium incorporation in cultured organisms.***

Organism [a]	Cd/Ca (µmol/mol) [b]	D_{Cd} [c]	F_{Cd} [d]	pCO_2 [e]
Mollusca				
Bay Scallop	0.020	0.29	unreal	400
	0.66	9.8	0.90	400
	0.0032	0.047	unreal	600
	0.0017	0.025	unreal	600
	0.0022	0.033	unreal	600
	2.0	29	0.98	900
	0.37	5.4	0.82	900
	0.012	0.18	unreal	2850
	22	330	1.1	2850
Oyster	0.025	0.36	unreal	400
	1.4	21	0.96	400
	0.014	0.20	unreal	600
	0.034	0.51	unreal	600
	0.020	0.29	unreal	600
	7.0	100	1.0	900
	0.019	0.28	unreal	900
	0.027	0.39	unreal	2850
	0.015	0.22	unreal	2850
Blue Mussel	0.010	0.15	unreal	400
	380	5500	1.2	400
	0.047	0.69	unreal	600
	0.034	0.50	unreal	600
	0.045	0.67	unreal	600
	5.9	87	1.0	900
	5.5	81	1.0	900
	0.0058	0.085	unreal	2850
Periwinkle	0.0036	0.053	unreal	400
	0.0030	0.043	unreal	400
	0.0010	0.014	unreal	400
	0.0079	0.12	unreal	600
	0.0025	0.037	unreal	600
	0.0030	0.045	unreal	600
	0.0014	0.021	unreal	900
	0.076	1.1	0.11	900
	0.0022	0.033	unreal	900
	0.0054	0.080	unreal	2850
	0.013	0.18	unreal	2850
Echinodermata				
Purple Urchin	0.22	3.3	0.72	400
	1.8	27	1.0	400

	0.42	6.1	0.81	600
	0.38	5.6	0.80	600
	0.57	8.4	0.86	600
	0.61	9.0	0.87	900
	0.35	5.2	0.79	900
	0.43	6.3	0.82	900
	0.37	5.4	0.80	2850
	0.40	5.9	0.81	2850
	0.52	7.7	0.85	2850
Rhodophyta				
Coralline Red Algae	9.0	130	1.1	400
	1.1	16	0.94	400
	0.60	8.9	0.90	400
	1.8	27	0.97	600
	2.2	32	0.98	600
	2.0	29	0.97	600
	0.60	8.8	0.90	900
	1.2	18	0.94	900
	1.3	19	0.95	900
	1.7	25	0.96	2850
	1.1	15	0.93	2850
	1.6	23	0.96	2850

[a] Common name of the organisms with the phyla names in shaded gray.
[b] Cadmium-to-Calcium ratio in units of micro-moles Cd / moles Ca.
[c] Empirical partition coefficient (D).
[d] Fraction of calcium remaining in the calcification reservoir after biomineralization (F).
[e] The pCO_2 treatment in which the organism was grown.

Table 32: ***A compilation of the standard deviations and standard errors for the U/Ca ratios of the cultured samples at their respective pCO_2 treatment levels.***

Organism [a]	Standard Deviation [b]	Standard Error [c]
Bay Scallop		
400 ppm	2.4	1.7
600 ppm	0.40	0.23
900 ppm	1.0	0.74
2850 ppm	2.8	2.0
Oyster		
400 ppm	36	25
600 ppm	8.3	4.8
900 ppm	2.4	1.7
2850 ppm	2.0	1.4
Blue Mussel		
400 ppm	1.1	0.76
600 ppm	39	22
2850 ppm	0.43	0.30
Hard Clam		
400 ppm	220	160
600 ppm	280	160
900 ppm	77	54
2850 ppm	5.6	4.0
Soft Clam		
600 ppm	25	17
900 ppm	33	23
2850 ppm	18	13
Conch		
400 ppm	2.9	1.7
600 ppm	9.3	5.4
900 ppm	6.0	3.5
2850 ppm	12	7.1
Periwinkle		
400 ppm	8.6	4.9
600 ppm	6.0	3.5
900 ppm	5.4	3.1
2850 ppm	4.3	2.5
Limpet		
400 ppm	4.8	2.8
600 ppm	17	9.7
900 ppm	85	49
2850 ppm	580	330
Purple Urchin		
400 ppm	180	130

600 ppm	0.63	0.36
900 ppm	30	18
2850 ppm	0.90	0.52
Temperate Coral		
400 ppm	0.51	0.14
600 ppm	1.1	0.26
900 ppm	0.67	0.17
2850 ppm	0.55	0.13
Coralline Red Algae		
400 ppm	10.5	6.1
600 ppm	22	13
900 ppm	13	7.7
2850 ppm	7.1	4.1

[a] The common name of the organism being studied.
[b] The standard deviation of the U/Ca ratios for the specified organism and pCO_2 treatment.
[c] The standard error of the U/Ca ratios for the specified organism and pCO_2 treatment.

Table 33: ***A compilation of the data for uranium incorporation in cultured organisms.***

Organism [a]	U/Ca (nmol/mol) [b]	D_U [c]	F_U [d]	pCO_2 [e]
Mollusca				
Bay Scallop	7.5	0.0060	140	400
	4.1	0.0033	310	400
	1.9	0.0015	850	600
	2.5	0.0020	590	600
	1.8	0.0014	920	600
	2.8	0.0022	530	900
	4.3	0.0034	300	900
	6.3	0.0050	180	2850
	2.3	0.0018	660	2850
Oyster	59	0.047	7.1	400
	8.6	0.0068	120	400
	6.4	0.0051	180	600
	6.0	0.0048	200	600
	21	0.016	33	600
	13	0.010	64	900
	10	0.0077	99	900
	8.4	0.0067	120	2850
	11	0.0089	80	2850
Blue Mussel	7.4	0.0059	148	400
	5.9	0.0047	206	400
	86	0.068	4.0	600
	16	0.013	46	600
	20	0.016	33	600
	44	0.035	11	900
	7.3	0.0058	150	900
	6.7	0.0053	170	2850
Hard Clam	210	0.17	unreal	400
	530	0.42	unreal	400
	140	0.11	unreal	600
	680	0.54	unreal	600
	290	0.23	unreal	600
	560	0.45	unreal	900
	460	0.36	unreal	900
	66	0.053	unreal	2850
	58	0.046	unreal	2850
Soft Clam	51	0.040	unreal	400
	50	0.040	unreal	600
	15	0.012	unreal	600
	71	0.056	unreal	900
	24	0.019	unreal	900

	49	0.039	unreal	2850
	23	0.019	unreal	2850
Conch	17	0.013	unreal	400
	18	0.015	unreal	400
	13	0.010	unreal	400
	9.4	0.0074	unreal	600
	28	0.022	unreal	600
	21	0.016	unreal	600
	24	0.019	unreal	900
	32	0.026	unreal	900
	20	0.016	unreal	900
	4.2	0.0034	unreal	2850
	7.7	0.0061	unreal	2850
	27	0.021	unreal	2850
Periwinkle	5.1	0.0040	240	400
	4.2	0.0033	310	400
	19	0.015	40	400
	17	0.013	48	600
	6.0	0.0047	190	600
	7.2	0.0057	150	600
	2.1	0.0017	750	900
	13	0.010	69	900
	6.3	0.0050	180	900
	6.4	0.0051	170	2850
	13	0.010	69	2850
	4.8	0.0038	250	2850
Limpet	79	0.062	unreal	400
	71	0.056	unreal	400
	80	0.064	unreal	400
	47	0.037	unreal	600
	77	0.061	unreal	600
	74	0.059	unreal	600
	190	0.15	unreal	900
	49	0.039	unreal	900
	34	0.027	unreal	900
	33	0.026	unreal	2850
	43	0.034	unreal	2850
	1000	0.82	unreal	2850
Echinodermata				
Purple Urchin	310	0.24	0.47	400
	52	0.041	7.7	400
	19	0.015	37	600
	20	0.016	34	600
	19	0.015	37	600

	65	0.051	5.4	900
	13	0.010	67	900
	12	0.010	75	900
	7.4	0.006	160	2850
	8.5	0.007	130	2850
	6.8	0.005	180	2850
Cnidaria				
Temperate Coral	6.8	5.4	0.97	400
	7.4	5.8	1.0	400
	7.8	6.2	1.0	400
	7.7	6.1	1.0	400
	7.9	6.2	1.0	400
	6.9	5.5	0.98	400
	7.1	5.6	0.98	400
	6.6	5.2	0.96	400
	7.0	5.5	0.98	400
	6.5	5.1	0.95	400
	6.5	5.1	0.95	400
	6.4	5.1	0.95	400
	6.8	5.4	0.97	400
	7.8	6.1	1.0	600
	8.7	6.9	1.1	600
	7.7	6.1	1.0	600
	4.4	3.5	0.80	600
	7.0	5.6	0.98	600
	7.3	5.8	1.0	600
	9.4	7.5	1.1	600
	6.9	5.5	0.98	600
	6.9	5.5	0.98	600
	6.9	5.5	0.98	600
	7.8	6.1	1.0	600
	7.0	5.5	0.98	600
	7.0	5.6	0.98	600
	6.7	5.3	0.96	600
	7.2	5.7	0.99	600
	7.6	6.0	1.0	600
	7.8	6.2	1.0	600
	9.4	7.4	1.1	600
	6.9	5.5	0.98	900
	7.2	5.7	0.99	900
	7.2	5.7	0.99	900
	9.5	7.5	1.1	900
	7.1	5.7	0.99	900
	7.1	5.6	0.98	900
	7.2	5.7	0.99	900

	7.4	5.9	1.0	900
	7.5	6.0	1.0	900
	6.8	5.4	0.97	900
	6.5	5.2	0.95	900
	7.0	5.6	0.98	900
	7.3	5.8	1.0	900
	7.6	6.1	1.0	900
	7.6	6.0	1.0	900
	8.0	6.3	1.0	2850
	7.8	6.2	1.0	2850
	7.9	6.3	1.0	2850
	8.0	6.3	1.0	2850
	7.3	5.8	1.0	2850
	7.8	6.2	1.0	2850
	8.0	6.3	1.0	2850
	7.4	5.9	1.0	2850
	7.8	6.2	1.0	2850
	8.1	6.4	1.0	2850
	7.0	5.6	0.98	2850
	7.1	5.6	0.98	2850
	7.4	5.8	1.0	2850
	7.2	5.7	0.99	2850
	9.3	7.4	1.1	2850
	7.5	5.9	1.0	2850
	7.2	5.7	0.99	2850
Rhodophyta				
Coralline Red Algae	140	0.11	1.2	400
	150	0.12	1.1	400
	130	0.10	1.5	400
	160	0.13	0.91	600
	120	0.10	1.7	600
	130	0.10	1.6	600
	140	0.11	1.2	900
	130	0.10	1.5	900
	120	0.093	1.8	900
	160	0.12	1.0	2850
	150	0.12	1.1	2850
	160	0.13	0.91	2850

[a] Common name of the organisms with the phyla names in shaded gray.
[b] Uranium-to-Calcium ratio in units of nano-moles U / moles Ca.
[c] Empirical partition coefficient (D).
[d] Fraction of calcium remaining in the calcification reservoir after biomineralization (F).
[e] The pCO_2 treatment in which the organism was grown.

Table 34: ***A compilation of the data for boron incorporation in the foraminifera*** **O. universa** ***studied by Allen et al., 2011.***

Organism [a]	B/Ca (µmol/mol) [b]	D_B [c]	F_B [d]	pH [e]	Temperature (°C) [f]
O. universa	61.5	0.0015	1.3	8.03	22.3
O. universa	62.3	0.0015	1.3	8.03	22.3
O. universa	61.1	0.0015	1.3	8.12	17.7
O. universa	62.9	0.0015	1.3	8.06	19.6
O. universa	64.9	0.0016	1.2	7.97	26.5
O. universa	55.7	0.0014	1.6	7.61	22.1
O. universa	69.3	0.0017	1.0	8.30	22.1
O. universa	92.0	0.0023	0.59	8.67	22.1
O. universa	55.2	0.0014	1.6	8.06	22.1
O. universa	52.9	0.0013	1.8	8.06	22.1
O. universa	66.5	0.0016	1.1	8.02	22.3
O. universa	65.0	0.0016	1.2	8.02	22.3
O. universa	71.7	0.0018	1.0	8.00	22.3

[a] Scientific genus and species name of the foraminfera.
[b] Boron-to-Calcium ratio in units of micro-moles B / moles Ca.
[c] Empirical partition coefficient (D).
[d] Fraction of calcium remaining in the calcification reservoir after biomineralization (F).
[e] The pH in which the organism matured in total pH scale.
[f] The temperature in which the organisms matured in degrees Celsius.

Table 35: ***A compilation of the data for boron incorporation in the foraminifera studied by Yu et al., 2007.***

Organism [a]	B/Ca (µmol/mol) [b]	D_B [c]	F_B [d]	pH [e]	Temperature (°C) [f]
G. inflata	58	0.0014	1.5	8.11	9.2
G. inflata	56	0.0014	1.6	8.09	9.17
G. inflata	53	0.0013	1.8	8.06	9.79
G. inflata	53	0.0013	1.8	8.05	9.8
G. inflata	54	0.0013	1.7	8.12	7.87
G. inflata	59	0.0014	1.4	8.10	9.48
G. inflata	57	0.0014	1.5	8.07	9.43
G. inflata	61	0.0015	1.3	8.09	10.31
G. inflata	62	0.0015	1.3	8.11	9.93
G. inflata	57	0.0014	1.5	8.08	9.26
G. inflata	58	0.0014	1.5	8.15	7.15
G. inflata	55	0.0013	1.7	8.11	7.86
G. inflata	57	0.0014	1.5	8.21	5.82
G. inflata	56	0.0014	1.6	8.16	6.83
G. inflata	62	0.0015	1.3	8.21	6.67
G. inflata	59	0.0014	1.4	8.13	8.27
G. inflata	59	0.0014	1.4	8.20	6.35
G. inflata	62	0.0015	1.3	8.22	6.28
G. inflata	58	0.0014	1.5	8.18	6.7
G. inflata	61	0.0015	1.3	8.22	6.32
G. inflata	60	0.0015	1.4	8.19	6.65
G. inflata	54	0.0013	1.7	8.17	6.14
G. inflata	61	0.0015	1.3	8.20	6.7
G. inflata	56	0.0014	1.6	8.18	6.3
G. inflata	53	0.0013	1.8	8.15	6.49
G. inflata	58	0.0014	1.5	8.14	7.92
G. inflata	63	0.0015	1.3	8.14	8.84
G. inflata	62	0.0015	1.3	8.13	9.1
G. inflata	61	0.0015	1.3	8.14	8.9
G. inflata	58	0.0014	1.5		7.4
G. inflata	58	0.0014	1.5		7.6
G. inflata	55	0.0013	1.7		7.7
G. inflata	58	0.0014	1.5		7.8
G. inflata	57	0.0014	1.5		8.1
G. inflata	54	0.0013	1.7		8.3
G. inflata	55	0.0013	1.7		8.3
G. inflata	52	0.0013	1.9		8.3
G. inflata	62	0.0015	1.3		8.6
G. inflata	59	0.0014	1.4		8.9
G. inflata	60	0.0015	1.4		9.1
G. inflata	59	0.0014	1.4		9.6

G. inflata	68	0.0017	1.1		12
G. inflata	69	0.0017	1.1		9.4
G. inflata	65	0.0016	1.2		10
G. inflata	69	0.0017	1.1		11.2
G. inflata	70	0.0017	1.0		12
G. inflata	71	0.0017	1.0		12.1
G. inflata	76	0.0019	0.87		12.5
G. inflata	62	0.0015	1.3		8.8
G. inflata	55	0.0013	1.7		9.1
G. inflata	70	0.0017	1.0		9.4
G. inflata	68	0.0017	1.1		9.7
G. inflata	75	0.0018	0.89		10
G. inflata	70	0.0017	1.0		10.6
G. inflata	72	0.0018	1.0		11.8
G. inflata	77	0.0019	0.85		12
G. inflata	76	0.0019	0.87		12
G. inflata	79	0.0019	0.80		12.1
G. inflata	79	0.0019	0.80		12.1
G. inflata	75	0.0018	0.89		12.1
G. inflata	65	0.0016	1.2		8.6
G. inflata	66	0.0016	1.2		9.5
G. inflata	73	0.0018	0.94		10.9
G. inflata	75	0.0018	0.89		11.1
G. inflata	74	0.0018	0.92		11.5
G. inflata	73	0.0018	0.94		11.5
G. inflata	74	0.0018	0.92		11.9
G. inflata	74	0.0018	0.92		12.1
G. inflata	70	0.0017	1.0		10.9
G. inflata	59	0.0014	1.4		11.5
G. inflata	58	0.0014	1.5		9.5
G. bulloides	42	0.0010	2.8		12.8
G. bulloides	50	0.0012	2.0		14.9
G. bulloides	46	0.0011	2.4		13.4
G. bulloides	44	0.0011	2.6		14.9
G. bulloides	35	0.0009	4.1		11.5
G. bulloides	31	0.0008	5.2		12.8
G. bulloides	34	0.0008	4.3		12.9
G. bulloides	46	0.0011	2.4		13.2
G. bulloides	49	0.0012	2.1		13.6
G. bulloides	50	0.0012	2.0		13.8
G. bulloides	49	0.0012	2.1		14.3
G. bulloides	44	0.0011	2.6		12.9
G. bulloides	36	0.0009	3.9		13.5
G. bulloides	48	0.0012	2.2		13.5
G. bulloides	49	0.0012	2.1		13.7

[a] Scientific genus and species name of the foraminfera.
[b] Boron-to-Calcium ratio in units of micro-moles B / moles Ca.
[c] Empirical partition coefficient (D).
[d] Fraction of calcium remaining in the calcification reservoir after biomineralization (F).
[e] The pH in which the organism matured in total pH scale.
[f] The temperature in which the organisms matured in degrees Celsius.

Table 36: ***A compilation of the data for magnesium incorporation in the foraminifera studied by Yu et al., 2007.***

Organism [a]	Mg/Ca (mmol/mol) [b]	D_{Mg} [c]	F_{Mg} [d]	pH [e]	Temperature (°C) [f]
G. inflata	1.27	0.00025	510	8.11	9.2
G. inflata	1.26	0.00025	510	8.09	9.17
G. inflata	1.35	0.00026	470	8.06	9.79
G. inflata	1.35	0.00026	470	8.05	9.8
G. inflata	1.10	0.00021	610	8.12	7.87
G. inflata	1.31	0.00026	490	8.10	9.48
G. inflata	1.30	0.00025	490	8.07	9.43
G. inflata	1.43	0.00028	440	8.09	10.31
G. inflata	1.37	0.00027	460	8.11	9.93
G. inflata	1.28	0.00025	500	8.08	9.26
G. inflata	1.02	0.00020	660	8.15	7.15
G. inflata	1.10	0.00021	610	8.11	7.86
G. inflata	0.88	0.00017	790	8.21	5.82
G. inflata	0.98	0.00019	700	8.16	6.83
G. inflata	0.97	0.00019	710	8.21	6.67
G. inflata	1.15	0.00022	570	8.13	8.27
G. inflata	0.94	0.00018	730	8.20	6.35
G. inflata	0.93	0.00018	740	8.22	6.28
G. inflata	0.97	0.00019	710	8.18	6.7
G. inflata	0.93	0.00018	740	8.22	6.32
G. inflata	0.97	0.00019	710	8.19	6.65
G. inflata	0.91	0.00018	760	8.17	6.14
G. inflata	0.97	0.00019	710	8.20	6.7
G. inflata	0.93	0.00018	740	8.18	6.3
G. inflata	0.95	0.00018	720	8.15	6.49
G. inflata	1.11	0.00022	600	8.14	7.92
G. inflata	1.22	0.00024	530	8.14	8.84
G. inflata	1.25	0.00024	520	8.13	9.1
G. inflata	1.23	0.00024	530	8.14	8.9

[a] Scientific genus and species name of the foraminfera.
[b] Magnesium-to-Calcium ratio in units of milli-moles Mg / moles Ca.
[c] Empirical partition coefficient (D).
[d] Fraction of calcium remaining in the calcification reservoir after biomineralization (F).
[e] The pH in which the organism matured in total pH scale.
[f] The temperature in which the organisms matured in degrees Celsius.

Table 37: ***A compilation of the data for magnesium incorporation in the foraminifera studied by Lea et al., 1999.***

Organism [a]	Mg/Ca (mmol/mol) [b]	D_{Mg} [c]	F_{Mg} [d]	pH [e]	Temperature (°C) [f]
G. bulloides	2.73	0.00053	200	8.15	16
G. bulloides	4.77	0.00093	98	8.15	22
G. bulloides	7.10	0.0014	59	8.15	25
G. bulloides	6.33	0.0012	69	7.6	22
G. bulloides	3.67	0.00071	140	8.5	22
G. bulloides	1.80	0.00035	340		10.4
G. bulloides	2.20	0.00043	260		13
G. bulloides	1.60	0.00031	390		8
G. bulloides	1.65	0.00032	370		11.5
G. bulloides	1.29	0.00025	510		9.7
O. universa	5.89	0.0011	75	8.15	17
O. universa	8.89	0.0017	45	8.15	22
O. universa	13.79	0.0027	26	8.15	27
O. universa	12.15	0.0024	30	8.15	17
O. universa	10.19	0.0020	38	8.15	22
O. universa	13.85	0.0027	26	8.15	27
O. universa	5.68	0.0011	79	8.15	22
O. universa	6.78	0.0013	63	8.15	22
O. universa	10.08	0.0020	38	8.15	22
O. universa	9.05	0.0018	44	8.15	22
O. universa	10.12	0.0020	38	7.8	22
O. universa	6.15	0.0012	71	8.6	22
O. universa	5.00	0.00097	92		27.2
O. universa	6.73	0.0013	63		27.2
O. universa	7.40	0.0014	56		27.5
O. universa	6.72	0.0013	64		27.2
O. universa	7.55	0.0015	55		22
O. universa	3.94	0.00077	125		27.4
O. universa	7.44	0.0014	56		27.4
O. universa	7.17	0.0014	59		27.4
O. universa	7.49	0.0015	55		27.4
O. universa	6.21	0.0012	70		27.4
O. universa	4.81	0.00094	97		27.4
O. universa	7.26	0.0014	58		27.4
O. universa	3.17	0.00062	164		27.4
O. universa	5.36	0.0010	85		23

[a] Scientific genus and species name of the foraminfera.
[b] Magnesium-to-Calcium ratio in units of milli-moles Mg / moles Ca.
[c] Empirical partition coefficient (D).
[d] Fraction of calcium remaining in the calcification reservoir after biomineralization (F).
[e] The pH in which the organism matured in NBS free hydrogen ion pH scale.
[f] The temperature in which the organisms matured in degrees Celsius.

Table 38: ***A compilation of the data for strontium incorporation in the foraminifera studied by Lea et al., 1999.***

Organism [a]	Sr/Ca (mmol/mol) [b]	D_{Sr} [c]	F_{Sr} [d]	pH [e]	Temperature (°C) [f]
G. bulloides	1.22	0.14	0.72	8.15	16
G. bulloides	1.29	0.15	0.63	8.15	22
G. bulloides	1.32	0.15	0.59	8.15	25
G. bulloides	1.25	0.14	0.68	7.6	22
G. bulloides	1.31	0.15	0.61	8.5	22
G. bulloides	1.14	0.13	0.83		10.4
G. bulloides	1.48	0.17	0.44		13
G. bulloides	1.28	0.15	0.64		11.5
G. bulloides	1.27	0.14	0.65		9.7
O. universa	1.27	0.14	0.65	8.15	17
O. universa	1.30	0.15	0.62	8.15	22
O. universa	1.40	0.16	0.51	8.15	27
O. universa	1.33	0.15	0.58	8.15	17
O. universa	1.32	0.15	0.59	8.15	22
O. universa	1.36	0.15	0.55	8.15	27
O. universa	1.26	0.14	0.67	8.15	22
O. universa	1.21	0.14	0.73	8.15	22
O. universa	1.35	0.15	0.56	8.15	22
O. universa	1.40	0.16	0.51	8.15	22
O. universa	1.26	0.14	0.67	7.8	22
O. universa	1.37	0.16	0.54	8.6	22
O. universa	1.64	0.19	0.33		22.9
O. universa	1.76	0.20	0.28		27.2
O. universa	1.64	0.19	0.33		27.2
O. universa	1.33	0.15	0.58		23

[a] Scientific genus and species name of the foraminfera.
[b] Strontium-to-Calcium ratio in units of milli-moles Sr / moles Ca.
[c] Empirical partition coefficient (D).
[d] Fraction of calcium remaining in the calcification reservoir after biomineralization (F).
[e] The pH in which the organism matured in NBS free hydrogen ion pH scale.
[f] The temperature in which the organisms matured in degrees Celsius.

Table 39: ***A compilation of the data for boron incorporation in the coccolithophores studied by Stoll et al., 2012.***

Organism [a]	Strain [b]	B/Ca (µmol/mol) [c]	D_B [d]	F_B [e]	pH [f]
C. braarudii	AC400	22	0.00054	8.2	8.57
C. braarudii	AC400	12	0.00029	19	8.28
C. braarudii	AC400	5.0	0.00012	66	8.03
C. braarudii	AC400	9.1	0.00022	28	7.89
C. braarudii	AC400	7.0	0.00017	41	8.51
C. braarudii	AC400	5.2	0.00013	63	8.20
C. braarudii	AC400	7.7	0.00019	36	8.03
C. braarudii	AC400	5.9	0.00014	52	7.91
E. huxleyi	RCC1256	27	0.00066	6.1	8.46
E. huxleyi	RCC1256	26	0.00064	6.5	8.46
E. huxleyi	RCC1256	36	0.00088	4.1	8.17
E. huxleyi	RCC1256	47	0.0012	2.8	8.00
E. huxleyi	RCC1256	40	0.00098	3.5	7.81
E. huxleyi	RCC1256	55	0.0013	2.2	7.81
E. huxleyi	RCC1212	7.3	0.00018	39	8.47
E. huxleyi	RCC1212	6.3	0.00015	48	8.18
E. huxleyi	RCC1212	8.6	0.00021	31	7.93
E. huxleyi	RCC1212	8.2	0.00020	33	7.77
E. huxleyi	RCC1238	39	0.00096	3.6	8.45
E. huxleyi	RCC1238	48	0.0012	2.7	8.45
E. huxleyi	RCC1238	25	0.00061	6.8	8.19
E. huxleyi	RCC1238	36	0.00088	4.1	7.96
E. huxleyi	RCC1238	56	0.0014	2.2	7.83
E. huxleyi	RCC1238	39	0.00096	3.6	7.83

[a] Scientific genus and species name of the coccolithophores.
[b] Strain of the organism studied
[c] Boron-to-Calcium ratio in units of micro-moles B / moles Ca.
[c] Empirical partition coefficient (D).
[d] Fraction of calcium remaining in the calcification reservoir after biomineralization (F).
[f] The pH in which the organism matured in total pH scale.

Table 40: ***A compilation of the data for strontium incorporation in cultured calcitic organisms using both the lowest and highest reported inorganic partition coefficients for the calculation of F.***

Organism [a]	Sr/Ca (mmol/mol) [b]	D_{Sr} [c]	F_{Sr}, α=0.020 [d]	F_{Sr}, α=0.35 [e]
Crustacea				
Lobster	6.45	0.73	5.9E-29	0.031
	6.43	0.73	7.5E-29	0.031
	5.78	0.66	2.8E-24	0.065
	4.41	0.50	1.1E-14	0.30
	3.63	0.41	3.0E-09	0.73
	4.64	0.53	2.7E-16	0.24
	5.80	0.66	2.1E-24	0.064
	6.25	0.71	1.3E-27	0.038
	4.43	0.50	7.4E-15	0.30
	5.26	0.60	1.3E-20	0.12
	5.17	0.59	5.2E-20	0.13
	4.31	0.49	5.4E-14	0.34
Blue Crab	5.17	0.59	5.4E-20	0.13
	4.51	0.51	4.6E-16	0.26
	5.46	0.62	9.1E-22	0.10
	5.85	0.66	4.6E-24	0.064
	5.27	0.60	1.2E-20	0.12
	5.37	0.61	3.5E-21	0.11
	5.14	0.58	7.6E-20	0.13
	5.63	0.64	9.8E-23	0.080
	5.46	0.62	9.5E-22	0.10
	5.46	0.62	9.7E-22	0.10
	4.97	0.56	7.8E-19	0.16
Shrimp	4.16	0.47	1.3E-14	0.35
	10.2	1.2	4.1E-46	0.00089
	4.63	0.53	4.7E-17	0.22
	5.03	0.57	4.3E-19	0.15
	4.96	0.56	1.0E-18	0.16
	7.59	0.86	2.3E-32	0.012
	5.08	0.58	2.2E-19	0.14
	5.01	0.57	5.1E-19	0.15
	5.94	0.67	8.1E-24	0.062
	4.07	0.46	4.1E-14	0.39
	5.00	0.57	5.7E-19	0.15
Mollusca				
Bay Scallop	1.48	0.17	0.00085	12
	1.36	0.15	0.0012	14
	1.51	0.17	0.00012	5.3

	1.40	0.16	0.00077	11
	1.47	0.17	0.0010	13
	1.48	0.17	0.00015	5.0
	1.38	0.16	0.00033	8.3
	1.51	0.17	0.0013	16
	1.49	0.17	0.00054	9.9
	1.41	0.16	0.00028	7.9
	1.29	0.15	0.0012	14
	1.34	0.15	0.00046	9.3
	1.33	0.15	0.00091	12
	1.38	0.16	0.00058	10
	1.36	0.15	0.0013	15
	1.38	0.16	0.00086	12
	1.40	0.16	0.00055	9.9
	1.43	0.16	0.0012	15
Oyster	1.21	0.14	6.3E-04	9.9
	1.26	0.14	4.6E-04	9.1
	1.23	0.14	5.6E-04	9.6
	1.27	0.14	4.3E-04	8.9
	0.921	0.10	4.2E-03	17
	0.975	0.11	2.9E-03	16
	0.869	0.10	5.8E-03	19
	0.938	0.11	3.7E-03	17
	1.02	0.12	2.2E-03	14
	0.904	0.10	4.6E-03	18
	0.936	0.11	3.7E-03	17
	0.971	0.11	3.0E-03	16
	0.956	0.11	3.3E-03	16
	0.987	0.11	2.7E-03	15
	0.943	0.11	3.6E-03	17
	1.13	0.13	1.1E-03	12
	0.984	0.11	2.7E-03	15
	1.14	0.13	9.9E-04	11
Blue Mussel	1.19	0.13	0.00073	10
	1.15	0.13	0.00092	11
	1.22	0.14	0.00059	9.9
	1.19	0.14	0.00071	10
	1.67	0.19	0.000029	4.9
	1.33	0.15	0.00028	8.3
	1.23	0.14	0.00055	9.7
	1.70	0.19	0.000023	4.7
	1.38	0.16	0.00019	7.6
	1.25	0.14	0.00048	9.4
	1.17	0.13	0.00080	11
	1.61	0.18	0.000041	5.3

	1.21	0.14	0.00064	10
	1.65	0.19	0.000032	5.0
	1.25	0.14	0.00050	9.5
	1.25	0.14	0.00050	9.5
	1.29	0.15	0.00036	8.8
	1.29	0.15	0.00038	8.9
Periwinkle	1.12	0.13	0.0011	12
	1.03	0.12	0.0021	14
	1.63	0.18	0.000038	5.1
	1.14	0.13	0.0010	11
	1.07	0.12	0.0016	13
	1.67	0.19	0.000029	4.8
	1.33	0.15	0.00029	8.5
	0.993	0.11	0.0027	15
	1.22	0.14	0.00057	10
	1.36	0.15	0.00024	8.1
	1.03	0.12	0.0021	14
	1.26	0.14	0.00045	9.4
	1.10	0.12	0.0013	12
	1.21	0.14	0.00062	10
	1.01	0.11	0.0024	14
	1.12	0.13	0.0012	12
	1.22	0.14	0.00057	10
	1.02	0.12	0.0022	14
	1.07	0.12	0.0016	13
	1.14	0.13	0.0010	11
	1.35	0.15	0.00025	8.2
	1.10	0.12	0.0013	12
	1.19	0.13	0.00074	11
	1.37	0.16	0.00022	7.9
Echinodermata				
Purple Urchin	3.55	0.40	2.5E-11	0.52
	2.15	0.24	8.4E-07	2.7
	3.55	0.40	2.4E-11	0.52
	2.20	0.25	6.0E-07	2.6
	2.05	0.23	1.9E-06	3.1
	2.05	0.23	1.7E-06	3.0
	2.08	0.24	1.5E-06	3.0
	2.03	0.23	2.0E-06	3.1
	2.03	0.23	2.1E-06	3.1
	2.06	0.23	1.7E-06	3.0
	2.15	0.24	8.3E-07	2.7
	2.18	0.25	6.7E-07	2.6
	2.08	0.24	1.4E-06	3.0

	2.17	0.25	7.5E-07	2.7
	2.16	0.25	7.7E-07	2.7
	2.07	0.23	1.5E-06	3.0
	2.25	0.26	4.1E-07	2.4
	2.13	0.24	1.0E-06	2.8
	2.04	0.23	1.9E-06	3.1
	2.22	0.25	5.2E-07	2.5
	2.11	0.24	1.1E-06	2.8
	2.07	0.23	1.5E-06	3.0
Pencil Urchin	2.14	0.24	8.9E-07	2.7
	2.03	0.23	2.1E-06	3.1
	2.26	0.26	3.7E-07	2.4
	2.36	0.27	1.7E-07	2.1
	2.24	0.25	4.3E-07	2.5
	2.24	0.25	4.3E-07	2.5
	2.25	0.26	3.9E-07	2.4
	2.20	0.25	6.0E-07	2.6
	2.30	0.26	2.7E-07	2.3
	2.18	0.25	7.0E-07	2.6
	2.25	0.26	3.9E-07	2.4
	2.20	0.25	5.8E-07	2.6
Rhodophyta				
Coralline Red Algae	3.31	0.38	5.6E-11	0.80
	3.29	0.37	7.1E-11	0.82
	3.18	0.36	2.0E-10	0.92
	3.18	0.36	1.8E-10	0.91
	3.17	0.36	2.1E-10	0.93
	3.10	0.35	3.9E-10	0.99
	3.16	0.36	2.3E-10	0.94
	3.47	0.39	1.3E-11	0.69
	3.20	0.36	1.5E-10	0.90
	3.02	0.34	8.4E-10	1.1
	3.24	0.37	1.1E-10	0.86
	3.08	0.35	4.9E-10	1.0
	2.91	0.33	2.2E-09	1.2
	3.21	0.36	1.4E-10	0.88
	3.41	0.39	2.3E-11	0.73
	2.82	0.32	5.0E-09	1.3
	3.11	0.35	3.6E-10	0.98
	3.29	0.37	6.6E-11	0.82
	3.77	0.43	8.7E-13	0.51
	3.49	0.40	1.1E-11	0.67
	3.12	0.35	3.2E-10	0.97
	3.61	0.41	3.7E-12	0.60

	3.34	0.38	4.3E-11	0.78
	3.00	0.34	1.0E-09	1.1

[a] Common name of the organisms with the phyla names in shaded gray.
[b] Strontium-to-Calcium ratio in units of milli-moles Sr / moles Ca.
[c] Empirical partition coefficient (D).
[d] Fraction of calcium remaining in the calcification reservoir after biomineralization (F) when the lowest reported inorganic partition coefficient ($\alpha = 0.020$ from Nehrke et al., 2007) is used for the calculation of F.
[e] Fraction of calcium remaining in the calcification reservoir after biomineralization (F) when the highest reported inorganic partition coefficient ($\alpha = 0.35$ from Gabitov and Watson, 2006) is used for the calculation of F.

Table 41: ***A compilation of the inorganic partition coefficients reported in the literature with their associated sources.***

X/Ca	Inorganic Partitioning Coefficient (α)	Reference	Notes
Calcite			
Sr/Ca	0.020	Nehrke et al., 2007	
	0.021	Tang et al., 2008	@25°C, from Tesoriero and Pankow, 1996
	0.040	Drake et al., 2012	from Lorens, 1981
	0.044	Elderfield et al., 1996	from Lea et al., 1995
	0.044	Dawber and Tripati, 2012	from Kitano et al., 1971
	0.070	Curti, 1999	from Katz, 1973
	0.080	Drake et al., 2012	from Pingitore and Eastman, 1986
	0.12	Gabitov and Watson, 2006	
	0.210	Nehrke et al., 2007	
	0.27	Drake et al., 2012	Mucci and Morse 1983
	0.35	Gabitov and Watson, 2006	
Mg/Ca	0.0123	Freitas et al., 2006	from Mucci and Morse, 1983
	0.017	Saulnier et al., 2012	
	0.0172	Freitas et al., 2006	from Mucci, 1987
	0.019	Freitas et al., 2006	from Oomori et al., 1987
	0.080	Dawber and Tripati, 2012	
	0.097	Drake et al., 2012	from Katz et al., 1973
Ba/Ca	0.015	Curti, 1999	from Tesoriero and Pankow, 1996
	0.060	Curti, 1999	
	0.080	Elderfield et al., 1996	from Pingitore and Eastman, 1986
	0.1	Gillikin et al., 2006	from Boyle et al., 1995
Mn/Ca	8.5	Drake et al., 2012	from Dromgoole and Walter, 1990
	14.8	Drake et al., 2012	from Lorens, 1981
	30	Elderfield et al., 1996	from Lea et al., 1995
B/Ca	0.00127	He et al., 2013	lowest value found
	0.0015	Allen et al., 2011	
	0.00213	He et al., 2013	highest value found
	1.2	Allen and Hönisch, 2012	lowest value found
	2.0	Allen and Hönisch,	highest value found

		2012	
Li/Ca	0.00025	Elderfield et al., 1996	from Murray, 1991
	0.00080	Marriott et al., 2004	lowest value found
	0.0031	Marriott et al., 2004	highest value found
	0.0040	Dawber and Tripati, 2012	from Okumura and Kitano, 1986
	3.82	Marriott et al., 2004a	
Cd/Ca	7	Elderfield et al., 1996	from Ólafsson, 1983
	14.7	Curti, 1999	from Lorens, 1981
	41	Curti, 1999	from Tesoriero and Pankow, 1996
	110	Curti, 1999	from Davis et al., 1987
U/Ca	0.046	Elderfield et al., 1996	from Russell et al., 1994
	0.046	Meece and Benninger, 1993	lowest value found
	0.2	Meece and Benninger, 1993	highest value found
Aragonite			
Sr/Ca	1.133	Gaetani and Cohen, 2006	@25°C
	1.174	Gaetani and Cohen, 2006	@25°C
	1.193	Dietzel et al., 2004	@25°C
	1.24	Gagnon et al., 2007	
Mg/Ca	0.000275	Gagnon et al., 2007	
	0.001027	Gaetani and Cohen, 2006	@25°C
	0.00133	Gaetani and Cohen, 2006	
Ba/Ca	1.521	Dietzel et al., 2004	@25°C
	2.11	Gaetani and Cohen, 2006	@25°C
	2.817	Gaetani and Cohen, 2006	@25°C
B/Ca	0.0016	Allison et al., 2010	
	0.981	Hemming et al., 1995	
U/Ca	1.8	Meece and Benninger, 1993	
	9.8	Meece and Benninger, 1993	

[a] Element-to-calcium ratio.
[b] Value of the inorganic partition coefficient used in this study.
[c] Literature source from which this value was obtained.
[d] Notes about the value.

References

Addadi L., Joester D., Nudelman F., and Weiner S. Mollusk shell formation: A source of new concepts for understanding biomineralization processes. *Chemistry, A European Journal* 12 (2006) 980-987. doi:10.1002/chem.200500980.

Ahearn G. A., and Zhuang Z. Cellular mechanisms of calcium transport in crustaceans. *Physiological Zoology* 69: 2 (1996) 383-402.

Albarède F. *Geochemistry, An Introduction*. Cambridge, UK: Cambridge University Press, (2003).

Alexander R. M. *The Invertebrates*. Cambridge, UK: Cambridge University Press (1979).

Alexandersson E. T. Carbonate cementation in coralline algal nodules in the Skagerrak, North Sea: biochemical precipitation in undersaturated waters. *Journal of Sedimentary Petrology* 44 (1974) 7-26.

Alexandersson E. T. Carbonate cementation in recent coralline algal constructions. IN: Flügel E. (ed.) *Fossil algae: Recent results and developments.* Berlin, Germany: Springer (1977) 261-269.

Allen K. A. and Hönisch B. The planktonic foraminiferal B/Ca proxy for seawater carbonate chemistry: A critical evaluation. *Earth and Planetary Science Letters* 345-348 (2012) 203-211. doi:10.1016/j.epsl.2011.07.010.

Allen K. A., Hönisch B., Eggins S. M., Yu J., Spero H. J. and Elderfield H. Controls on boron incorporation in cultured tests of the planktonic foraminifer *Orbulina universa*. *Earth and Planetary Science Letters* 309 (2011) 291-301. doi:10.1016/j.epsl.2011.07.010.

Allison N., Finch A. A. and EIMF. δ^{11}B, Sr, Mg and B in a modern *Porites* coral: the relationship between calcification site pH and skeletal chemistry. *Geochimica et Cosmochimica Acta* 74 (2010) 1790-1800. doi:10.1016/j.gca.2009.12.030.

Bach L. T., Riebesell U. and Schulz K.G. Distinguishing between the effects of ocean acidification and ocean carbonation in the coccolithophore Emiliania huxleyi. *Limnology and Oceanography* 56: 6 (2011) 2040-2050. doi:10.4319/lo.2011.56.6.2040.

Bailey A., and Bisalputra T. A preliminary account of the application thin-sectioning, freeze-etching and scanning microscopy to the study of coralline algae. *Phycologia* 9 (1970) 83-101.

Barker S., Greaves M., Elderfield H. A study of cleaning procedures used for foraminiferal Mg/Ca paleothermometry. *Geochimica et Cosmochimica Acta* 4: 9 (2003). doi:10.1029/2003GC000559.

Barker S., Cacho I., Benway H., and Tachikawa K. Planktonic foraminiferal Mg/Ca as a proxy for past oceanic temperatures: a methodological overview and data compilation for the Last Glacial Maximum. *Quaternary Science Reviews* 24 (2005) 821-834. doi:10.1016/j.quascirev.2004.07.016.

Beniash E., Aizenberg J., Addadi L., and Weiner S. Amorphous calcium carbonate transforms into calcite during sea urchin larval spicule growth. *Proceedings of The Royal Society of London, Biological Sciences* 264: 1380 (1997) 461-465. doi:10.1098/rspb.1997.0066.

Benson S. C., and Wilt F. H. Calcification of spicules in the sea urchin embryo. IN Bonucci E. (ed.) *Calcification in Biological Systems*. Boca Raton, FL: CRC Press Inc. (1992) 157-178.

Bentov S., Brownlee C., and Erez J. The role of seawater endocytosis in the biomineralization process in calcareous foraminifera. *PNAS* 106: 51 (2009). doi:10.1073/pnas.0906636106.

Bernhardt A. M., Manyak D. M., and Wilbur K. M. In vitro recalcification of organic matrix of scallop shell and serpulid tubes. *Journal of Molluscan Studies*, Oxford, 51 (1985) 284-289.

Boiteau R., Greaves M., and Elderfield H. Authigenic uranium in foraminiferal coatings: A proxy for ocean redox chemistry. *Paleoceanography* 27 (2012). doi:10.1029/2012PA02335.

Borowitzka M. A. Calcium exchange and the measurement of calcification rates in the calcareous coralline red alga *Amphiroa foliacea*. *Marine Biology* 50 (1979) 339-347.

Borowitzka M. A. Photosynthesis and calcification in the articulated coralline red algae *Amphiroa anceps* and *A. foliacea*. *Marine Biology* 62 (1981) 17-23.

Borowitzka M. A. and Larkum A. W. D. Calcification in the green alga *Halimeda*. III: The sources of inorganic carbon for photosynthesis and calcification and a model of the mechanism of calcification. *Journal of Experimental Biology* 27: 100 (1976) 879-893

Borowitzka M. A. and Larkum A. W. D. Calcification in the green alga *Halimeda*. I: An ultrastructure study of thallus development. *Journal of Phycology* 13 (1977) 6-16.

Bosence D. W. J. Coralline algae: Mineralization, taxonomy, and paleoecology. IN: Riding R. E. (ed.) *Calcareous algae and stromatolites*. Berlin, Germany: Springer-Verlag (1991) 98-113.

Bosence D. W. J. Preservation of coralline-algal reef frameworks. IN: *Proceedings of the 5th International Coral Reef Congress*. Tahiti 6 (1985) 623-628.

Boyle E. A., Labeyrie L., and Duplessy J.-C. Calcitic foraminiferal data confirmed by cadmium in aragonitic *Hoeglundina*: Application to the last glacial maximum in the northern Indian Ocean. *Paleoceanography* 10: 5 (1995) 881-900.

Broecker W. S. and Peng T. H. *Tracers in the Sea*. Palisades, NY: Lamont-Doherty Geological Observatory, Columbia University. 1982.

Bruland K. W., Coale K. H., and Mart L. Analysis of seawater for dissolved cadmium, copper and lead: an intercomparison of voltammertics and atomic absorption methods. *Marine Chemistry* 17 (1985) 285-300.

Buitenhuis E. T., de Baar H. J. W., and Veldhuis M. J. W. Photosynthesis and calcification by *Emiliania huxleyi* (Prymnesiophyceae) as a function of inorganic carbon species. *Journal of Phycology* 35 (1999) 949-959.

Cardinal D., Hamelin B., Bard E., and Pätzold J. Sr/Ca, U/Ca and $\delta^{18}O$ records in recent massive corals from Bermuda: relationships with sea surface temperature. *Chemical geology* 176 (2001) 213-233.

Cohen A. L., Layne G. D., Hart S. R., and Lobel P. S. Kinetic control of skeletal Sr/Ca in a symbiotic coral: Implications for the paleotemperature proxy. *Paleoceanography* 16: 1 (2001) 20-26.

Cohen A. L. and Holcomb M. Why corals care about Ocean Acidification: Uncovering the mechanism. Oceanography 22:4 (2009) 118-127.

Cohen A. L. and McConnaughey T. A. Geochemical Perspectives on Coral Mineralization. *Reviews in Mineralogy and Geochemistry* 54: 1 (2003) 151-187.

Constanz B. *The skeletal ultrastructure of Scleractinian Corals*. Santa Cruz, CA: University of California, Santa Cruz. 1986.

Cossa D., Michel P., Noel J., and Auger D. Vertical mercury profile in relation to arsenic, cadmium and copper at the eastern North Atlantic ICES reference station. *Oceanologica Acta* 15: 6 (1992) 603-608.

Curti E. Coprecipitation of radionuclides with calcite: Estimation of partition coefficients based on a review of laboratory investigations and geochemical data. *Applied Geochemistry* 14 (1999) 433-445.

Cusack M. and Freer A. Biomineralization: Elemental and organic influence in carbonate systems. *American Chemical Society* 108 (2008) 4433-4454. doi:10.1021/cr078270o.

Dauphin Y. Comparative studies of skeletal soluble matrices from some scleractinian corals and molluscs. *International Journal of Biological Macromolecules* 28 (2001) 293-304.

Davis J. A., Fuller C.C., and Cook A. D. A model for trace metal sorption processes at the calcitic surface: Adsorption of Cd^{2+} and subsequent solid solution formation. *Geochimica et Cosmochimica Acta* 51 (1987) 1477-1490.

Dawber C. F. and Tripati A. Relationships between bottom water carbonate saturation and element/Ca ratios in coretop samples of the benthic foraminfera Oridorsalis umbonatus. *Biogeosciences* 9 (2012) 3029-3045. doi:10.5194/bg-9-3029-2012.

Dawson E. Y. *Marine Botany: An Introduction*. New York, NY: Holt, Rinehart and Winston, Inc. (1966).

De Beer D., and Larkum A. W. D. Photosynthesis and calcification in the calcifying *Halimeda discoidea* studied with microsensors. *Plant, Cell and Environment* 24 (2001) 1209-1217.

de Nooijer L. J., Toyofuku T. and Kitazato H. Foraminifera promote calcification by elevating their intracellular pH. *PNAS* 106: 36 (2009). doi:10.1073/pnas.0904306106.

de Villiers S., Greaves M., and Elderfield H. An intensity ratio calibration method for the accurate determination of Mg/Ca and Sr/Ca of marine carbonates by ICP-AES. *Geochimica et Cosmochimica Acta* 3 (2002).

Delaney M. L., Popp B. N., Lepzelter C. G., and Anderson T. F. Lithium-to-calcium ratios in modern Cenozoic, and Paleozoic articulate brachiopod shells. *Paleoceanography* 4: 6 (1989) 681-691.

Dickson A. G. The carbon dioxide system in sea water: equilibrium chemistry and measurements. IN: Riebesell U., Fabry V. J., Hansson L. and Gattuso J.-P. eds. Guide to best practices for ocean acidification research and data reporting. *European Commission*, Brussels (2010).

Dietzel M., Gussone N. and Eisenhauer A. Co-precipitation of Sr^{2+} and Ba^{2+} with aragonite by membrane diffusion of CO_2 between 10 and 50°C. *Chemical Geology* 203 (2004) 139-151. doi:10.1016/j.chemgeo.2003.09.008.

Doney S. C., Balch W. M., Fabry V. J. and Feely R. A. Ocean acidification: A critical emerging problem for the ocean sciences. *Oceanography* 22: 4 (2009a) 16-25.

Doney S. C., Fabry V. J., Feely R. A. and Kleypas J. A. Ocean acidification: The other CO_2 problem. *Annual Review of Marin Science* 1 (2009b) 169-192.

Drake H., Tullborg E.-L., Hogmalm K. J. and Åström M. E. Trace metal distribution and isotope variations in low temperature calcite and groundwater in granitoid fractures down to 1km depth. *Geochimica et Cosmochimica Acta* 84 (2012) 217-238. doi:10.1016/j.gca.2012.01.039.

Dromgoole E. L. and Walter L. M. Iron and manganese incorporation into calcite: Effects of growth kinetics, temperature and solution chemistry. *Chemical Geology* 81 (1990) 311-336.

Dueñas-Bohórquez A., Raitzch M., de Nooijer L. J., and Reichart G.-J. Independent impacts of calcium and carbonate ion concentration on Mg and Sr incorporation in cultured benthic

foraminifera. *Marine Micropaleontology* 81 (2011) 122-130. doi:10.1016/j.marmicro.2011.08.002.

Elderfield H., Bertram C. J. and Erez J. A biomineralization model for the incorporation of trace elements into foraminiferal calcium carbonate. *Earth and Planetary Science Letters* 142 (1996) 409-423.

Erez J., Bentov S., Grinstein M., and de Beer D. A novel carbon concentrating mechanism for foraminiferal calcification and its potential effects on paleoceanographic proxies. *Geochimica et Cosmochimica Acta* 72: 12 (2008) A245.

Erez J. The source of ions for biomineralization in foraminifera and their implications for paleoceanographic proxies. *Reviews in Mineralogy and Geochemistry: Biomineralization* 54 (2003) 115-150.

Fallon S. J., McCulloch M. T., Woesik R., and Sinclair D. J. Corals and their latitudinal limits: laser ablation trace element systematics in *Porites* from Shirigai Bay, Japan. *Earth and Planetary Science Letters* 172 (1999) 221-238.

Foster G. L. Seawater pH, pCO_2 and $[CO_3^{2-}]$ variations in the Caribbean Sea over the last 130 kyr: A boron isotope and B/Ca study of planktic foraminifera. *Earth and Planetary Science Letters* 271 (2008) 254-266. doi:10.1016/j.epsl.2008.04.015.

Freitas P. S., Clarke L. J., Kennedy H., Richardson C. A., and Abrantes F. Environmental and biological controls on elemental Mg/Ca Sr/Ca and Mn/Ca ratios in shells of the king scallop *Pecten maximus*. *Geochimica et Cosmochimica Acta* 70 (2006) 5119-5133. doi:10.1016/j.gca.2006.07.029.

Furla P., Galgani I., Durand I., Allemand D. Sources and mechanisms of inorganic carbon transport for coral calcification and photosynthesis. *The Journal of Experimental Biology* 203 (2000) 3445-3457.

Gabitov R. I. and Watson E. B. Partitioning of strontium between calcite and fluid. *Geochemistry Geophysics Geosystems* 7: 11 (2006). doi:10.1029/2005GC001216

Gaetani G. A. and Cohen A. L. Element partitioning during precipitation of aragonite from seawater: A framework for understanding paleoproxies. *Geochimica et Cosmochimica Acta* 70 (2006) 4617-4634. doi:10.1016/j.gca.2011.01.010.

Gaetani G. A., Cohen A. L., Wang Z., and Crusius J. Rayleigh-based, multi-element coral thermometry: A biomineralization approach to developing climate proxies. *Geochimica et Cosmochimica Acta* 75 (2011) 1920-1932. doi:10.1016/j.gca.2006.07.008.

Gagnon A. C., Adkins J. F., Fernandez D. P., and Robinson L. F. Sr/Ca and Mg/Ca vital effects correlated with skeletal architecture in a scleractinian deep-sea coral and the role of

Rayleigh fractionation. *Earth and Planetary Science Letters* 261 (2007) 280-295. doi:10.1016/j.epsl.2007.07.013.

Gagnon A. C., Adkins J. F., and Erez J. Seawater transport during coral biomineralization. *Earth and Planetary Science Letters* 329-330 (2012) 150-161. doi:10.1016/j.epsl.2012.03.005.

Gagnon A. C., Adkins J. F., Erez J., Eiler J. M., and Guan Y. Sr/Ca sensitivity to aragonite saturation site in cultured samples from a single colony of coral: Mechanism of biomineralization during ocean acidification. *Geochimica et Cosmochimica Acta* 105 (2013) 240-254. doi:10.1016/j.gca.2012.11.038.

Gao K., Aruga Y., Asada K., Ishihara T., Akano T., and Kiyohara M. Calcification in the articulated coralline alga *Corallina pilulifera*, with special reference to the effect of elevated CO_2 concentration. *Marine Biology* 117 (1993) 129-132.

Garbary D. J. An introduction to the scanning electron microscopy of the red algae. IN: Irvine D. E. G., and Price J. H. (eds.) *Modern approaches to the taxonomy of red and brown algae*. Academic Press, London (1978) 205-222.

Gattuso J.-P., Allemand D., and Frankignoulle M. Photosynthesis and calcification at cellular, organismal and community levels in coral reefs: A review on interactions and control by carbonate chemistry. *American Zoologist* 39 (1999) 160-183.

Gillikin D. P., Dehairs F., Lorrain A., Steenmans D., Baeyens W., and André L. Barium uptake into the shells of the common mussel (*Mytilus edulis*) and the potential for estuarine paleo-chemistry reconstruction. *Geochimica et Cosmochimica Acta* 70 (2006) 395-407. doi:10.1016/j.gca.2005.09.015.

Glock N., Eisenhauer A., Liebetrau V., Weidenbeck M., Hensen C., and Nehrke G. EMP and SIMS studies on Mn/Ca and Fe/Ca systematics in benthic foraminifera from the Peruvian OMZ: a contribution to the identification of potential redox proxies and the impact of cleaning protocols. *Biogeosciences* 9 (2012) 341-359. doi:10.5194/bg-9-341-2012.

Goreau T. F. The physiology of skeleton formation in corals. I: A method for measuring the rate of calicium deposition by corals under different conditions. *Biological Bulletin* 116: 1 (1959) 59-75.

Gussone N., Langer G., Thoms S., Nehrke G., Eisenhower A., Riebesell U. and Wefer G. Cellular calcium pathways and isotope fractionation in Emiliania huxleyi. *Geology* 34:8 (2006) 625-628. doi:10.1130/G22733.1.

Hall J. M., and Chan L.-H. Li/Ca in multiple species of benthic and planktonic foraminifera: Thermocline, latitudinal, and glacial-interglacial variation. *Geochimica et Cosmochimica Acta* 68: 3 (2004) 529-545.

Hastings D. W., Russell A. D., and Emerson S. R. Foraminiferal magnesium in *Globeriginoides sacculifer* as a paleotemperature proxy. *Paleoceanography* 13:2 (1998) 161-169.

Hathorne E. C., and James R. H. Temporal record of lithium in seawater: A tracer for silicate weathering? *Earth and Planetary Science Letters* 246 (2006) 393-406.

Hathorne E. C., James R. H., and Lampitt R. S. Environmental versus biomineralization controls on the intratest variation in the trace element composition of the planktonic foraminifera *G. inflata* and *G. scitula*. *Paleoceanography* 24: PA4204 (2009). doi:10.1029/2009PA001742.

He M., Xiao Y., Jin Z., Liu W., Ma Y., Zhang Y., Luo C. Quantification of boron incorporation into synthetic calcite under controlled pH and temperature conditions using a differential solubility technique. *Chemical Geology* 337-338 (2013) 67-74. doi:10.1016/j.chemgeo.2012.11.013.

Hemming N. G., Reeder R. J., and Hanson G. N. Mineral-fluid partitioning and isotopic fractionation of boron in synthetic calcium carbonate. *Geochimica et Cosmochimica Acta* 59: 2 (1995) 371-379.

Hemming N. G., and Hanson G. N. Boron isotopic composition and concentration in modern marine carbonates. *Geochimica et Cosmochimica Acta* 56 (1992) 537-543.

Hickman C. P. *Biology of the Invertebrates*, 2nd ed. St. Louis, MO: C. V. Mosby Company (1973).

Hönisch B., Allen K. A., Russell A. D., Eggins S. M., Bijma J., Spero H. J., Lea D. W., and Yu J. Planktonic foraminifers as recorders of seawater Ba/Ca. *Marine Micropaleontology* 79 (2011) 52-57. doi:10.1016/j.marmicro.2011.01.003.

Horta-Puga G., and Carriquiry J. D. Coral Ba/Ca molar ratios as a proxy of precipitation in the northern Yucatan Peninsula, Mexico. *Applied Geochemistry* 27 (2012) 1579-1586. doi:10.1016/j.apgeochem.2012.05.008.

Iglesias-Rodriguez M. D., Brown C. W., Doney S. C., Kleypas J., Kolber D., Kolber Z., Hayes P. K., and Falkowski P. G. Representing key phytoplankton functional groups in ocean carbon cycle models: Coccolithophorids. *Global Biogeochemical Cycles* 16: 4 (2002). doi:10.1029/1002GB001454.

Jensen P. R., Gibson R. A., Littler M. M., and Littler D. S. Photosynthesis and calcification in four deep-water *Halimeda* species (Chlorophyceae, Caulerpales. *Deep Sea Research* 32: 4 (1985) 451-464.

Katz A. The interaction of magnesium with calcite during crystal growth at 25-90°C and one atmosphere. *Geochimica et Cosmochimica Acta* 37 (1973) 1563-1586.

Kawaguti S. and Sakumoto D. The effect of light on the calcium deposition of corals. *Bulletin of the Oceanographical Institute of Taiwan* 4 (1948) 65-70.

Kisakürek B., Eisenhauer A., Böhm F., Garbe-Schönberg D., and Erez J. Controls on shell Mg/Ca and Sr/Ca in cultured planktonic foraminiferan, *Globigerinoides ruber* (white). *Earth and Planetary Science Letters* 273 (2008) 260-269. doi:10.1016/j.epsl.2008.06.026.

Kitano Y., Kanamori N., and Oomori T. Measurements of distribution coefficients of strontium and barium between carbonate precipitate and solution – Abnormally high values of distribution coefficients measured at early stages of carbonate formation *Geochemical Journal* 4 (1971) 183-206.

Klochko K., Cody G. D., Tossell J. A., Dera P., and Kaufman A. J. Re-evaluating boron speciation in biogenic calcite and aragonite using ^{11}B MAS NMR. *Geochimica et Cosmochimica Acta* 73 (2009) 1890-1900. doi:10.1016/j.gca.2009.01.002.

Lea D. W., and Spero H. J. Experimental determination of barium uptake in shells of the planktonic foraminifera *Orbulina universa* at 22°C. *Geochimica et Cosmochimica Acta* 56 (1992) 2673-2680.

Lea D. W., Martin P. A., Chan D. A., and Spero H. J. Calcium uptake and calcification rate in the planktonic foraminifer *Orbulina universa*. *Journal of Foraminiferal Research* 25: 1 (1995) 14-23.

Lea D. W., Mashiotta T. A., and Spero H. J. Controls on magnesium and strontium uptake in planktonic foraminifera determined by live culturing. *Geochimica et Cosmochimica Acta* 63: 16 (1999) 2369-2379.

Lea D. W. Elemental and isotopic proxies of past ocean temperatures. *The oceans and marine geochemistry* 6: 365 (2006).

Lear C. H., Elderfield H., and Wilson P. A. Cenozoic deep-sea temperatures and global ice volumes from Mg/Ca in benthic foraminiferal calcite. *Science* 287 (2000) 269-272. doi:10.1126/science.287.5451.269.

Lear C. H., Mawbey E. M., and Rosenthal Y. Cenozoic benthic foraminiferal Mg/Ca and Li/Ca records: Toward unlocking temperatures and saturation states. *Paleoceanography* 25 (2010). doi:10.1029/2009PA001880.

Leonardos N., Read B., Thake B., and Young J. R. Mechanistic dependence of photosynthesis on calcification in the coccolithophorid *Emiliania huxleyi* (Haptophyta). *Journal of Phycology* 45 (2009) 1046-1051. doi:10.1111/j.1529-8817.2009.00726.x.

Lorens R. B. Sr, Cd, Mn and Co distribution coefficients in calcite as a function of calcite precipitation rate. *Geochimica et Cosmochimica Acta* 45 (1981) 553-561.

Luquet G., and Marin F. Biomineralizations in crustaceans: storage strategies. *General Palaeontology (Paleobiochemistry)* 3 (2004) 515-534. doi:10.1016/j.crpv.2004.07.015.

Mackinder L., Wheeler G., Schroeder D., Riebesell U. and Brownlee C. Molecular mechanisms underlying calcification in coccolithophores. *Geomicrobiology Journal* 27: 6-7 (2010) 585-595. doi:10.1080/01490451003703014.

Mackinder L., Wheeler G., Schroeder D., von Dassow P., Riebesell U. and Brownlee C. Expression of biomineralization-related ion transport genes in *Emiliania huxleyi*. *Environmental Microbiology* 13: 12 (2011) 3250-3265. doi:10.1111/j.1462-2920.2011.02561.x.

Mann S. Biomineralization: Principles and concepts in bioinorganic materials chemistry. *Oxford University Press*, Oxford. (2001).

Marchitto T. M., and Broecker W. S. Deep water mass geometry in the glacial Atlantic Ocean: A review of constraints from the paleonutrient proxy Cd/Ca. *Geochemistry Geophysics Geosystems* 7: 12 (2006). doi:10.1029/2006GC001323.

Marriott C. S., Henderson G. M., Belshaw N. S. and Tudhope A. W. Temperature dependence of δ^7Li, δ^{44}Ca and Li/Ca during growth of calcium carbonate. *Earth and Planetary Science Letters* 222 (2004a) 615-624. doi:10.1016/j.epsl.2004.02.031.

Marriott C. S., Gideon M. H., Crompton R., Staubwasser M., and Shaw S. Effect of mineralogy, salinity, and temperature on Li/Ca and Li isotope composition of calcium carbonate. *Chemical Geology* 212 (2004b) 5-15. doi:10.1016/j.chemgeo.2004.08.002.

Marshal J. F., and McCulloch M. T. An assessment of the Sr/Ca ratio in shallow water hermatypic corals as a proxy for sea surface temperature. *Geochimica et Cosmochimica Acta* 66: 18 (2002) 3263-3280.

Mashiotta T. A., Lea D. W., and Spero H. J. Experimental determination of cadmium uptake in shells of the planktonic foraminifera *Orbulina universa* and *Globigerina bulloides*: Implications for surface water paleoreconstructions. *Geochimica et Cosmochimica Acta* 61: 19 (1997) 4053-4065.

Matthews K. A. Cadmium in coral skeleton: Natural variability and in situ calibration. Doctoral dissertation at the University of Pennsylvania (2007).

McConnaughey T. ^{13}C and ^{18}O isotopic disequilibrium in biological carbonates: II. *In vitro* simulation of kinetic isotope effects. *Geochimica et Cosmochimica Acta* 53 (1989) 163-171.

McConnaughey, T. A. *Oxygen and carbon isotope disequilibria in Galapagos corals: isotopic thermometry and calcification physiology*. Seattle, WA: Washington University, Seattle. 1986.

McCorkle D. C., Martin P. A., Lea D. W., and Klinkhammer G. P. Evidence of a dissolution effect on benthic foraminiferal shell chemistry: $\delta^{13}C$, Cd/Ca, Ba/Ca, and Sr/Ca results from the Ontong Java Plateau. *Paleoceanography* 10: 4 (1995) 699-714.

McCulloch M., Falter J., Trotter J., and Montagna P. Coral resilience to ocean acidification and global warming through pH up-regulation. *Nature Climate Change* 2 (2012) 623-627. doi:10.1038/nclimate1473.

McManus J., Berelson W. M., Hammond D. E., and Klinkhammer G. P. Barium cycling in the North Pacific: Implications for the utility of Ba as a paleoproductivity and paleoalkalinity proxy. *Paleoceanography* 14: 1 (1999) 53-61.

Meece D. E. and Benninger L. K. The coprecipitation of Pu and other radionuclides with $CaCO_3$. *Geochimica et Cosmochimica Acta* 57 (1993) 1447-1458.

Millero F. J., Feistel R., Wright D. G., McDougall T. J. The composition of Standard Seawater and the definition of the Reference-Composition Salinity Scale. *Deep-Sea Research I* 55 (2008) 50-72. doi:10.1016/j.dsr.2007.10.001.

Min G., Edwards R., Taylor F., Gallup C., and Beck J. Annual cycles of U/Ca in coral skeletons and U/Ca thermometry. *Geochimica et Cosmochimica Acta* 59: 10 (1995) 2025-2042.

Murray J. W. Ecology and distribution of benthic foraminifera. IN: *Biology of the Foraminifera*. Lee J. J., Anderson O. R. eds. London, UK: Academic (1991) 221-253.

Muscatine L. Nutrition of corals. IN: Jones O. A., and Endean R. (eds.) *Biology and Geology of Coral Reefs, Volume II: Biology I.* New York and London: Academic Press (1973) 77-115.

Neff J. M. Ultrastructure of the outer epithelium of the mantle in the clam *Mercenaria mercenaria* in relation to calcification of the shell. *Tissue and Cell* 4: 4 (1972) 591-600.

Nehrke G., Reichart G. J., Van Cappellen P., Meile C., and Bijma J. Dependence of calcite growth rate and Sr partitioning on solution stoichiometry: Non-Kossel crystal growth. *Geochimica et Cosmochimica Acta* 71 (2007) 2240-2249. doi:10.1016/j.gca.2007.02.002.

Nesse W. *Introduction to Mineralogy*, 1st edition. Oxford, UK: Oxford University Press (2004).

Ni Y., Foster G. L., Bailey T., Elliott T., Schmidt D. N., Pearson P., Haley B. and Coath C. A core top assessment of proxies for the ocean carbonate system in surface-dwelling foraminifers. *Paleoceanography* 22 (2007). doi:10.1029/2006PA001337.

Okumura M., and Kitano Y. Coprecipitation of alkali metal ions with calcium carbonate. *Geochimica et Cosmochimica Acta* 50 (1986) 49-58.

Ólafsson J. Mercury concentrations in the North Atlantic in relation to cadmium, aluminum and oceanographic parameters. IN: *Trace metals in sea water*. Wong C. S., Boyle E., Bruland K. W., Burton J. D., Goldberg E. D. eds. New York, NY: Plenum 475-485.

Paasche E. A review of the coccolithophorid *Emiliania huxleyi* (Prymnesiophyceae), with particular reference to growth, coccolith formation, and calcification-photosynthesis interactions. *Phycologia* 40: 6 (2002) 503-529.

Palmer M. R., Brummer G. J., Cooper M. J., Elderfield H., Greaves M. J., Reichart G. J., Schouten S. and Yu J. Multi-proxy reconstruction of surface water pCO_2 in the northern Arabian Sea since 29ka. *Earth and Planetary Science Letters* 295 (2010) 49-57. doi:10.1016/j.epsl.2010.03.023.

Patton G. M., Martin P. A., Voelker A., and Salgueiro E. Multiproxy comparison of oceanographic temperature during Heinrich Events in the eastern subtropical Atlantic. *Earth and Planetary Science Letters* 310 (2011) 45-58. doi:10.1016/j.epsl.2011.07.028.

Pearse V. B. Incorporation of metabolic CO_2 into coral skeleton. *Letters to Nature* 228 (1970) 383. doi:10.1038/228383a0.

Pearse V. B. Sources of carbon in the skeleton of the coral *Fungia scutaria*. IN: Lenhoff H., Muscatine L., and Davis L. V. (eds.) *Experimental Coelenterate Biology*. Honolulu, Hawaii: University of Hawaii Press (1971) 239-245.

Pechenik J. A. *Biology of the Invertebrates*, 2nd ed. Dubuque, IA: Wm. C. Brown Publishers (1991).

Pingitore N. E., and Eastman M. P. The coprecipitation of Sr^{2+} with calcite at 25°C and 1 atm. *Geochimica et Cosmochimica Acta* 50 (1986) 2195-2203.

Prakash Babu C., Brumsack H.-J., Schnetger B., and Böttcher M. E. Barium as a productivity proxy in continental margin sediments: a study from the eastern Arabian Sea. *Marine Geology* 184 (2002) 189-206.

Rae J. W. B., Foster G. L., Schmidt D. N., and Elliott T. Boron isotopes and B/Ca in benthic foraminifera: Proxies for the deep ocean carbonate system. *Earth and Planetary Science Letters* 302 (2011) 403-413. doi:10.1016/j.epsl.2010.12.034.

Raitzch M., Dueñas-Bohórquez A., Reichart G.-J., de Nooijer L.J., and Bickert T. Incorporation of Mg and Sr in calcite of cultured benthic foraminifera: impact of calcium concentration and associated calcite saturation state. *Biogeosciences* 7 (2010) 869-881.

Rayleigh O. M. *LIX On the distillation of binary mixtures*. London, Edinburgh, and Dublin: *Philosophical Magazine and Journal of Science* (1902).

Rickaby R. E. M., and Elderfield H. Planktonic foraminiferal Cd/Ca: Paleonutrients or paleotemperature? *Paleoceanography* 14: 3 (1999) 293-303.

Rickaby R. E. M., Henderiks J. and Young J. N. Perturbing phytoplankton response and isotope fractionation with changing carbonate chemistry in two coccolithophore species. *Climate of the Past* 6 (2010) 771-785. doi:10.5194/cp-6-771-2010.

Riebesell U., Fabry V. J., Hansson L. and Gattuso J.-P. eds. Guide to best practices for ocean acidification research and data reporting. *European Commission*, Brussels (2010).

Ries J. B., Cohen A. L., and McCorkle D. C. Marine calcifiers exhibit mixed responses to CO_2-induced ocean acidification. *Geology* 37: 12 (2009) 1131-1134. doi:10.1130/G30210A.1.

Ries J. B. A physiochemical framework for interpreting the biological calcification response to CO_2-induced ocean acidification. *Geochimica et Cosmochimica Acta* 75 (2011) 4053-4064. doi:10.1016/j.gca.2011.04.025.

Roer R. and Dillaman R. The structure and calcification of the crustacean cuticle. *American Zoology* 24 (1984) 893-909.

Roer R. D. Mechanisms of resorption and deposition of calcium in the carapace of the crab *Carcinnus maenas*. *Journal of Experimental Biology* 88 (1980) 205-218.

Rollion-Bard C. and Erez J. Intra-Shell Boron isotope ratios in the symbiont bearing benthic foraminifera *Amphistegina lobifera*: Implications for $\delta^{11}B$ vital effects and paleo-pH reconstructions. *Geochimica et Cosmochimica Acta* 74:5 (2009) 1530-1536. doi:10.1016/j.gca.2009.11.017.

Rosenthal Y., Boyle E. A., and Slowey N. Temperature control on the incorporation of magnesium, strontium, fluorine, and cadmium into benthic foraminiferal shells from Little Bahama Bank: Prospects for thermocline Paleoceanography. *Geochimica et Cosmochimica Acta* 61: 17 (1997) 3633-3643.

Russell A. D., Emerson S. R., Nelson B. K., Erez J., and Lea D. Uranium in foraminiferal calcite as a recorder of seawater uranium concentrations. *Geochimica et Cosmochimica Acta* 58 (1994) 671-681.

Russell A. D., Hönisch B., Spero H. J., and Lea D. W. Effects of seawater carbonate ion concentration and temperature on shell U, Mg, and Sr in cultured planktonic foraminifera. *Geochimica et Cosmochimica Acta* 68: 21 (2004) 4347-4361. doi:10.1016/j.gca.2004.03.013.

Saenger C., Cohen A. L., Oppo D. W., and Hubbard D. Interpreting sea surface temperature from strontium/calcium ratios in *Montastrea* corals: Link with growth rate and implications for proxy reconstructions. *Paleoceanography* 23 (2008). doi:10.1029/2007PA001572.

Sarmiento J. L. and Gruber N. *Ocean Biogeochemical Dynamics*. Princeton, NJ: Princeton University Press, 2006.

Saulnier S., Rollion-Bard C., Vigier N., Chaussidon M. Mg isotope fractionation during calcite precipitation: An experimental study. *Geochimica et Cosmochimica Acta* 91 (2012) 75-91. doi:10.1016/j.gca.2012.05.024.

Shaw D. *Trace elements in magmas: a theoretical treatment*. Cambridge, UK: Cambridge University Press (2006).

Shen G. T., and Dunbar R. B. Environmental controls on uranium in reef corals. *Geochimica et Cosmochimica Acta* 59: 10 (1995) 2009-2024.

Sinclair D. J., Kinsley L. P. J., and McCulloch M. T. High resolution analysis of trace elements in corals by laser ablation ICP-MS. *Geochimica et Cosmochimica Acta* 62: 11 (1998) 1889-1901.

Stoll H. M. and Schrag D. P. Coccolith Sr/Ca as a new indicator of coccolithophorid calcification and growth rate. *Geochemistry Geophysics Geosystems* 1:1 (2000). doi:10.1029/1999GC000015.

Stoll H., Langer G., Shimizu N., and Kanamaru K. B/Ca in coccoliths and relationship to calcification vesicle pH and dissolved inorganic carbon concentrations. *Geochimica et Cosmochimica Acta* 80 (2012) 143-157. doi:10.1016/j.gca.2011.12.003.

Sun Y., Sun M., Wei G., Lee T., Nie B., and Yu Z. Strontium contents of a *Porites* coral from Xisha Island, South China Sea: A proxy for sea-surface temperature of the 20th century. *Paleoceanography* 19 (2004). doi:10.1029/2003PA000959.

Tambutté S., Holcomb M., Ferrier-Pagès C., Reynaud S., Tambutté É., Zoccola D., and Allemand D. Coral biomineralization: From the gene to the environment. *Journal of Experimental Marine Biology and Ecology* 408 (2011) 58-78.

Tang J., Dietzel M., Böhm F., Köhler S. J., and Eisenhauer A. Sr^{2+}/Ca^{2+} and $^{44}Ca/^{40}Ca$ fractionation during inorganic calcite formation: II. Ca isotopes. *Geochimica et Cosmochimica Acta* 72 (2008) 3733-3745. doi:10.1016/j.gca.2008.05.033.

Tanur A. E., Gunari N., Sullan R. M. A., Kavanagh C. J., and Walker G. C. Insights into the composition, morphology, and formation of the calcareous shell of the serpulid *Hydroides dianthus*. *Journal of Structural Biology* 169 (2010) 145-160.

Taylor A. R., Chrachri A., Wheeler G., Goddard H. and Brownlee C. A voltage-gated H^+ channel underlying pH homeostasis in calcifying coccolithophores. *PLoS Biology* 9: 6 (2011). doi:10.1371/journal.pbio.1001085.

Tesoriero A. J., and Pankow J. F. Solid solution partitioning of Sr^{2+}, Ba^{2+}, and Cd^{2+} to calcite. *Geochimica et Cosmochimica Acta* 60: 6 (1996) 1053-1063.

Travis D. F. The molting cycle of the spiny lobster, *Panulirus argus* Latreille. II: Pre-ecdysial histological and histochemical changes in the hepatopancreas and integumental tissues. *The Biological Bulletin* 108 (1955) 88-112.

Travis D. F. The deposition of skeletal structures in the Crustacea. V: The histomorphological and histochemical changes associated with the development and calcification of the branchial exoskeleton in the crayfish, *Orconectes virilis* Hagen. *Acta Histochemical* 20 (1965) 193-222.

Tripati A. K., Roberts C. D., Eagle R. A. and Li G. A 20 million year record of planktic foraminiferal B/Ca ratios: Systematics and uncertainties in pCO_2 reconstructions. *Geochimica et Cosmochimica Acta* 75 (2011) 2582-2610. doi:10.1016/j.gca.2011.01.018.

Vandermeulen J. H., Davis N. D., and Muscatine L. The effect of inhibitors of photosynthesis on zooxanthellae in corals and other marine invertebrates. *Marine Biology* 16 (1972) 185-191.

Vinn O. The role of an internal organic tube lining in the biomineralization of serpulid tubes. *Carnets de Géologie / Notebooks on Geology - Letters* (January 2011).

Watabe N., Meenakshi V. R., Blackwelder P. L., Kurtz E. M., and Dunkelberger D. G. Calcareous spherules in the gastropod *Pomacea paludosa*. IN: *The mechanisms of mineralization in the invertebrates and plants*. Columbia, SC: *University of South Carolina Press* (1976) 283-308.

Wei G., Sun M., Li X., and Nie B. Mg/Ca, Sr/Ca and U/Ca ratios of a porites coral from Sanya Bay, Hainan Island, South China Sea and their relationships to sea surface temperature. *Palaeogeography, Palaeoclimatology, Palaeoecology* 162 (2000) 59-74.

Westbroek P., Young J. R. and Linschooten K. Coccolith production (Biomineralization) in the marine alga *Emiliania huxleyi*. *Journal of Protozoologists* 36: 4 (1989) 368-373.

Young J. R. and Henriksen K. Biomineralization within vesicles: The calcite of coccoliths. *Reviews in Mineralogy and Geochemistry: Biomineralization* 54 (2003) 189-215.

Yu J., Day J., Greaves M., and Elderfield H. Determination of multiple element/calcium ratios in foraminiferal calcite by quadrupole ICP-MS. *Geochimica et Cosmochimica Acta* 6:8 (2005). doi:10.1029/2005GC000964.

Yu J., and Elderfield H. Benthic foraminiferal B/Ca ratios reflect deep water carbonate saturation state. *Earth and Planetary Science Letters* 258 (2007) 73-86. doi:10.1016/j.epsl.2007.03.025.

Yu J., Elderfield H. and Hönisch B. B/Ca in planktonic foraminifera as a proxy for surface seawater pH. *Paleoceanography* 22 (2007). doi:10.1029/2006PA001347.

Yu J., Elderfield H., Jin Z., and Booth L. A strong temperature effect on U/Ca in planktonic foraminiferal carbonates. *Geochimica et Cosmochimica Acta* 72 (2008) 4988-5000. doi:10.1016/j.gca.2008.07.011.